Nanoscale Horizons

ROYAL SOCIETY OF CHEMISTRY

REVIEW

View Article Online
View Journal | View Issue

Cite this: *Nanoscale Horiz.*, 2021, **6**, 505

Chitin and chitosan on the nanoscale

Tony Jin,[a] Tracy Liu,[a] Edmond Lam *[b] and Audrey Moores *[ac]

Received 21st December 2020,
Accepted 10th May 2021

DOI: 10.1039/d0nh00696c

rsc.li/nanoscale-horizons

In a matter of decades, nanomaterials from biomass, exemplified by nanocellulose, have rapidly transitioned from once being a subject of curiosity to an area of fervent research and development, now reaching the stages of commercialization and industrial relevance. Nanoscale chitin and chitosan, on the other hand, have only recently begun to raise interest. Attractive features such as excellent biocompatibility, antibacterial activity, immunogenicity, as well as the tuneable handles of their acetylamide (chitin) or primary amino (chitosan) functionalities indeed display promise in areas such as biomedical devices, catalysis, therapeutics, and more. Herein, we review recent progress in the fabrication and development of these bio-nanomaterials, describe in detail their properties, and discuss the initial successes in their applications. Comparisons are made to the dominant nanocelluose to highlight some of the inherent advantages that nanochitin and nanochitosan may possess in similar application.

1. Introduction

Biomass-based nanomaterials have become a vast area of research globally. Owing to their unique abilities to combine intricate nanostructure design with biocompatibility and sustainable resourcing, important work has been done to investigate and derive value from these nanomaterials. Within the domain of biomass-based nanomaterials, cellulose nanocrystals (CNCs) have dominated the field thus far, both in terms of the quantity of publications and the numerous applications that have been researched and commercialized.[1–3] More recently, interest

[a] *Center in Green Chemistry and Catalysis, Department of Chemistry, McGill University, 801 Sherbrooke St. West, Montreal, Quebec, H3A 0B8, Canada. E-mail: Audrey.moores@mcgill.ca*
[b] *Aquatic and Crop Resource Development Research Centre, National Research Council of Canada, Montreal, Quebec, H4P 2R2, Canada. E-mail: edmond.lam@cnrc-nrc.gc.ca*
[c] *Department of Materials Engineering, McGill University, 3610 University Street, Montréal, Québec, H3A 0C5, Canada*

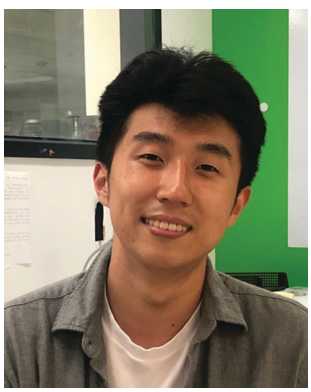

Tony Jin

Tony Jin obtained his BS degree in Chemistry from University of Alberta in 2018 studying under Prof. Vladimir Michaelis. Since then, he has been pursuing a PhD degree in Chemistry under the guidance of Prof. Audrey Moores at McGill and in close collaboration with the National Research Council of Canada under Dr Edmond Lam. He is currently supported by the postgraduate doctoral scholarship from the Natural Sciences and Engineering Research Council (NSERC) and the Dr Lawrence Light Graduate Fellowship in Sustainability. His research focus is in developing the synthesis, properties, and applications of chitosan nanocrystals.

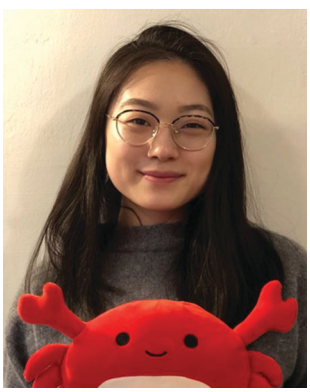

Tracy Liu

Tracy Liu completed her Bachelor of Science degree in Food Chemistry from McGill University in 2021. She spent 2 years working under the guidance of Prof. Audrey Moores on several projects focusing on the mechanochemical synthesis, properties, and applications of chitin products, notably chitosan and chitosan nanocrystals. Her current research interests include sustainable materials, green chemistry, and biological polymers.

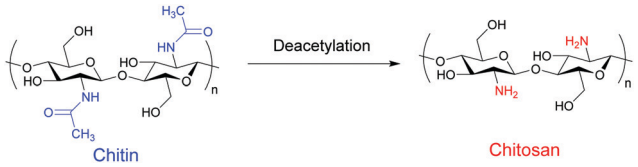

Scheme 1 Chemical structures of chitin and chitosan *via* deacetylation.

has expended towards other sources of biomass resources that can create similar nanostructures as cellulose. Chitin, the second most abundant biopolymer in the world behind cellulose, is a natural alternative to study. Chemically, it is a linear polysaccharide with repeat units of β-(1 → 4)-2-acetamido-2-deoxy-β-D-glucose, with the characteristic acetamide group on the C2 position (Scheme 1).[4] It is a common polymer found in the shells of crustaceans, insects, and certain fungi, and has an annual global availability that is in the order of billions of tonnes.[5] Indeed, marine biowaste is an incredibly important waste stream that is in need of valorisation, with remarkable growth in comparison to other sources.[6] Moreover, the concept of a shell biorefinery that can extract value-added resources, including chitin, has gained increasing interest, with potential for implementation within the coming years.[7] Yet, the implementation of this biorefinery is still in need of value-adding technologies from materials such as chitin that are capable of commercialization.[8] While there are possibilities in using raw chitin as a feedstock for fertilizer in the agricultural industry, research involving the upgrading of chitin is still needed to meet the supply demands necessary for the shell biorefinery sector to thrive.[9] The creation of value-added chemicals such as N-containing furans,[10] and chitin-based oligosaccharides,[11] among others has all helped in realizing the potential for biorefinery commercialization.[12]

As opposed to the acetamide group found in chitin, chitosan, a derivative of chitin, contains repeat units of β-(1 → 4)-2-amino-2-deoxy-β-D-glucose and features a primary amine functionality (Scheme 1). This functionality is typically afforded through deacetylation of chitin in basic media, resulting in hydrolysis of the acetamide group to form chitosan and acetic acid. A known unit of measurement to quantify this procedure is the degree of deacetylation (DDA), where pure chitin has a DDA of 0–15%, primarily containing acetamide groups at the C2 position, while chitosan has a DDA of 75–80%, with mostly amine functionalities on the C2 position.[13] For the purpose of this review, anything referred to as "partially deacetylated chitin" will not be viewed as chitosan, as long as the DDA is below 30%. Due to this chemical modification *via* deacetylation, chitosan has a noted advantage in solubility in acidic, aqueous media compared to chitin, making chitosan highly applicable to current challenges.[14] For example, chitosan is known to possess beneficial antimicrobial[15] and antioxidant[16] properties, while also displaying characteristics that are attractive for applications involving hydrogel formation for drug delivery,[17] water purification,[18] and metal ion scavenging,[19] among others.

Both chitin and chitosan have been explored extensively as bulk systems. More recently, the idea to explore their properties at the nanoscale has emerged. Similar to envisaging the conversion of biowaste materials to value-added chemicals, the creation of functional nanomaterials is another major avenue in the pursuit to create a shell biorefinery. The forestry biorefinery serves as a model here, as it was discovered that treating cellulose pulp with various strong acids enabled the hydrolysis of the amorphous regions of the material and allowed for the release of well-defined nanocrystalline particles with high aspect ratios (on average 5 × 150 nm).[20] These materials feature remarkable capabilities, such as mechanical strength greater than Kevlar,[21] adhesive capabilities,[22] and long-range nematic ordering behaviour[23] among many others.[24] Based on this initial framework, CNCs are now commercially produced worldwide by companies such as Celluforce (Canada), American Process (USA), and Melodea (Israel), with more applications and strengths being discovered.[24,25] Applications for CNCs

Edmond Lam

Dr Edmond Lam is a Research Officer and Team Lead (Advanced Biomaterials and Chemical Synthesis) within the Aquatic and Crop Resource Development research centre of the National Research Council of Canada (NRC). He previously served as Technical Service Lead for the NRC's Bio-based Specialty Chemicals program which aimed to accelerate the commercial readiness of firms by improving the technologies used to produce higher-value, bio-based specialty chemicals. His current research interests include biomass valorization, catalysis, sustainable materials, and synthetic chemistry.

Audrey Moores

Audrey Moores is a professor of chemistry at McGill University and associate editor of ACS Sustainable Chem. Eng. She leads a research group focused on sustainable processes to access metal and biomass-based nanomaterials, to catalyse organic transformations and to convert waste into functional materials. She has received the 2019 McGill University Fessenden Professorship and the 2021 Canadian Chemistry and Chemical Engineering Award for Green Chemistry. She is also member of 2020 class of the College of New Scholars, Artists and Scientists of the Royal Society of Canada.

have been researched extensively[26] in a number of domains, including agriculture,[27] biomedicine,[28] adhesives,[22] and food packaging.[29] Within this mind-set, exploration of both chitin and chitosan on the nanoscale is imperative to develop and even enhance current bio nanomaterial technology based on CNCs as a pathway to addressing similar challenges towards shell biorefinery.[30]

While terminologies vary in the literature, for the sake of this review, we will consider three main types of chitin and chitosan-based nanomaterials: nanocrystals, nanoparticles, and nanofibers. Nanocrystals are defined as nanorod-shaped biopolymers that are crystalline, spanning between 5–20 nm in width and hundreds of nm in length, depending on the source and treatment. Nanoparticles are nano-scaled materials, yet they do not feature the high aspect ratio and crystallinity typical of nanocrystals. While maintaining one of their dimensions in the nanoscale, nanofibers reach much larger dimensions in length, typically to micron sizes. For both chitin and chitosan, all three types of nanomaterials have been developed. Yet, chitosan in the nanoscale has seen fewer developments. Since the deacetylation treatment of chitin into chitosan typically comes with major structural and morphological changes in the bulk material, relying on naturally occurring order to develop these nano-scaled materials is more challenging. Recent developments are showcasing exciting avenues to achieve this goal.[31,32]

In Section 2, various fabrication procedures will be outlined for nanochitin such as chitin nanofibers (ChNFs), chitin nanocrystals (ChNCs), and chitin nanoparticles (ChNPs), as well as nanochitosan in the form of chitosan nanofibers (ChsNFs), chitosan nanocrystals (ChsNCs), and chitosan nanoparticles (ChsNPs). From this, Section 3 will address specific properties of these nanomaterials such as liquid crystalline behaviour, antibacterial properties, and also thermal and mechanical stability. Section 4 will highlight applications in which these nanostructures can be used, including tissue engineering, wound dressing, drug delivery, and catalysis. Finally, a future outlook in Section 5 will be provided on addressing future challenges and directions. Throughout the text, we have highlighted communalities and differences between chitin and chitosan *versus* cellulose to draw comparisons with the well-established field of nanocellulose.

2. Synthesis of nanoscale chitin and chitosan

While a number of chitin- and chitosan-based nanomaterials syntheses are described in the literature (Scheme 2), they proceed *via* similar general methods, as outlined below. Therefore, the approaches and mechanisms of fabrication will be discussed succinctly for the fabrication of the three main nanomaterial forms of chitin and chitosan. Where relevant, the reader will be pointed to existing reviews on specific synthetic methods. This section will not cover how chitin is extracted from the raw resource itself, such as crustaceans, insects, or fungi. For this, the reader is directed to numerous reviews and research articles that define how the deproteinization and demineralization process occurs.[4,33–35] Fabrication procedures outlined below all start from ''purified'' chitin which is deproteinized and demineralized, unless noted in the text.

Two main types of approaches are used for nanochitin/chitosan formation. The first type is called ''top-down'' approaches and consist of extracting the nanomaterial by deconstruction of the bulk phase (Scheme 2), taking advantage of the inherent crystalline structure of the starting material as detailed in Section 2.1. For reasons explained below, this strategy is only accessible for chitin. The second type of approaches, referred to as ''bottom-up'' approaches, involve a dissolution step, followed by some form of ''nanoshaping,'' using crosslinking of electrospinning or ionotropic gelation (Scheme 2). Finally, deacetylation may be used as a means to convert chitin to chitosan in the nanoscale and is the method of choice of ChsNC fabrication.

2.1. Nanochitin preparation

Chitin is a crystalline material with long-range order in the form of the three polymorphs of chitin, namely α-, β-, and γ-chitin.[42–44] The origin of these polymorphs stems from the chitin source itself. α-Chitin is the most abundant form found in crustaceans such as crab.[45] β-Chitin comes from squid pen and cuttlefish,[46] while γ-chitin is present in cocoon fibers in *Ptinus* beetles.[44] Accordingly, a general rule follows that α-chitin is found in hard structures, while β-, and γ-chitin are found in soft structures.[43] The structure of these polymorphs involves H-bonding arrangements of the chitin polymer chains through the amide functionality, with the key difference being how these chains stack with respect to one another. For example, α-chitin has the chitin polymer chains stacked in an anti-parallel fashion, while β-chitin has polymer chains stacked parallel to one another, as seen in Scheme 3.[47] In contrast, γ-chitin has both anti-parallel and parallel polymer chain arrangements.

2.1.1. Chitin nanofibers (ChNFs). The nanofibril arrangements of chitin are naturally occurring architectures. For example, the exoskeleton of crustaceans such as crab contain a hierarchical organization of chitin nanofibrils surrounded by sheets of proteins. These chitin–protein bundles exist as an interwoven network embedded within a matrix of calcium carbonate. The components of this network can then be separated into layers, forming a ''twisted plywood structure,'' as seen in Fig. 1. The main methods for harnessing ChNFs are ''top-down'' and thus rely on taking advantage of this naturally occurring order. Specifically, ChNFs extraction takes place from the treatment of bulk chitin mechanically and/or chemically. Alternatively, ''bottom-up'' approaches involve electrospinning a highly solubilized chitin solution to yield ChNFs.[48]

Extracting chitin nanofibers from bulk chitin through mechanical force is a common procedure and draws common features found in the production of cellulose nanofibers.[50] In 2008, Isogai and coworkers prepared ChNFs from β-chitin

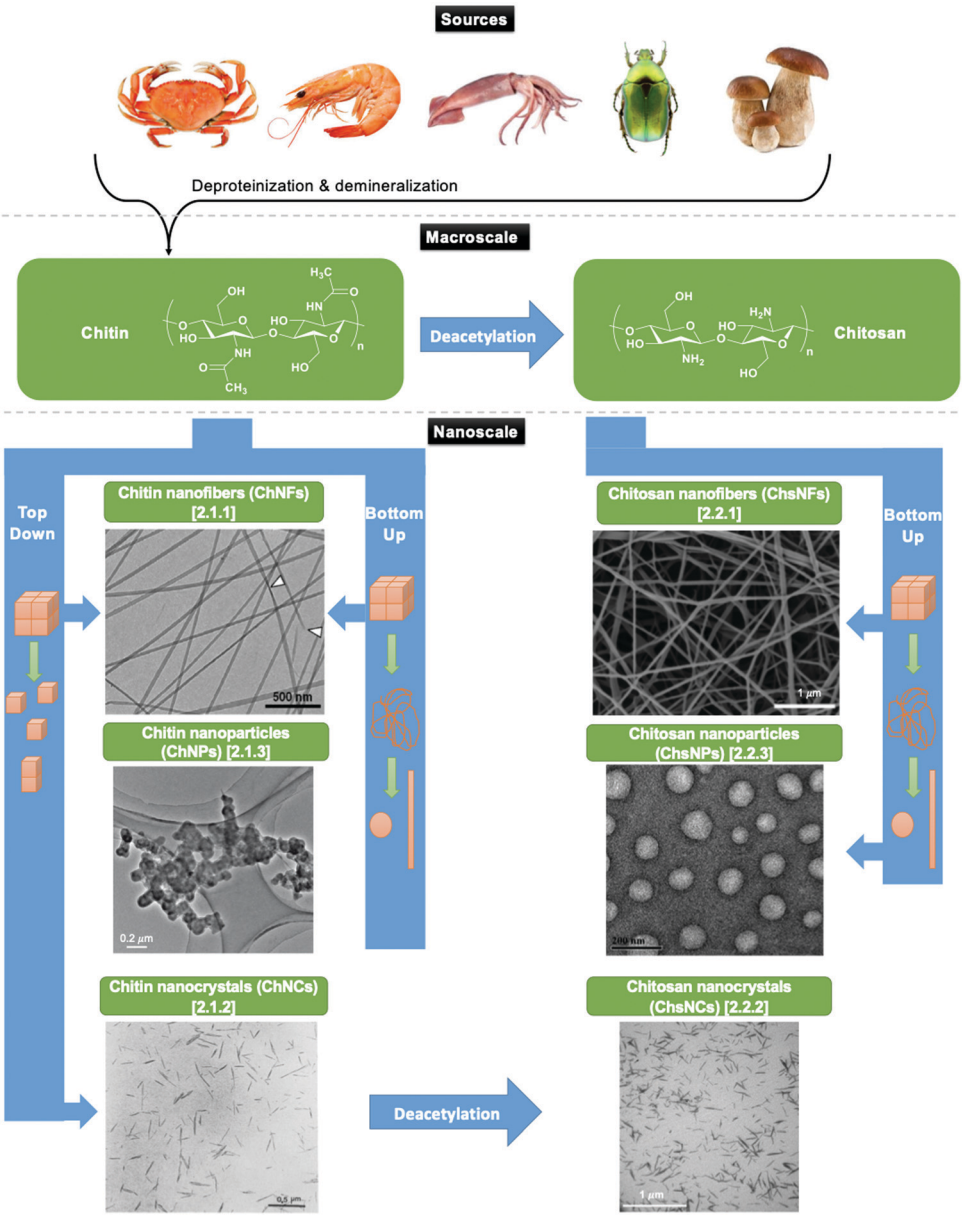

Scheme 2 Depiction of the various subsections in this review and the pathways from the raw resources to the nanomaterial. In this review, the term "top-down" is used for methods whereby bulk materials are deconstructed down to the nanoscale, while "bottom-up" is used for methods where the material is dissolved before reshaping, for instance by crosslinking or electrospinning. Electron microscopy images are reprinted with permission from ref. 36–41.

extracted from squid pens through mechanical disintegration *via* ultrasonication.[46] By testing conditions at various pH and concentration, ChNFs were produced at a pH of 3–4 and at a relatively low concentration of chitin at 0.1–0.3 wt % in aqueous conditions. They reported a width of the ChNFs at 3–4 nm, with an aspect ratio greater than 500.

Furthermore, Ifuku *et al.* have also reported a simple grinding technique to cause fibrillation to yield ChNFs with 10–20 nm widths.[51] The authors indicated that an acidic condition is key to fabricating ChNFs, as a very small number of amino groups on the ChNFs can be charged, promoting electrostatic repulsion and subsequently fibrillation of the bulk fibrillar matrix.

The use of a purely chemical methodology can also be used to make ChNFs. For instance, Isogai and coworkers used 2,2,6,6-tetramethylpiperidine-1-oxyl radical (TEMPO) as an oxidant to fabricate ChNFs from β-chitin extracted from tubeworms.[37] β-Chitin found in tubeworms contains higher crystallinity than those found in squid pens, which explains the retention of its structure to form ChNFs after TEMPO oxidation, instead of depolymerizing further into nanocrystallites and subsequent formation of ChNCs. Fig. 2 shows the transmission electron microscopy (TEM) of the as-synthesized ChNFs, along with electron diffraction.

For "bottom-up" approaches, the most crucial aspect lies in the ability to obtain highly solubilized chitin, essential for

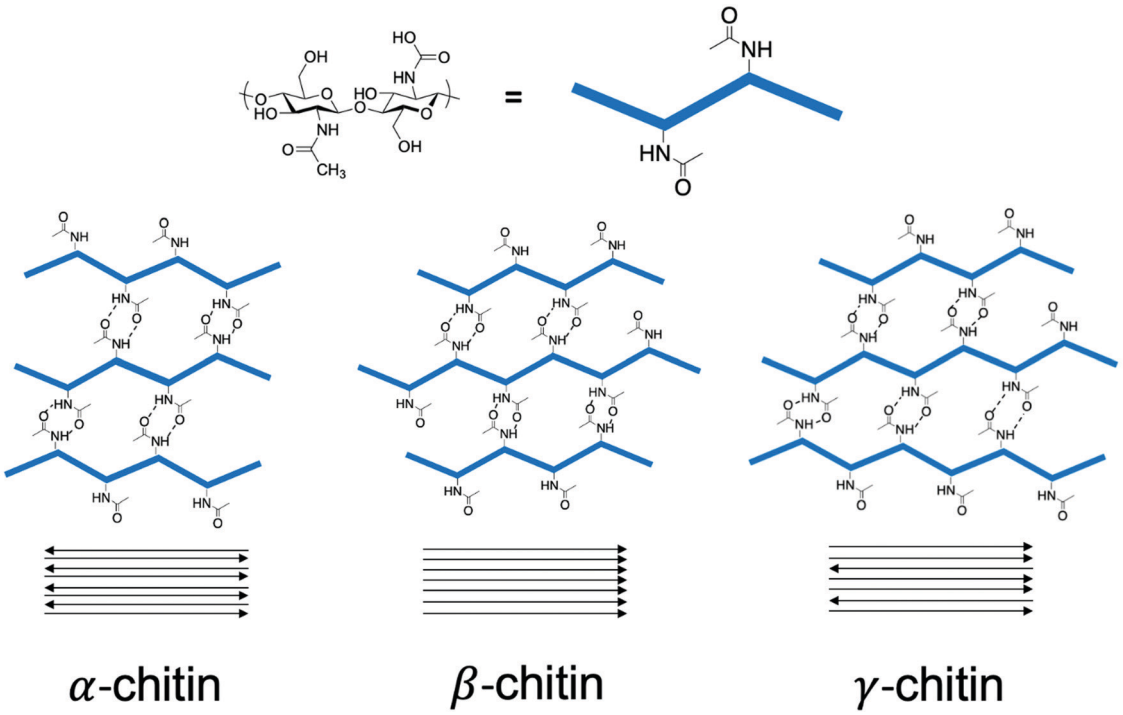

Scheme 3 Schematic outlining the differences in the three polymorphs of chitin. The upper portion depicts how the chains are stacked *via* hydrogen-bonding interactions, while the lower portion illustrates how the direction of the chains changes as they are stacked.

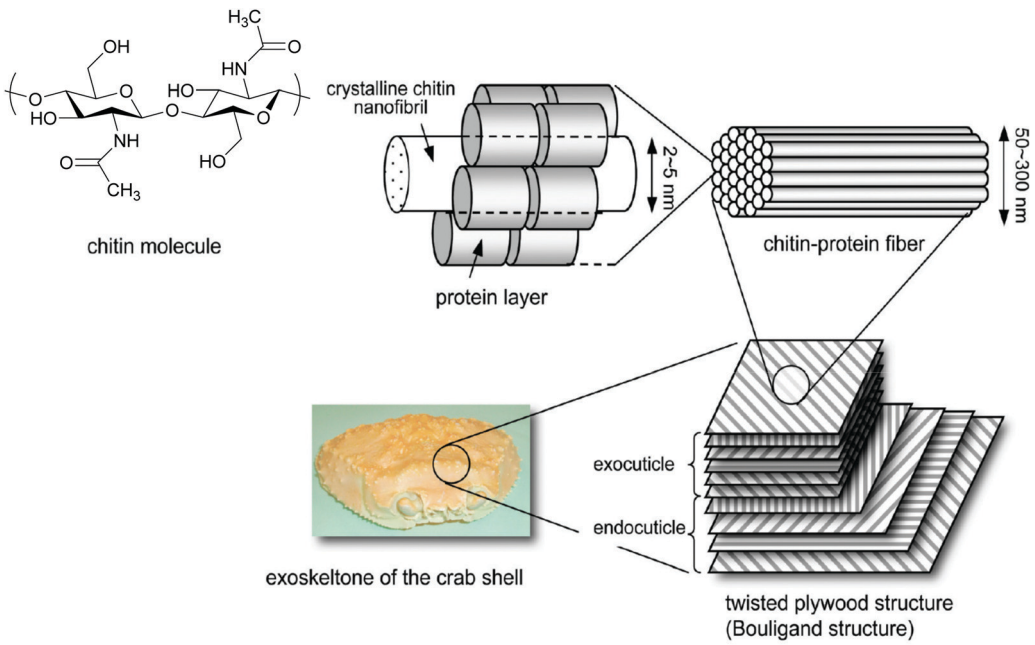

Fig. 1 Representation of the exoskeleton structure of crab. Adapted and formatted from ref. 49.

effective electrospinning.[52] For example, Min *et al.* used γ-radiation to depolymerize bulk chitin to a tenth of its original molecular weight (~900 kDa to 91 kDa) such that it can be soluble in aqueous media.[53] Other works, such as Barber *et al.* involve the use of ionic liquids to dissolve higher molecular weight chitin, such as 1-ethyl-3-methylimidazolium acetate.[48]

2.1.2. Chitin nanocrystals (ChNCs). In contrast to the synthesis of ChNFs, where a ''bottom-up'' approach can be utilized, ChNCs can only be accessed through a ''top-down'' approach. In brief, native polysaccharides such as cellulose and chitin feature high crystallinity. Upon either acid hydrolysis or oxidation pathways, cleavage of the glycosidic oxygen units in

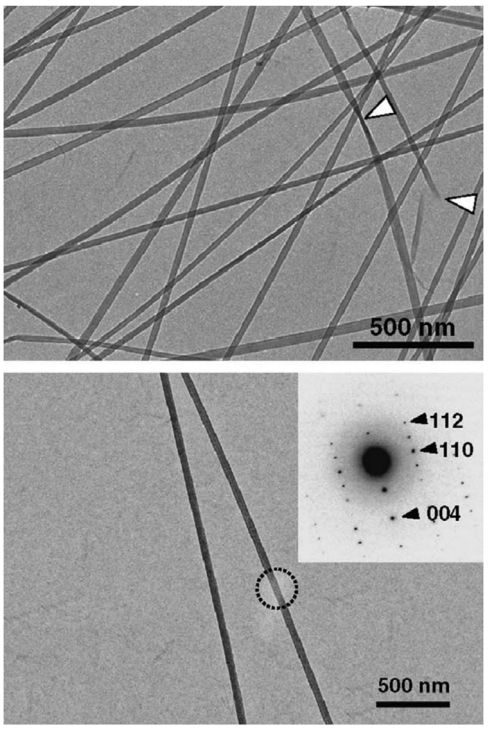

Fig. 2 Bright-field TEM micrograph of ChNFs prepared by TEMPO-oxidation of tubeworm chitin. (top) White arrows depict ''twists'' in the ChNFs (top). (bottom) Bright-field TEM micrograph of ChNF, with electron diffraction diagram shown in insert, with labelled Miller indices. Adapted from ref. 37.

the polymeric backbone can depolymerize amorphous sections of the biopolymeric chain while also releasing fragments of the nanocrystalline domains, effectively freeing ChNCs (Table 1).[54,55]

Marchessault and co-workers first prepared ChNCs using 3 M hydrochloric acid as the acidic medium, while also evidencing the liquid crystalline behaviour of these ChNCs.[38] Based on this methodology of acid hydrolysis, numerous papers have described the preparation of ChNC.[56] Chitin extracted from various sources such as squid pen,[57] riftia tubes,[58] crab shells,[59–63] and shrimp shells,[64–70] were then treated with HCl solutions at concentrations of 2.5 to 3 M to produce ChNC of lengths varying from 50 to 600 nm, and widths between 8 and 50 nm. Variability in this context originates from the chitin source.[71] Since 2011, numerous modifications to this extraction procedure have been conducted to include exchanging the mineral acid used for hydrolysis. Sulfuric acid was first used instead of hydrochloric acid for the synthesis of ChNCs by Qin *et al.*, with a broad distribution of ChNCs extracted, from 100 to 400 nm in length and 10–50 nm in width.[72] This technique has gained traction as other groups have adapted this method for ChNC synthesis using chitin from crab shells.[73,74] Similar to what has been reported for cellulose-based nanocrystals, these methods have afforded sulphate half-ester functionalities at the surface of the as-made ChNCs.[75]

However, the above-described mineral acid hydrolysis for ChNCs synthesis is potentially detrimentally with respect to sustainability due to the hazards associated with corrosive solution handling and wasteful effluents. Other more sustainable, yet more expensive, synthetic methods include a method by Isogai and coworkers to employ a radical oxidation pathway *via* TEMPO to selectively oxidize amorphous regions of chitin.[76–78] In their study, TEMPO was added to NaClO as a co-oxidant, which led to the cleavage of ether linkages within the polysaccharide, and the oxidation of the C6 hydroxyl group into the carboxyl moiety. Isogai and coworkers noticed that increased NaClO concentration caused decreased ChNC length through more intense depolymerization at the ends of the ChNC.

Isogai and co-workers also demonstrated that a O_2-laccase/TEMPO system could yield carboxylated ChNCs.[77] In the presence of oxygen, laccase enzymes have been shown to catalyse the oxidation of phenols, anilines, and aliphatic amines.[79,80] However, macromolecules such as chitin cannot access the laccase site due to their large size. Therefore, TEMPO is used as a shuttle to mediate this one-electron reaction. With this method, the fabrication of ChNCs with dimensions of 400 nm and 24 nm in length and width, respectively, was made possible.

Other methods for ChNC synthesis involve milder treatments, with the goal of sustainability and minimizing environmental

Table 1 Comparison between methods to fabricate ChNCs either through acid hydrolysis or oxidation

Product	Method	Dimensions (length/width) (nm)	Advantages	Ref.
ChNCs	Chitin extraction followed by acid hydrolysis with 2.5–3 M HCl	50–600/8–50	''Classic method''	38 and 56–70
	Chitin extraction followed by acid hydrolysis with H_2SO_4	100–400/10–50	Similar to HCl method	72–74
	Using acidic deep eutectic solvents (DES) to induce acid hydrolysis	206–1000/12–44	Avoid excess usage of mineral acid Acidic medium becomes recyclable	82 and 83
Carboxylated ChNCs	Radical oxidation pathway *via* TEMPO	480/24	More sustainable compared to classic method	76–78
	O_2-laccase–TEMPO system	400/24	More sustainable compared to classic method	77, 79 and 80
	Oxidation through ammonium persulfate (APS)	239 ± 7/4.60 ± 0.06	Milder, greener conditions, Cheaper reagent	42

waste. We demonstrated the use of ammonium persulfate (APS) as a mild oxidant in the fabrication of ChNCs.[42] Like TEMPO, APS afforded fully carboxylated ChNCs, while relying on milder conditions and the use of a more economical reagent. This process was adapted from previous works that converted bulk cellulose into CNCs, highlighting a typical example of how inspiration from CNC research can be applied towards ChNCs.[81]

Recently, strategies using acidic deep eutectic solvents (DES) have been developed to fabricate ChNCs.[82,83] While this method also induced acid hydrolysis to form ChNCs, it avoided the use of stoichiometric amounts of mineral acid during synthesis and made the acidic medium recyclable. For example, Cao *et al.* prepared ChNC with *p*-toluenesulfonic acid/choline chloride (*p*TA–ChCl) DES, yielding ChNCs with a width between 12–44 nm and length between 206–399 nm.[82] Furthermore, Mukesh *et al.* prepared ChNC using choline chloride/urea DES.[83] They demonstrated the recyclability of the DES by preparing a subsequent batch of ChNCs with the same DES, with the composition and morphology of the second batch of ChNC being similar to the first batch.

2.1.3. Chitin nanoparticles (ChNPs). Aside from the slender rod-like morphologies driving much of the nanochitin literature, other types of architectures can be prepared, such as spherical and amorphous ChNPs. These procedures are inherently ''bottom-up'' in nature as they proceed *via* chitin solubilisation before some crosslinking event.

In one approach, an ionic crosslinker such as tripolyphosphate (TPP) reacts with the few protonated amino groups on chitin to form a nanosized particle. Critically, these methodologies rely on the presence of amine groups within the chitin polymer. Thus, they are restricted to chitins which have undergone sufficient deacetylation to possess enough of this functional group, and which have been amorphized, so that that can be solubilized and reacted with the crosslinker. For instance, Jayakumar and coworkers reported the synthesis of amorphous ChNPs using a 1 wt% TPP solution added dropwise to a 0.01 wt% solution of amorphous bulk chitin with a DDA of 40%.[84] The as-synthesized ChNPs have a relative diameter of 120 ± 50 nm. Later, Jayakumar and coworkers used a similar procedure with 35% DDA–chitin starting material.[85] The average size of the ChNPs produced were 324 ± 17 nm, which is on the boundary between nano and micro dimensions.

Other ChNP formation procedures include using chemically modified chitin as the substrate. Jayakumar and coworkers reported the fabrication of carboxymethyl (CM) ChNPs for use in drug delivery *via* a cross-linking method that uses $CaCl_2$ and $FeCl_3$.[86] It can be noted that CM ChNPs are of particular interest for biomedical applications due to their higher solubility for hydrogel fabrication. In the case of drug delivery, crosslinking of the CM ChNPs can help decrease the rate of CM ChNP degradation within the body, which directly affects the rate of drug delivery within the body. Further, the nanoscale range of the CM ChNPs is required for elective passive targeting, such as a diameter between 200–300 nm needed for passive liver targeting. From their procedure, they succeed in producing CM ChNPs with a diameter between 200–250 nm.

2.2. Nanochitosan preparation

While there are numerous methods already in place for fabricating chitin-based nanomaterials, development of chitosan into the nanoscale offers less options. Effectively, two main strategies are possible in making chitosan nanomaterials, as shown in Scheme 2. The first strategy involves the deacetylation of bulk chitin to afford chitosan, which is then converted into nanochitosan *via* a ''bottom-up'' approach. Such chitosan made from bulk chitin deacetylation can then be converted into ChsNPs and ChsNFs. In contrast, the second strategy involves using already fabricated nanochitin, before deacetylation is performed to make nanochitosan. Deacetylation at the nanoscale has only recently been investigated as a pathway to form ChsNCs, as it has been met with multiple challenges including retention of crystallinity and structure.

2.2.1. Chitosan nanofibers (ChsNFs). Because chitin deacetylation causes amorphization, there is no possibility to attain ChsNFs by the ''top-down'' approaches used for ChNFs preparation. Additionally, unlike both chitin and cellulose, chitosan can readily dissolve in dilute acidic conditions. Thus, only ''bottom-up'' approaches are able to afford ChsNFs. There are many methods using electrospinning to produce ChsNFs with a variety of acids and additives, which have been extensively covered in previous reviews and articles.[41,53,87–89] In this process, a high voltage is used to create a stream of charged polymer solution, which are subsequently dried to form nanofibers as a non-woven fabric.[87] As this field has largely grown in a separate direction from the other types of chitin- and chitosan-based nanomaterials, this will not be covered in this review, and the reader can be directed to the reviews highlighted above.

2.2.2. Chitosan nanocrystals (ChsNCs). Initial attempts at using the ''classic'' conditions of basic media deacetylation (*e.g.*, a concentrated aqueous solution of NaOH) for bulk chitin was observed to destroy the nanorod morphology of the ChNCs. Chirachanchai and coworkers first reported the synthesis of a chitosan ''nanoscaffold'' by first fabricating ChNC *via* acid hydrolysis, and subsequently subjecting ChNC to basic media in the form of aqueous NaOH (40% w/v) at reflux for 3 days.[32] While they achieved a high DDA value of 95%, drastic structural changes took place during the procedure. For instance, from the nanorod-shaped ChNCs (Fig. 3a), swelling and aggregation occurred through the basic deacetylation process, creating an interwoven network of nanochitosan (Fig. 3b). Secondly, X-ray diffraction (XRD) spectra of both the ChNC and chitosan nanoscaffold material (Fig. 3c) found that severe changes in terms of packing and crystallinity took place during the deacetylation process. For instance, the reflections found at 9° and 20° on ChNC (**1** on Fig. 3c) had shifted to a higher 2θ angle for the chitosan nanoscaffold. While the authors did not rationalize this shift, one may hypothesize that amorphization of the ChNC shifted and broadened these reflections for the chitosan nanoscaffold.

The same group further analysed synthesized ChNCs through gel permeation chromatography (GPC) measurements and observed that the obtained chitosan nanoscaffold featured

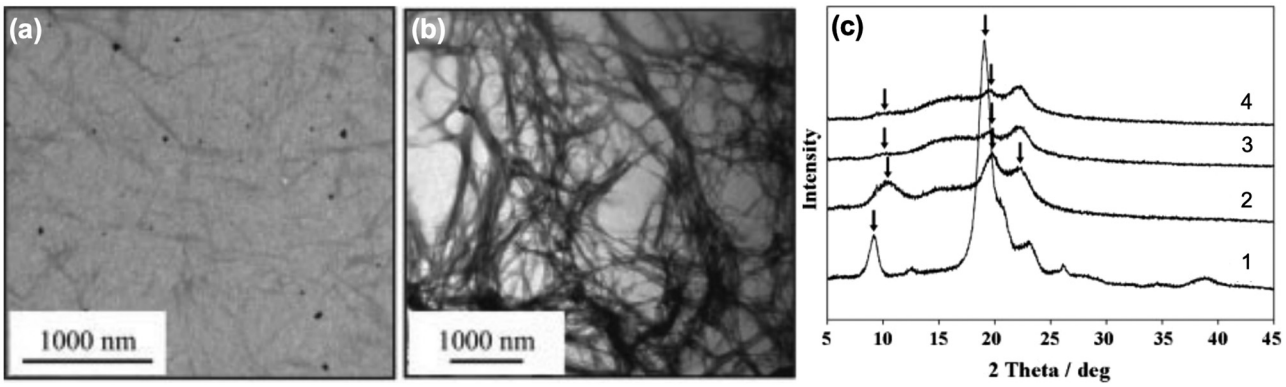

Fig. 3 Bright-field TEM micrographs of (a) ChNCs and (b) the as-prepared chitosan nanoscaffold. XRD patterns of (1) ChNCs, (2) chitosan nanoscaffold, (3) lactose-conjugated chitosan nanoscaffold, and (4) maltose-conjugated chitosan nanoscaffold. Black arrows represent notable reflections of interest. Adapted from ref. 32.

increased molecular weight (137 kDa) compared to the original ChNCs (63 kDa).[69] This is in stark contrast to bulk chitin reactivity, since concentrated NaOH solutions cause molecular weight reduction in bulk chitin deacetylation.

In order to prevent destruction of the ChNC morphology, careful tuning of parameters and much milder conditions are needed. As such, Hsieh and co-workers studied ChNC deacetylation with much milder conditions to retain a rod-like shape.[90] Instead of deacetylation at reflux temperatures approaching 120 °C, they used a mild temperature of 50 °C. DDA reached 40% after 6 h of reaction and plateaued thereafter, even beyond 24 h. Importantly, the rod-like morphology was retained after this treatment at 6 h (Fig. 4a). The authors suggested that with these milder conditions, only the surface of the ChNC was deacetylated into chitosan, while the interior remained as ChNC, thus creating a core–shell structure. The XRD of the

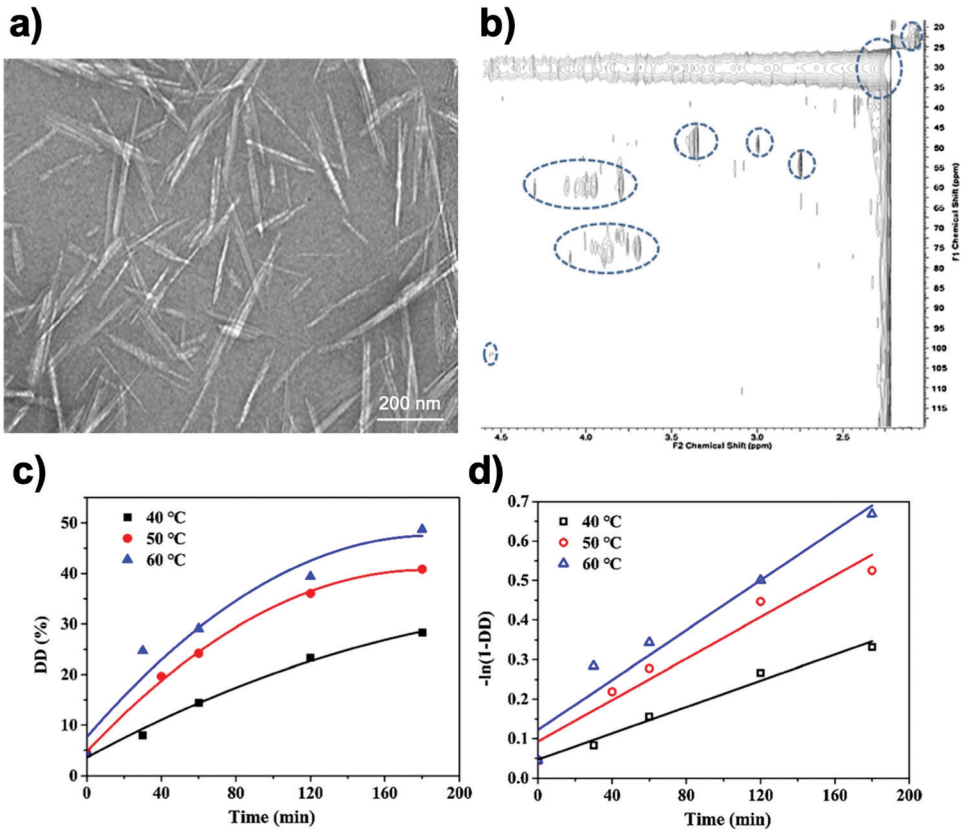

Fig. 4 (a) Bright-field TEM micrograph of chitin–chitosan core–shell nanocrystals. 2% uranyl acetate was used as a staining agent. (b) 2-D heteronuclear single quantum coherence (HSQC) NMR experiment of chitin–chitosan core–shell nanocrystals. (c) Kinetic curves of DD (degree of deacetylation) at different reaction temperature. (d) Curve-fitting results to deduce rate constants at different temperatures. Adapted from ref. 90–92.

core–shell chitin–chitosan (Ch–Chs) nanocrystal also retained the structure found for the α-chitin polymorph, additionally implying the interior ChNC structure had not be altered by this treatment.

A subsequent report from the Hsieh group used high resolution liquid-state ^{1}H NMR as a spectroscopic tool to provide further evidence of the chitin–chitosan core–shell configuration.[91] To do so, they used 2-D heteronuclear single quantum coherence (HSQC) since in a ^{1}H–^{13}C HSQC experiment, mobile polymer strands are more susceptible to magnetization as compared to H-bonded ones (Fig. 4b). Thus, they used this method to specifically analyse mobile chains floating at the surface of prepared Ch–Chs core–shell nanocrystals, while the ChNC core remained silent. Thus, this method effectively deduced the differences between the outer chitosan shell of Ch–Chs core–shell nanocrystals and the interior chitin core.

Further works on the study of chitin–chitosan core–shell structures involved plotting kinetic curves towards the deacetylation procedure, where the rate of ChNC deacetylation could be determined at various temperatures (Fig. 4c and d).[92] In addition, Arrhenius plots were conducted to determine the activation energy of deacetylation for ChNC, which was 28 kJ mol^{-1}, a much lower number than the one for bulk chitin at 92 kJ mol^{-1}. This has been ascribed to the higher surface area of ChNC, which made deacetylation more accessible to the surface of the ChNC.

A challenge in all of these works has been the ability to reach a DDA >75%, while also keeping the morphology of ChNCs intact in order to truly obtain rod-like ChsNCs. To solve this, our group used $NaBH_4$ as an additive to combat nanorod degradation[39] and inhibit the ''end-peeling'' phenomenon known for polysaccharides in a basic environment.[93,94] This phenomenon is based on the alkaline pulping process of cellulose, which involves the elimination of the reducing end-groups *via* β-alkoxy elimination to carboxylic acids, thus degrading the polysaccharides one monomeric unit at a time.[93] Simply, the hydrides from $NaBH_4$ can reduce the alditol ends, thereby preventing end-peeling from occurring.

This method allowed for the retention of the nanorod morphology with DDA values well over 80% (Fig. 5a). Without $NaBH_4$, aggregated spheres of what is likely degraded chitin/chitosan oligomers were imaged by TEM imaging (Fig. 5b).

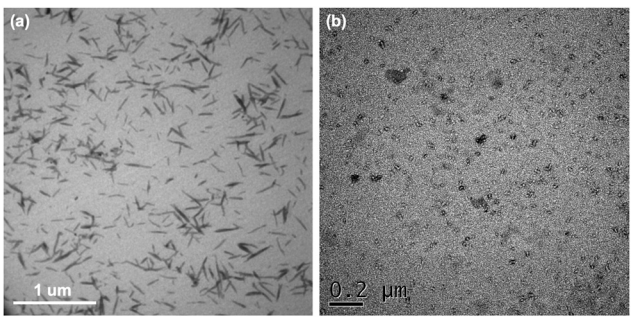

Fig. 5 Bright-field TEM micrographs after deacetylation of ChNCs (a) with $NaBH_4$ and (b) without $NaBH_4$. Adapted from ref. 42.

Currently, this is the only known synthesis path towards the formation of ChsNCs with both rod-like morphology and DDA > 80%.

2.2.3. Chitosan nanoparticles (ChsNPs). A variety of methods have been explored in preparing ChsNPs, including ionic cross-linking (similar to what was described for ChNP), as well as emulsion droplet coalescence and precipitation.[94] In 1989, Bodmeier *et al.* first synthesized ChsNPs as a novel drug delivery system.[95] This was achieved upon adding a TPP solution drop-wise into a positively charged chitosan in acetic media, while stirring constantly. The intermolecular cross-linking between the chitosan-free amino groups and TPP anions afforded ionotropically gelled, spherical beads of TPP–chitosan complex. The process was observed to progress from solution, to aggregation, and finally an opalescent suspension, implying that the fabrication process is complete.[96] Adopting this principle of ChsNP formation, Huang *et al.* explored the effect of bulk chitosan molecular weight on the size and zeta potential of the corresponding nanoparticles.[94] Samples with different molecular weights were first prepared by initial H_2O_2 treatments. The resulting ChsNPs were isolated by high-speed centrifugation, washing and freeze-drying for analysis. The authors concluded that a lower molecular weight chitosan (LWCS) produced smaller nanoparticle sizes, and that the optimal LWCS/TPP mass ratio for the cross-linking reaction was 5 : 2. At that ratio, ChsNPs were obtained, and further increasing the TPP content appeared to form a precipitate, possibly from excess ChsNP coagulation. Yang *et al.* also employed the same method to produce highly uniform ChsNPs with a size of ~50 nm.[97] This ionic gelation approach appears to be favourable due to its simple and mild procedure.[97–100] The physical cross-linking based on electrostatic interaction was also reversible, avoiding potential toxicity in reagents.[98] Similarly, Moura and coworkers dissolved chitosan in methacrylic acid (MAA) solution and used potassium persulfate as the source of anions – a method that is also commonly used for ChsNP synthesis.[101–103]

Alternatively, Tokumistu *et al.* used an emulsion-droplet coalescence technique to prepare ChsNPs loaded with gadopentetic acid for gadolinium neutron-capture cancer therapy.[104] This was achieved by first combining a chitosan solution with an emulsifier agitated at high speed, followed by mixing the emulsion with another NaOH emulsion. Upon stirring and centrifugation, this emulsion-droplet coalescence method afforded ChsNPs of 426 nm in size. A similar method using an emulsifier was employed by Tang *et al.* where 1% chitosan solution was poured into a medium of petroleum ether, mineral oil, and an emulsifier.[98] This dispersion medium was then stirred for 10 min at 1000–2000 rpm before isolating the desired ChsNPs. The group then compared this emulsion polymerization method with the ionic cross-linking method using TTP solution previously described. It was observed that the emulsion method produced larger nanoparticles (>200 nm), compared to the nanoparticles made in water phase using TTP solution which were too small to be collected by super-centrifugation.

While the diverse application of ChsNPs in various fields will be discussed in the sections ahead, much less can be said of the fundamental research on the mechanisms of the synthesis for these nanomaterials. Similar to the best practices in reporting inorganic colloidal nanomaterials, much more work must be done in achieving a similar level of control and characterization on these organic nanoparticles.[105] For example, further studies that implement control in creating monodisperse nanoparticles are crucial in controlling directed delivery of pharmaceuticals *via* nanoparticles. Details regarding the structural arrangements of the ChsNP can be more thoroughly developed with tools such as XRD and solid-state NMR, which can directly probe the crystalline and amorphous nature of these nanoscale objects.

2.3. Surface characteristics of nanochitin and nanochitosan

With the number of fabrication strategies for each type of nanochitin and nanochitosan described in Sections 2.1 and 2.2, the structure and morphological characteristics of the above-mentioned nanomaterials can be quite different from each other. Table 2 outlines the general structure and morphological properties of each type of nanomaterial.

The average dimensions and length-scales for each type of nanomaterial are generally consistent within the literature, though there is a dependence on which raw biomass the initial bulk chitin was extracted from (*e.g.*, shrimp, crab, squid, fungi). Table 1 goes into more detail on specific types of ChNCs in Section 2.1.2. Similar to nanocellulose, the aspect ratios for nanofibers and nanocrystals vary significantly depending on chitin source.[56]

One unique property that differs between the chitin and chitosan nanomaterials is the surface charge which is quantified by measuring the zeta-potential of a suspension of the nanomaterials. In Table 2, there are distinct differences in zeta potential between the nanomaterial types associated with the variance in DDA between chitin and chitosan. There is a pH dependency on the zeta potential of chitosan linked to the presence of the amine functionality. The zeta potential of chitosan-based nanomaterials reached values up to +60 mV in acidic conditions, while values of −10 to −20 mV were found for chitosan nanomaterials at pH > 8. Most chitosan nanomaterials form very stable colloidal solutions in slightly acidic aqueous conditions (pH ≈ 5) due to the pK_a of bulk chitosan being ∼ 6.2.[106] Chitin nanomaterials do not show this dramatic increase in zeta potential at low pH due to the limited number of amines that can be protonated.

The last parameter is the crystallinity of the material, which can be quantified by calculating the crystallinity index (CrI) based on the XRD diffractogram of the nanomaterial. In general, it can be seen that for chitin nanomaterials, moderate to high crystallinities are seen with respect to their chitosan-based counterparts. In the macroscale, it is noted that bulk chitin has relatively high crystallinity while chitosan is amorphous, due to the fact that the fabrication of chitosan involves harsh conditions of deacetylation from chitin, which disrupts the inherent crystalline structure of chitin. Therefore, chitosan nanomaterials made from bulk chitosan will always be amorphous. Other parameters include surface functionalization groups, which depends on the process used to make the nanomaterials, or if further surface functionalization has been performed. For example, carboxylated ChNCs have been covered in Section 2.1.2, while carboxylated ChNFs are also known and reviewed in Section 2.1.1.

3. Properties of nanoscale chitin and chitosan

Both bulk form chitin and chitosan display numerous biological properties that have been analysed and utilized for a variety of applications. At the nanoscale, these properties may be enhanced with increased effective surface area, or even new characteristics unique to these materials. In this section, key characteristics of nanoscale chitin and chitosan materials will be discussed. Specifically, liquid crystalline, antibacterial, antioxidant, thermal, and mechanical properties will be discussed in the context of their initial development. Macroscopic properties such as antibacterial, thermal and mechanical properties are intrinsically difficult to evaluate on nanomaterials directly, which is also seen for the CNC literature, because of their nanoscale.[2,107] Thus, much of these studies involve the incorporation of nanochitin or nanochitosan within a specific system (*e.g.* hydrogel, aerogel, coating, film) rather than evaluating them independently. Comparisons with similar systems without nanochitin/chitosan may be used to extract the true role of such nanomaterials.

3.1. Liquid crystalline behaviour

Akin to the helicoidal arrangement of cellulose fibers inside plant walls, the exoskeleton of many arthropods such as crab and shellfish are made up of an assembly of one dimensional

Table 2 Shape, Morphology, surface, and structural characteristics of the various types of nanochitin and nanochitosan

	Nanofibers		Nanocrystals		Nanoparticles	
	ChNFs	ChsNFs	ChNCs	ChsNCs	ChNPs	ChsNPs
Shape	Long fibers		Short rods		Spheres	
Average dimensions	3–20 nm in width, 50–100 μm in length	10–40 nm in width, 50–100 μm in length	8–44 nm in width, 50–1000 nm in length	5–20 nm in width, 150–250 nm in length	100–300 nm in diameter	50–200 nm in diameter
Surface charge (ξ-potential) at neutral pH	−20 to −25 mV	+10 to +20 mV	0 to −10 mV	+15 to +20 mV	+20 mV	+50 mV
Crystallinity	Moderate – low	Low	High	Low	Moderate	Low

chitin fibers embedded within a matrix of proteins and cations.[108–110] Both cellulose and chitin have a unique twisted plywood structure (coined the Bouligand-type structure) that is characteristic of chiral nematic ordering, a property that plays a central role in the structure's load-bearing properties. Ordering at the nanoscale is interesting as it may result in the emergence of structural colour as seen in the shell of some insects such as the jewel beetle.[111] The colour of the exoskeleton can change with variation in the polarization of light, which is one of the more profound characteristics in the self-assembly of chitin on the nanoscale.

3.1.1. Nanochitin liquid crystal behaviour. The exploration of the liquid crystalline properties of nanochitin-based systems are still at its infancy, with different research groups dedicated to this work. Importantly, much of the research involved in the liquid crystalline properties of nanochitin derives mainly from work done on CNCs, which is elegantly compared in a recent review by MacLachlan and co-workers.[112] In 1993, Revol and Marchessault confirmed that ChNCs made through acid hydrolysis demonstrated liquid crystal-like behaviour through the formation of a chiral nematic phase.[38] Two phases – one isotropic and one anisotropic – were made after letting a 5 wt% aqueous ChNC suspension sit at room temperature overnight. The two-phase suspension was then vigorously shaken, and TEM revealed droplets with a birefringence pattern known as tactoids similar to cellulose crystallites. The chiral nematic ordering can be seen when the suspension is left to settle for one day, optically visualized through crossed polars (Fig. 6). It can be seen that the spacings can be measured to produce the length of half of the cholesteric pitch ($p/2$). The authors suspected that the apparent chiral nematic ordering originated from a helical twist located in the effective electric envelope of the ChNC itself, since no inherent chirality or charge distribution is found within the nanocrystals themselves.

Further work from the same group investigated the mechanism of phase separation and self-assembly of ChNCs, as well as the role that electrostatic repulsion plays in the ChNC structure.[113] Through phase diagrams, it was shown that varying the NaCl concentration (and thereby the ionic strength of the medium) did not change the overall phase diagram for concentrated samples of ChNCs, as the contribution of the ChNCs themselves were large. They also reported zeta potential measurements as well as interaction energy calculations that were comparable to theoretical calculations made using Onsager theory.

Based on this framework, Belamie *et al.* further examined the chirality of ChNC suspensions by quantifying nematic properties such as the nematic order parameter and cholesteric pitch.[114] Measurements of the cholesteric pitch as a function of HCl concentration were conducted (Fig. 7) by measuring optical micrographs of the anisotropic phase. From these measurements, it was observed that the liquid-like positional order is stronger at lower ionic strengths, which is very common with electrostatically stabilized colloids. Phase diagrams were also reported with a ChNC concentration range between 1 to 7 wt% and ionic strength ranging between 10^{-5} to 10^{-2} M, which further confirms the experimental results of Marchessault and coworkers that the system exhibits bulk phase separation with a large pH range, but there is minimal contribution to ionic strength.[113]

Polarized optical microscopy (POM) is an extensively-used technique to investigate the optical birefringence typically observed for lyotropic liquid crystalline phases.[115] As seen in work by Liu *et al.*, the optical birefringent patterns of ChNC dispersions appear at 5 wt% concentration in aqueous media (Fig. 8a).[116] Further POM imaging of ChNC suspension droplets in silicone oil (Fig. 8b–e) demonstrated the formation of the cholesteric phase, indicating that self-assembly occurred due to concentric ordering within the droplet surrounded by an oil medium. This feature is similar to the observations made with CNCs.[117]

More recently, Oh *et al.* explored the formation of the chiral nematic phase with ChNFs as opposed to ChNCs.[118] A ''natural'' method was used involving the dispersion of bulk chitin into a Ca–methanol gel, which was then solvent exchanged with other isopropyl alcohol (IPA) and water. While a nematic liquid crystalline phase could be observed after solvent exchange with IPA, a chiral nematic phase formed after solvent exchange with water. The incorporation of Ca^{2+} cations was key during the formation of the chiral nematic phase, likely due to the high binding affinity of Ca on chitin, which can then screen the hydrogen-bonding interactions that make ChNFs aggregate in the bulk form. These gels were then incorporated into an epoxy resin, whereby Young's modulus and toughness tests demonstrated that the ChNF hydrogel featured the highest mechanical durability, likely due to the highly ordered nature of the gel.

Recently, further investigations have been performed in studying how specific fabrication parameters and conditions can affect the self-assembly behaviours of ChNC. These parameters include acid concentration and hydrolysis time during ChNC formation, as well as DDA, pH, and ionic strength conditions when making the liquid crystalline phases. Vignolini and coworkers conducted an in-depth study on these parameters,

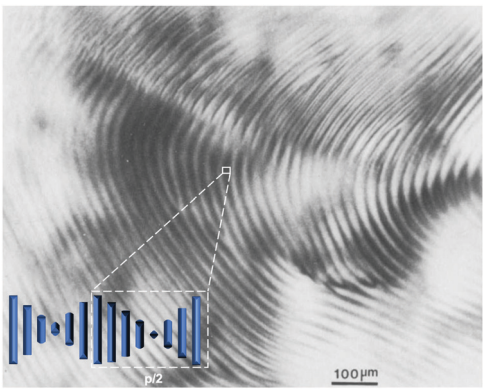

Fig. 6 Optical micrograph (with crossed polars) of the anisotropic phase of a 5 wt% suspension of ChNCs. The fingerprint-like pattern, characteristic of a cholesteric texture, exhibits periodic lines with a spacing of ~30 µm, corresponding to half the cholesteric pitch ($p/2$). Inset depicts a visualisation of how the nanocrystals arrange to produce this pattern, subsequently showing how the spacing depicts $p/2$. Adapted from ref. 38.

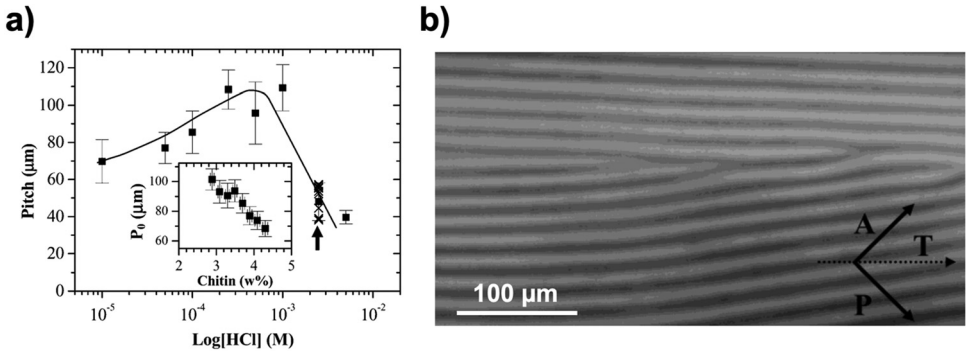

Fig. 7 (a) Variation in the average cholesteric pitch in biphasic samples prepared at different HCl concentrations. Each data point is the average value of data taken along a dilution series in the biphasic domain. The entire set of pitch values is shown for HCl = 2.5×10^{-3} M (crosses). The line represents a visual guide of the trend. The inset shows the evolution of the pitch as a function of chitin concentration for the case where HCl = 10^{-4} M. Every pitch value reported in the graph is an average taken over 10–50 measurements made along the capillary tube axis. The measurements were made through measuring (b) an optical image of the anisotropic phase. The *T* axis depicts the capillary axis. *A* and *P* vectors represent the crossed polars. Adapted from ref. 114.

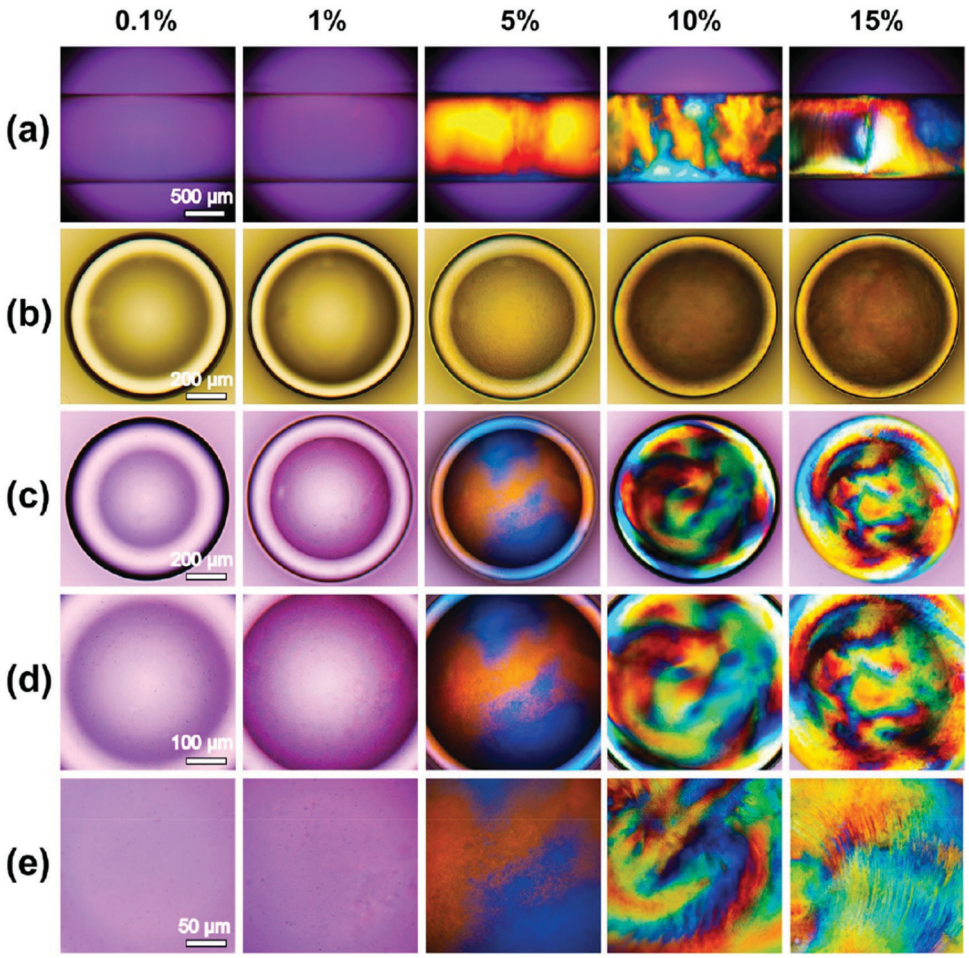

Fig. 8 POM images of different concentrations (top) of ChNC dispersions in (a) capillary form; (b) ordinary light images of the droplets of ChNCs dispersions in silicone oil with different concentrations; (c–e) POM images of the droplets of different concentrations of ChNCs dispersion in silicone oil with varying magnifications. Reproduced with permission from ref. 116.

in which they used ChNC synthesized from the acid hydrolysis of prawn shell chitin.[119] In general, increasing reaction time and concentration of HCl during acid hydrolysis results in smaller ChNCs, which increased the cholesteric pitch of the liquid

crystalline suspension. Further, ultrasonic tip sonication was also a variable, in which larger energy and time spent on tip sonication of the ChNC suspension could break up large bundles present in the suspension. Thus, sonication can induce a smaller twist and higher pitch value. Specifically, they compared using raw chitin (DDA ~ 2%) and partially deacetylated raw chitin (DDA ~ 11%) to produce ChNCs. However, after acid hydrolysis, it was evidenced that the DDA for both synthetic variations of ChNC produced similar values, and that hydrolysis conditions exfoliated the crystalline areas in a way to remove deacetylated portions of the chitin. The main parameter in changing the cholesteric pitch value was the adjustment of ionic strength and pH, producing opposing effects on the self-assembly characteristics. When the HCl concentration was increased while maintaining a similar ionic strength with NaCl, the pitch increased. This relationship was expected due to the repulsive forces involved with the protonation of the few amines present at low pH. When ionic strength is not controlled with increasing HCl concentration, a non-linear trend in pitch emerges: the pitch increases up to a certain peak concentration, and then substantially shortens at elevated HCl concentrations beyond this peak concentration, indicating that ionic strength is the dominant factor in determining pitch rather than the repulsive forces that were previously dominant.

3.1.2. Nanochitosan liquid crystal behaviour. The liquid crystalline behaviour of nanochitosan have been sparsely reported compared to nanochitin, mostly due to the difficulty in fabricating individual ChsNCs (see Section 2.2.2). The loss of crystallinity and shape control involved in the process of deacetylating ChNCs may also explain the difficulties in studying this system. More work in this area will be needed to better understand this system. For instance, how different the interchain hydrogen-bonding strengths may affect cholesteric pitch and order of these ChsNCs, as well as how these come into effect while applying this nanomaterial to various processing technologies. This knowledge will be incredibly useful for future applications of ChsNCs in optoelectronics and liquid-crystalline displays. Factors such as cholesteric pitch and swelling behaviour can directly affect the structural coloration of the nanomaterial.

However, there is one existing report by the group of MacLachlan to organize ChsNFs into a left-handed chiral nematic structure within a hydrogel.[120] The ChsNFs were prepared through sequential soaking of shrimp with acid and alkali baths to remove protein and minerals, and then treated three times with concentrated NaOH at 80 °C. Interestingly, the ChsNFs were then acetylated with acetic anhydride to create a hydrogel with reversible swelling behaviour through water absorption. This swelling substantially increased the thickness of the hydrogel by several-fold, which is reported to be much higher than the pristine ChsNF hydrogel with nematic ordering. Further experiments included the incorporation of a poly(methylmethacrylate) (PMMA) polymer into the acetylated ChsNF matrix increases the response to swelling behaviour as well as mechanical durability. The PMMA–ChsNF hydrogel exhibited varied colours based on the swelling of the gel, as well as retention of the left-handed chiral nematic structure.

3.2. Antibacterial and antioxidant properties

3.2.1. Nanochitin-based antibacterial and antioxidant properties. As it is well established that deacetylation confers improved antibacterial properties to chitin in the bulk phase, the differences in antibacterial properties between varying levels of deacetylation at the nanoscale has been recently studied.[121] In 2019, Xu *et al.* measured the antibacterial properties of ChNCs while varying their DDA values from 16 to 47%.[122] In their study monitoring *E. coli* bacteria growth, they reported that both pH and DDA were important parameters with respect to antibacterial activity, with low pH and high DDA creating the optimal conditions. In both of these parameters, the increase of cationic amino groups was likely the main factor in the inhibition of bacteria growth. The minimum inhibitory concentration (MIC) was used as a general parameter to quantify the activity of antibacterial agents against an organism.[123] It was observed that with increasing DDA, the MIC decreased (Fig. 9a). Further, the MIC decreased with respect to the amount of cationic amino groups found on each sample (Fig. 9b), which was calculated using the DDA value and pH at which the experiment was conducted. Prior to this experiment, it was noted that

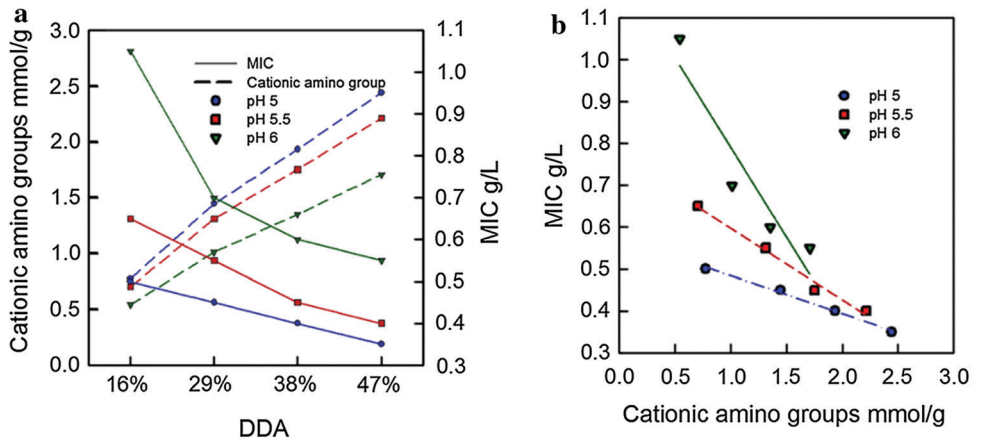

Fig. 9 Minimum inhibitory concentration (MIC) as a function of (a) DDA and (b) quantity of cationic amino groups on the ChNC. Adapted from ref. 122.

positive amino groups can interact electrostatically with the negatively charged microbial membrane in bulk chitosan, promoting leakage of intracellular electrolytes such as potassium, and effectively inhibiting cell growth.[124]

These results are further supported by another study from Oh and coworkers, in which they also demonstrated the importance of the positively charged protonated amino group.[125] Through comparison of as-made partially deacetylated ChNCs with other types of nanochitin material such as ChNF, ChNCs, and carboxylated ChNCs made through TEMPO-mediated oxidation, they showed excellent antibacterial behaviour of the partially deacetylated ChNC based on presence of positive charges.

Much of the literature of the antibacterial properties of ChNCs and ChNFs have been based on blending these nanomaterials with other polymers to make polymer nanocomposite materials. For instance, Shankar *et al.* investigated using ChNCs as nanofillers for carrageenan to create a homogeneous nanocomposite film.[126] In this study, the incorporation of ChNCs promoted antibacterial activity towards *L. monocytogenes* and *E. coli* bacteria. While a clear mechanism for antibacterial behaviour has yet to be proven, the authors suggested a possible pathway in which the ChNFs made the bacteria flocculate, thereby preventing growth through a lack of nutrients and dioxygen.

Copello and co-workers further investigated the use of ChNCs in antimicrobial finishings of textiles.[127] In this case, ChNCs were used primarily for their durability, biocompatibility, and high surface area for methylparaben adsorption, which was the antimicrobial agent of choice. A major challenge with antimicrobial coatings of textiles is leaching during washing cycles (*i.e.*, laundering the textile after use). Controlled release of methylparaben was observed after 20 washing cycles, indicating that the ChNCs embedded in a silica matrix can act to reduce leaching of methylparaben in textiles, thus prolonging the antimicrobial finishing. Further, consistent bacterial reduction for various bacteria strains such as *P. aeruinosa* and *S. aureus* were seen for the composite material, as opposed to control variables without ChNCs (Fig. 10). This demonstrates that ChNCs have enormous potential in antimicrobial coatings, with potential for further development with other systems.

Other applications for antibacterial and antioxidant properties of ChNCs involve food packaging material, where microbial spoilage is a major issue in food quality and preservation.[128] Sun and coworkers demonstrated that, compared to free lysozymes, lysozymes immobilized onto ChNCs can promote antimicrobial activity.[129] This study spurred the possibility of ChNCs as a key nanomaterial for use as an antibacterial agent in food preservation.

3.2.2. Nanochitosan-based antibacterial and antioxidant properties. Although multiple chitosan-based nanomaterials can be fabricated, investigations into antimicrobial activity of ChsNPs appears more than any of the other nanomaterials. A 2004 study by Qi *et al.* evaluated the antibacterial activity of ChsNPs prepared through ionic gelation using TPP anions.[130] The antibacterial assessment was performed in both water and

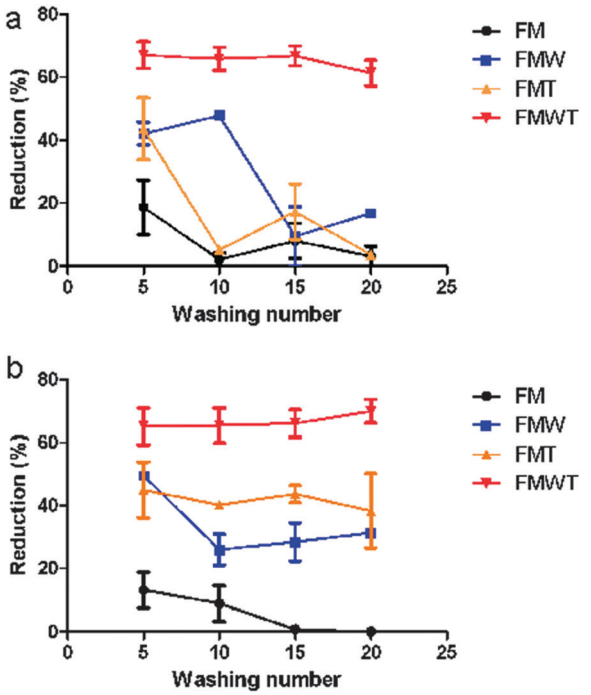

Fig. 10 Bacterial reduction (%) *versus* washing cycle number for (a) *P. aeruginosa* and (b) *S. aureus*. FM = only methylparaben mixed with textile, FMW = methylparaben adsorbed onto ChNC mixed with textile, FMT = FM immersed in mixture of tetraethyl orthosilicate (TEOS) then mixed with textile, FMWT = FMW in mixture of TEOS then mixed with textile. Adapted from ref. 127.

0.25% acetic acid, of which lower antibacterial activity was exhibited in water, as chitosan is less soluble in water. Against *E. coli*, *S. choleraesuis*, *S. typhimurium* and *S. aureus*, both the MIC and MBC (minimum bactericidal concentration) of the ChsNPs were found to be significantly higher than that of bulk chitosan and doxycycline, a common tetracycline antibiotic. By observing bacteria morphology, atomic force microscopy (AFM) showed that *S. cholerasesuis* cells began to fragment after 3 h of ChsNP treatment. The interaction between cationic amino groups and the anionic cell surface was also postulated to be the main mechanism for antimicrobial activity. Therefore, it was subsequently hypothesized that the much greater surface charge density in ChsNPs accounts for their increased interaction with bacteria compared to their bulk counterpart. ChsNPs tightly adsorb onto its target site, the negatively charged plasma membrane, leading to cytosolic leakage.[16,130,131] In fact, Leonida *et al.* found the nano-size dimension of ChsNPs increased chitosan antimicrobial activity by 1.25–4.00 times.[132] Another study by Du *et al.* showed similar results *in vitro*, but further extended this work by loading ChsNPs onto Ag^{+}, Cu^{2+}, Zn^{2+}, Mn^{2+}, and Fe^{2+}, each individually.[133] The antibacterial activity of these metal-chitosan composite nanomaterials was shown to be enhanced compared to bare ChsNPs or metal ions – except for Fe^{2+}. While Ag^{+} ions were shown to exhibit the strongest antibacterial property out of all samples, Cu^{2+} was enhanced by 21–42 times when loaded onto ChsNPs. However, the MIC and MBC values of Ag^{+}–ChsNPs were slightly higher than that

of chlortetracycline, another common tetracycline – implying the antibacterial activity of that novel nanomaterial could not compare to antibiotics already in use for medical treatment. Furthermore, this study found a clear and direct correlation between the ChsNP positive zeta potential and their antibacterial activity – which again led to the hypothesized electrostatic mechanism previously explained. Chang *et al.* also suggested that there could be additional binding between chitosan and teichoic acids, found in mostly Gram-positive bacteria, which led to lipid membrane extraction and thus cell content leakage.[134] Gram-positive bacteria have also been suggested to be particularly vulnerable to ChsNP antibacterial activity, as they lack an outer lipid membrane, and the thick peptidoglycan layer they do possess is in fact weaker towards antibacterial agents.[135]

Due to the water solubility of ChsNPs, Anitha *et al.* further investigated antibacterial activity of chitosan's water-soluble derivatives, *O*-carboxymethyl chitosan (*O*-CMC) and *N*,*O*-carboxymethyl chitosan (*N*,*O*-CMC), in nanoparticle form.[100] *N*,*O*-CMC was found to have the strongest antibacterial effect for its higher degree of carboxymethyl substitution, most likely due to its greater solubility in aqueous media.[136] A study conducted by Xing *et al.* on oleoyl-chitosan nanoparticles (OCNPs) also found that this material exhibited an ability to permeate *E. coli* and *S. aureus* cells, causing pore formation on the cell membrane and the release of intracellular components.[137] Based on this work, OCNP was shown to be a novel antibacterial dispersion system with great potential.

Nanochitosan has also been explored for its antifungal properties. Divya *et al.* found ChsNPs inhibit four different strains of fungi, mostly with increased inhibition rates at higher concentrations (Fig. 11).[138] Its antifungal activity was also shown to be more effective than amphotericin, a common antifungal medication. The group elucidated the antifungal mechanism of ChsNPs through microscopic observation, and concluded that disruption of the cell membrane, and thus cell lysis, was caused by the ChsNP's cationic character, as was explained previously for bacteria. Sathiyabama and Parthasarathy also observed higher antifungal activity for nanochitosan than for bulk chitosan against multiple phytopathogens, and assumed that it is a result of the material's increased permeability towards cell membranes in the nanoscale.[139] The higher zeta potential and lower polydispersity index of the ChsNPs also contributed to the improved stability and effectiveness of its antifungal activity. Furthermore, antifungal properties were also observed in nanochitosan blended with Zn and Cu, along with additional benefits such as enhanced plant defence enzymes.[140] In a biomedical context, Mubarak Ali *et al.* compared the antimicrobial activity of ChsNPs against pathogenic bacteria and fungi and found that *C. albicans* required a higher concentration of the ChNPs for effective fungicidal activity.[141] The thick cell wall was hypothesized to explain this finding, as the complex components can delay or hinder cellular lysis more effectively against the ChsNPs, further supporting the postulated antimicrobial mechanism for ChsNPs.

Nanochitosan's anti-pathogenic properties against bacteria and fungi have been exploited for many agricultural products, including as a coating material for refrigerated fish fillets, as an edible coating for bell pepper, and as a supplement for plant growth and protection – all of which aim to improve or maintain product quality.[140,142,143] The material is also ideal for many biomedical applications. For instance, Ikono *et al.* used ChNPs for inhibition of *S. mutans* and *C. albicans*, the bacterium and fungus responsible for dental caries.[144] Bone cement has also been impregnated with ChNPs as a promising candidate for combating infection from a joint implant.[145]

There have also been many composite materials produced that incorporate nanochitosan, and then applied as antimicrobial agents. For example, Ngo *et al.* observed that pectin:nanochitosan films for functional packaging inhibited growth of spoilage bacteria, fungus, and yeast while also altering water and oxygen permeability.[146] Furthermore, nanochitosan-grafted flocculants were synthesized by Chen *et al.*, and were used to successfully treat low turbidity and salmonella in water and had a superior performance to traditional organic flocculants.[147]

Lastly, nanochitosan has antioxidant activities. Oxidation occurs through the action of highly unstable free radicals, causing chain reactions that can damage living cells in organisms and food product quality. Antioxidant substances inhibit or delay oxidation by quenching environmental free radicals. In 2018, Alboghbeish *et al.* explored the effects of coating

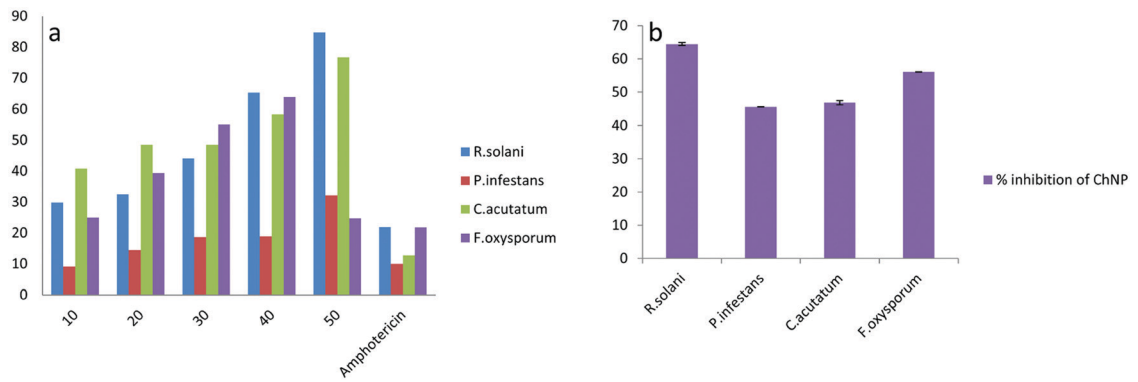

Fig. 11 Percent rate inhibition against four strains of fungi (a) by increasing concentration of ChNP (10–50 mg ml^{-1}) (b) by ChNPs grown in potato dextrose agar. Adapted from ref. 138.

refrigerated fish with chitosan and ChsNPs for storage. 2-Thiobarbituric acid (TBA) reactive substances were used as an indicator for lipid peroxidation through the detection of fat degradation products.[142] Results demonstrated that not only did the ChsNP have stronger antibacterial activity, but it also seemed to effectively protect against lipid oxidation in fish: the concentration of breakdown products was significantly reduced in ChsNP coated samples, compared to bulk chitosan. The group hypothesized that compared to bulk chitosan, the larger surface area per volume in nanoscale chitosan improved the scavenging power for OH radicals, thereby further reducing lipid oxidation. Divya *et al.* and Mohammed *et al.* also observed significant antioxidant activity in ChsNPs with different assays and reached a similar conclusion, with the intent of applying ChsNPs as an edible coating on vegetables to extend shelf-life, displaying favourable properties for the agricultural industry.[34,138] In addition, in a study of ChsNPs synthesized from a fungal enzyme (T-CSNP), their antioxidant activity also appeared promising when evaluated with four different tests, including total antioxidant assay, 2,2-diphenyl-1-picrylhydrazyl (DPPH) radical scavenging, total reducing power and H_2O_2 radical scavenging.[100] A positive correlation was again observed between increasing T-CSNP concentration and antioxidant activity, yet none of the synthesized systems surpassed the positive standard, ascorbic acid.[131] The free-radical scavenging ability of T-CSNPs was attributed to their amine and amino group, which explained why their antioxidant activity is higher than that of TPP-crosslinked ChsNPs.[131] The antioxidant and antimicrobial effect of ChsNPs has also been exploited for biomedical purposes, such as treatment for cutaneous leishmaniasis, a skin lesion caused by a single-celled parasite.[141,148,149]

Overall, the amine group confers to ChsNCs their unique functionalities, which include antibacterial, antifungal, and antioxidant properties, in contrast to un-modified nanocellulose, providing a distinct advantage for nanochitin and nanochitosan to be deployed preferentially in different biological applications, as reviewed in Section 4. As seen in Section 3.2.1, any significant antimicrobial activity for nanochitin was due to partial deacetylation in order to increase the number of amines groups on the surface of the nanomaterial. Scheme 4 summarizes the trends in functional properties of all nanochitin and nanochitosan recently reported in the literature, along with the bacteria strains that were studied.

3.3. Thermal and mechanical properties

In this section, the thermal and mechanical properties of nanochitin and nanochitosan are explored. In much of the literature, thermal and mechanical properties are investigated in the context of a composite material.

3.3.1. Nanochitin thermal and mechanical properties. While much of the literature is that of composite materials, there is one report by Tran *et al.* where various types of nanochitin thermal degradation properties were assessed.[125] ChNFs, ChNCs, and carboxylated ChNCs were among the ones tested, where their respective temperatures where 5 wt% of the initial mass degraded (T_{d5}) were 301 °C, 277 °C, and 256 °C, respectively. Compared to the T_{d5} of bulk chitin of 285 °C, thermal stability of chitin decreases when it is transformed into ChNCs, while slightly increasing when made into ChNFs. Comparing these values with the T_{d5} of CNCs (250 °C), it could be seen that nanochitin materials have higher thermal stability than nanocellulose, outlining the potential for such materials as better nanofillers for material composites.[150]

Initial tests using ChNC-incorporated composites as thermoplastics were done by Paillet and Dufresne in 2001.[57] They fabricated a nanocomposite film of latex mixed with colloidal ChNCs, with a weight fraction of ChNCs between 0–20%. No noticeable effect on the shear modulus was observed for temperatures below the glass transition temperature (T_g). However, above T_g, the relaxed modulus increased by 160 times with 10 wt% (w/w) ChNC. The authors attributed this finding to the high aspect ratio of the ChNC.

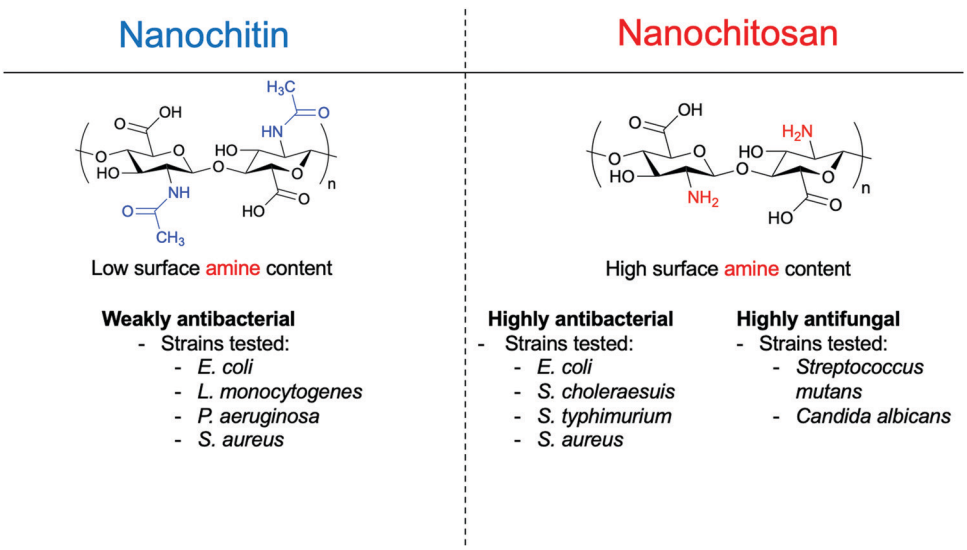

Scheme 4 Summary of the antibacterial properties and the bacteria strains used for nanochitin and nanochitosan-based systems.

ChNCs have also been incorporated into hydrogels for use as cell scaffolds and drug delivery vehicles as studied by Chen and coworkers[151] Specifically, injectable hydrogels have received a lot of attention as a tool for the creation of tissue scaffolds as they can successfully offset the need for surgeries.[152] To this end, hydrogels featuring high tensile strength and elastic modulus are in high demand.[153] This study found that with 5% (w/w) incorporation of ChNCs into a beta-glycerophosphate-based hydrogel, gelation time of the hydrogel decreased from 6038 s to 25 s. Furthermore, the same study also observed increased mechanical durability for the hydrogels. The authors attributed these remarkable mechanical enhancements to the hydrogen bonding interactions between the glycerophosphate hydrogel and ChNC. Drug release behaviour of this hydrogel composite has also been studied, with *in vitro* acetylsalicylic acid (ASA) release done as the model test. With the incorporation of ChNCs, there was a much slower release of ASA likely due to the much greater crosslinking densities of the hydrogel nanocomposite. Similar results were found by Pang *et al.* while using ChNCs as an additive for a chitosan/dextran-based hydrogel, including shortened gelation time, increased compressive stress, as well as higher bonding strength to tissues, indicating a potential application in tissue adhesives.[74] Other properties that can seemingly be enhanced by ChNCs have been demonstrated in the work of Xiong and coworkers in which gelation temperature, as well as salt and pH resistance, was increased for the ChNC enhanced gelatin.[73]

ChNCs can also be chemically modified using available functional groups to support other substrates. Gu and co-workers described a process in which poly(3-hydroxybutyrate-*co*-3-hydroxyvalerate) (PHBV) can be grafted onto ChNCs *via* chlorination. The polymeric ends of PHBV are chlorinated with thionyl chloride before covalently bonded to the ChNCs through the hydroxyl group. The authors reported higher melting point temperatures for ChNC-incorporated PHBV nanocomposites compared to the native PHBV. In these examples, ChNCs were able to afford the desired heightened mechanical durability due to their high aspect ratio (similar to CNCs), as well as the tuneable handle of both their acetamide and amine functionalities.

Aside from mechanical tests, the thermal parameters of these nanomaterials have also been reported. These properties include thermal expansion determined using a thermomechanical analyser, onset and peak temperature determined using differential scanning calorimetry, and thermal stability profiles determined using thermogravimetric analysis (TGA). Thermal properties are very important in applications where a material needs to be very resistant to degradation at high temperatures, such as food packaging films. Qin *et al.* incorporated ChNCs of up to 5 wt% into maize starch films and saw an overall increase in both onset temperature and peak temperature, showing an optimal ChNC loading of 0.5 wt% with respect to the maize film.[72] Interestingly, TGA measurements showed that the maximum degradation temperature decreased with incorporation of ChNCs into the films, which the authors attributed to the decreased flexibility of the amylopectin chains in starches with ChNCs as a filler.

The mechanical durability of ChNFs have also been reported and tested for a variety of applications by Ifuku *et al.*[154] A ChNF–(meth)acrylic resin nanocomposite film was created that was optically transparent (Fig. 12a) and exhibited good tensile strength of at least 30 MPa, depending on the type of resin used. With the inclusion of ChNF within the (meth)acrylic resin, the film's Young's modulus increased by up to 3.0 GPa, as seen in Fig. 12b. Fan *et al.* also observed this finding with ChNC–poly(lactic acid) (PLA) films as the thermal degradation point decreased with respect to bulk α-chitin.[155] In general, this is to be expected since the nanoscale structure of ChNCs, along with all other types of nanochitin and nanochitosan, confers higher surface area, and therefore a lower threshold for withstanding higher temperature. Similar results have also been reported by Salaberria *et al.* by incorporating ChNCs into a starch-based thermoplastic[156] and for CNC composites as well.[157,158]

Gelatin-based nanocomposites were also reported to be reinforced by ChNFs. For instance, Rolandi and coworkers demonstrated that the incorporation of ChNFs within gelatin methacryloyl increased the hydrogel elastic modulus 1000-fold, while also increasing stress-to-strain failure by more than 200%.[159]

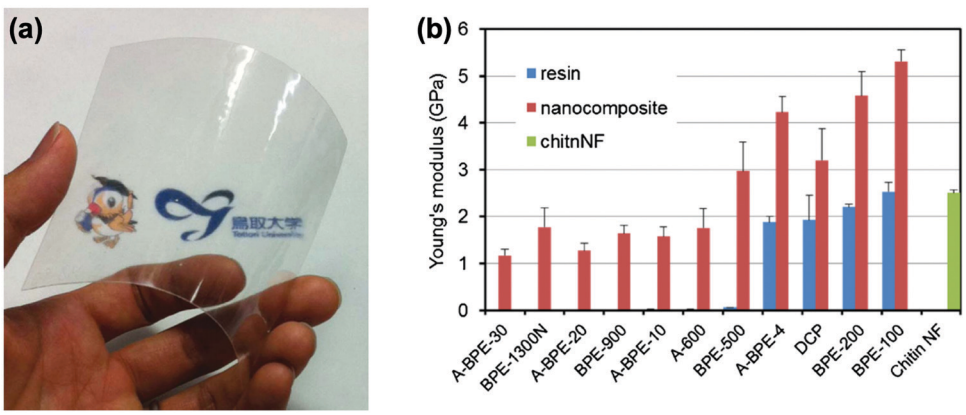

Fig. 12 (a) Photo of Tricyclodecanedimethanoldimethacrylate (DCP) film with ChNF; (b) Young's modulus of various meth(acrylic)–ChNF films and their nanocomposites. Error bars show standard deviation. Adapted from ref. 154.

Surface deacetylation of the ChNFs were observed to be an important parameter, as Li and co-workers had demonstrated using ChNFs with surface deacetylation to produce gelatin-based nanocomposites.[160] Namely, the Young's modulus of the surface-deacetylated ChNF-containing gelatin increased 2.5-fold compared to gelatin on its own. Neat ChNFs that did not undergo a deacetylation treatment showed less pronounced results than the surface-deacetylated ChNFs. The authors suggested that improved hydrogen bonding from the amines played an important role in increasing the tensile strength of the nanocomposite.

ChNFs have also been directly applied to enhance CNC-based films used for packaging materials. The group of Meredith have shown that the incorporation of ChNFs into CNC-based films can greatly augment the film's ultimate tensile strength (UTS), with a 1 : 3 ratio of CNC : ChNF being the optimum conditions.[161] Interestingly, even though the mixed CNC/ChNF film performed the best, a film based only on ChNF demonstrated only slightly lower UTS results. Furthermore, authors also reported that lower acetylation of the ChNF (*i.e.*, more amines instead of acetamides) provided better results for both UTS and breaking strain. These results indicated that the positive electrostatic charge of the low acetylation ChNF can enhance aggregation with the negative charge of the CNC, therefore creating a much more compact film. Another study from the same group further validated the enhancement that ChNFs provided to CNC-based films through O_2 permeability tests, in which the combination of ChNF and CNC layers could provide much less O_2 permeability for use as barrier materials for food packaging.[162]

The coefficient of thermal expansion was also analysed for ChNF-containing nanocomposites, which typically possess an inverse relationship with the Young's modulus of a material. Ifuku *et al.* reported a decrease in the coefficient of thermal expansion with the incorporation of ChNFs into chitosan-based films, which is an improvement from neat chitosan films.[163] This was further validated by the same group with the incorporation of glycerol in a ChNF-based film.[164] This improvement was in contrast to the previously noted negative performance for ChNC-incorporated polymeric films. A direct comparison between ChNF and ChNCs was made by Salaberria *et al.*, in which the authors realized an increase in the thermal degradation temperature in a starch-based nanocomposite with ChNFs as nano-fillers, while a decrease occurred when using ChNCs.[156] They hypothesized that the as-made ChNFs contained more amino groups that can interact with the hydroxyl groups of the starch matrix, along with the minor accumulation of glycerol due to its web-like morphology.

Aside from ChNF–polymer composites, Nam *et al.* measured the thermal degradation behaviour of ChNFs with varying DDA values, and observed a decrease in the maximum degradation temperature of ChNFs with respect to bulk chitin.[165] Furthermore, they noticed that with increasing DDA value, the maximum degradation temperature decreased. The authors attributed this finding to the lower crystallinity for the ChNFs at higher DDA.

3.3.2. Nanochitosan thermal and mechanical properties. Nanochitosan have been reported to enhance mechanical properties of polymer-based nanocomposites and films. For example, Rachtanapun and coworkers described using ChsNPs to reinforce pectin-based films.[146] With the incorporation of ChsNPs, the film was found to have increased tensile strength, along with decreased water vapor and oxygen permeability. Other reports utilized ChsNPs as a reinforcement in glass-ionomer cements (GICs) for use as dental restorative materials.[166] Incorporation of ChsNPs into conventional GICs *via* mixing increased tensile strength by 70 MPa, compared to the maximum tensile strength of 110 MPa of the conventional GIC.

In general, the thermal stability of ChsNPs has been observed to decrease with respect to bulk chitosan, similar to that of ChNCs. For instance, Sivakami *et al.* reported a decrease in thermal stability of ChsNP made using ionic gelation compared to bulk chitosan.[167] Furthermore, Shajan and coworkers also indicated that the addition of ChsNPs decreased the thermal stability of a plasticized polymer nanocomposite electrolyte based on poly(ethylene oxide) for application in lithium ion batteries.[168] Indeed, as more developments in the field of nanochitosan are made, much more analysis and determination of these fundamental physical properties must be assessed and understood.

3.4. Life cycle assessment and biodegradation

In addition to physical, chemical, biological and self-assembly properties described in the previous sections, nanomaterials made from polysaccharides feature the distinct advantage to align with the principles of green chemistry and sustainability.[169] Utilizing biomass and especially biomass waste as a source for accessing functional nanomaterials is an attractive feature of nanochitin and nanochitosan in considering their downstream applications.[170] The life cycle assessment (LCA) of a material details a ''cradle-to-grave'' scenario for these new nanomaterials, quantifying details such as material extraction, processing, manufacturing, distribution, use and maintenance, recycling, and disposal.[171] Currently most processes for producing nanochitin and nanochitosan are at low technology readiness levels (TRLs), and as a result, no in-depth LCA studies have been performed on them yet. However, there have been some studies into closely related materials that could be serve as guides for future investigations. For example, one recent review highlights the efforts in addressing LCA on the field of nanocellulose[172] while another recent review highlights the LCA of bulk chitosan production.[173] Indeed, LCA studies will be crucial in identifying and alleviating the environmental impact on the processing of these nanomaterials as they approach higher TRL associated with commercialization. Thus, a sustainable pathway to an efficient shell bioeconomy will require more than an environmental assessment. There is the need to evaluate the sustainability of industry-standard processing technologies that may use decision support tools, low-carbon procurement tools, and frameworks for monetizing undervalued streams through economic assessment.[174] More important is the understanding and evaluating of trade-offs

among product quality and functionality, technical efficiency, and techno-economic viability.

On a similar vein to LCA, biodegradation is a characteristic that is often touted for materials made from polysaccharides.[175] While bulk chitin and chitosan have been tested for biodegradation in soil, nanochitin and nanochitosan studies have not yet been reported.[176] The impacts of their end of life treatment, handling, and performance in various environments also needs to be understood and mitigated in order to realize a net environmental benefit and enable a circular shell bioeconomy. Thus, following the framework of research that led to the development and commercialization of nanocellulose-based materials, we believe it is imperative that this gap in the literature must be filled in order to move forward in making materials sustainably as well as maintaining commercial value.

4. Applications of nanoscale chitin and chitosan

The attractive properties of nanoscale chitin and chitosan, as described in detail in Section 3, have led to their use in a multitude of applications within the last two decades. In this section, we will provide an in-depth discussion of the research sectors actively using nanoscale chitin and chitosan, and the relationship between these applications and the unique properties listed above. Particularly, the wide area of biomedical applications will be split into drug delivery, medical devices, and other applications that have been lesser reported such as cosmetology, textile coatings, and filtration devices. Agricultural applications including plant growth and food packaging will also be included, along with a section on catalysis, which is at its infancy and has huge potential in sprouting into a large field.

4.1. Biomedical applications

Both chitin and chitosan have been extensively studied at both the bulk and nanoscale in biomedical applications, thanks to their abundance, low-cost, and antibacterial and biocompatible properties. Biomedical applications have been divided into three main categories: (1) drug delivery, (2) medical devices, and (3) other miscellaneous applications. Drug delivery includes studies involving encapsulation, release, and targeting. Medical devices will incorporate aspects such as tissue engineering applications for bone scaffolding, wound healing in bandaging and suture applications, and dental devices. Finally, miscellaneous applications will include unique works that are not covered in the previous two sections such as cosmetology, textile coatings, among other fascinating functions.

4.1.1. Drug delivery. Similar to nanocellulose, there are many reports that describe the use of chitinous nanomaterials for drug delivery applications. Due to their high solubility, along with the nitrogen functional handle to coordinate with various pharmaceutical molecules, extensive reviews have been written that describe the use of bulk/nanoscale chitin and chitosan.[86,177–179] It should be noted that nanocomposite materials that use bulk chitosan or chitin as a coating or as a nanofiller without directly converting to the nanoscale first will not be covered, and instead we would like to direct the reader to a number of excellent reviews.[180–184] For example, this includes magnetically targeted NPs in which chitosan was used to coat magnetic NPs.[185–189] Furthermore, a huge focus in this section is based on utilizing ChsNPs in particular, a subject of a number of reviews that document their successful use in encapsulating a diverse subset of small molecule drugs.[190–192] ChsNPs are the dominant nanomaterial of choice for drug encapsulation, as it possess the following desirable traits: high biocompatibility, high stability, and low toxicity properties, along with being very easy to synthesize using ionotropic gelation.[193] With this in mind, this section will focus on covering the most recent advancements in the field, exploring the advantages in using nano-chitin and -chitosan, while also giving a brief overview on some of the current challenges to their applications.

Table 3 lists the variety of drugs that currently use nanochitin- and chitosan-based delivery systems. This list is only a representative portion of the amount of literature found for using chitin- and chitosan-based nanomaterials in drug delivery with the oldest being from 2012.

In order to move away from molecular target therapy which focuses on a specific kinase or receptor within cancer cells, much of the research for ChsNP relies on the enhanced permeability and retention (EPR) effect, coined by Matsumura *et al.*[214] The EPR effect relies on the fact that many solid tumours have defect sites located in their blood vessels. These defect sites produce vascular permeability factors such that large macromolecules will accumulate in tumour tissues, passing through the tumour blood vessels instead of the normal blood vessels.[215,216] Fang and coworkers utilized this effect when fabricating ChsNPs with biotin, a substance known to enhance binding of macromolecules to tumour cells.[209,217] This material was then loaded with bufalin, a candidate drug for cancer chemotherapy. Bufalin induces cell arrest and apoptosis in many cancer cells, yet it also has the central problem of all chemotherapeutic agents: the severe toxic effect it has on cells across the entire body.[218] This application makes selective targeting especially important, which can be achieved by a dual-targeting mechanism of the EPR effect of the ChsNPs, as well as selectively binding to tumour cells that express biotin receptors. The biotin–ChsNP material loaded with bufalin demonstrated much higher cytotoxicity to MCF-7 cells, as well as improved therapeutic effects in a human MCF-7 breast cancer nude mice model.

Co-encapsulation is also possible with ChsNPs, as reported by Deng *et al.* with the loading of doxorubicin and microRNA-34a (miR-34a) into ChsNPs made *via* ionic gelation with hyaluronic acid and TPP (Fig. 13).[40] An important factor in this dual loading capability is the oppositely charged nature of doxorubicin (DOX), which is positive, and miR-34a, which is negative, which can electrostatically bind to each other within the ChsNP–TPP matrix. Another notable factor is that hyaluronic acid is also known to bind to the CD44 molecule on

Table 3 A representative list of various small molecules that have been encapsulated by nanochitin- and nanochitosan-based drug delivery carriers

Nanomaterial	Type of drug encapsulated	Application of drug	Ref.
ChsNP *via* ionic gelation	Ellagic acid	Anticancer	194
ChsNP *via* ionic gelation	Lansoprazole	Antiulcer	195
ChsNP on polycaprolactone nanofibers	Ferulic acid and resveratrol	Non-melanoma skin cancer	196
ChsNP *via* ionic gelation	Chlorogenic acid	Antioxidant/anticancer	197
Quaternary ammonium palmitoyl glycol ChsNPs	Leucine–enkaphaline peptide	Anticancer	198
ChsNPs with hyaluronic acid	Curcuminoid	Anticancer	199
ChsNP *via* ionic gelation	Jasmine oil	Anticancer	200
ChsNP *via* ionic gelation	Recombinant antigens rEIT and rStx2B	*E. coli* vaccine candidate	201
ChsNP *via* filtration	Plasmid DNA vaccine	Swine flu vaccine	202
Thiolated ChsNP	Insulin	Oral delivery of insulin	203
ChsNP *via* ionic gelation	Eugenol	Rheumatoid arthritis	204
Carboxymethyl chitosan and ChsNP	Doxorubicin	Colorectal cancer therapy	205
ChsNP *via* succinic anhydride	Herceptin targeted antibody and doxorubicin	Breast cancer	206
ChsNP *via* ionic gelation	Curcumin with epidermal growth factor conjugation	Anticancer	207
ChsNP with EGFR antibody shell	Curcuminoids	Anticancer	208
Biotin-conjugated ChsNP	Bufalin	Anticancer	209
ChsNP *via* ionic gelation	IL-2	Colorectal cancer	210
Cetuximab-conjugated ChsNP	Paclitaxel	Anticancer	211
ChsNP with hyaluronic acid	MiR-34a and doxorubicin	Breast cancer	40
cm-ChNPs	5-Fluorouracil	Anticancer	86
Poly(lactic acid)–Chs NP composite	Lamivudine	Anti-HIV	212
ChNC–glutaraldehyde gel	Circumin loaded with Tween 20 surfactant	Anticancer	213

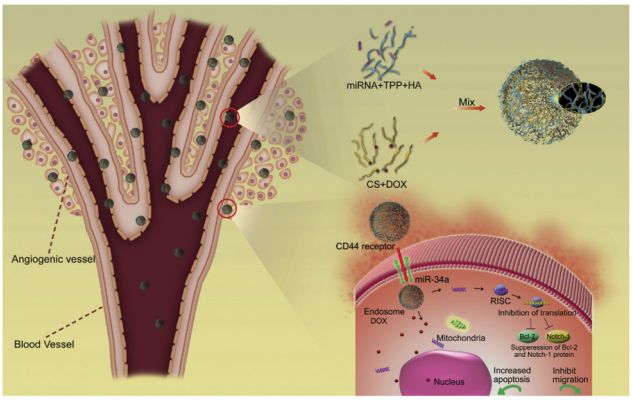

Fig. 13 Schematic illustration of the construction of ChsNPs made from chitosan (CS) and ionic gelation with hyaluronic acid (HA) and TPP (top right in the figure) for the simultaneous co-delivery of DOX and miR-34a to MDA-MB-231 human breast cancer cells for enhanced anti-cancer effects. Retrieved from ref. 40.

the MDA-MB-231 breast cancer cells, making it another ideal candidate in creating targeted drug therapeutics.[219] Fig. 13 depicts the process of how the ChsNPs loaded with DOX and miR-34a are delivered into tumour cells directed by the CD44 receptor.

As opposed to using only one form of chitosan for ionic gelation to form ChsNPs, Feng *et al.* implemented the use of both carboxymethyl (CM)-chitosan and "pure" chitosan to form a NP through electrostatic interactions between the positively charged chitosan and negatively charged CM-chitosan.[205] Furthermore, CM-chitosan has higher aqueous solubility than chitosan, along with having a higher chance of binding Ca^{2+}, increasing parallular permeability of the epithelium.[220] Thus, CM-chitosan provides a unique access to higher solubility as well as chelating ability in NP form. The group reported a surface charge effect of loading DOX, with the positively charged CM-chitosan/pure-chitosan NP cross-linked with TPP outcompeting the negatively charged CM-chitosan/pure-chitosan NP cross-linked with Ca^{2+}, with the former achieving enhanced cellular uptake.

Among other applications for ChsNPs in drug delivery, a wide breadth of literature exists for DNA conjugated ChsNPs as well as gene therapy, on which an excellent review was written.[221] Further, other types of nanochitosan such as ChsNFs acquired from electrospinning have also received some attention in drug delivery, which has been highlighted in a recent review.[222]

To a lesser extent, nanochitin has also been explored for use in drug delivery. Jayakumar and coworkers fabricated magnetic CM–ChNPs crosslinked with $CaCl_2$ and $FeCl_3$ for *in vitro* delivery of 5-fluorouricil.[86] This system combined the drug delivery capabilities of ChNPs with potential drug-tracking potential due to its magnetic nature, with sustained and controlled drug release as well as enhanced toxicity with KB cells. In an effort to increase mechanical durability of hydrogel for drug delivery and prolong the sustained release of the loaded drugs, ChNCs have been incorporated into the hydrogel itself. The first report of ChNC usage was claimed by Liu and coworkers in 2018, in which they used ChNCs as a cross-linker with glutaraldehyde to form a hydrogel drug carrier for the incorporation of Tween-20 loaded curcumin.[213] Improved stiffness as well as mechanical strength of the hydrogel was observed. They also proposed hydrogen-bond interactions between curcumin and the hydrogel itself which enabled its prolonged release in phosphate-buffered saline (PBS). Yet, a direct mechanism for such a release was not proposed. Additional work has also been done on reinforcing alginate-based hydrogels reported by Petrova *et al.*,[223] as well as reinforcing a chitosan/β-glycerophosphate injectable hydrogel done

by Wang *et al.*[151] The use of ChNCs conferred high mechanical durability to the materials, thanks to the highly crystalline nature of nanochitin, while ChsNPs' amorphous nature afforded a loose structure conducive to high drug loading and sustainable release. Due to the high crystalline nature of ChNCs relative to other types of nanochitin, it is the ideal nanofiller for strengthening other composites in drug delivery vehicles.

Importantly, chitosan is one of the major polysaccharides used in current research, with ChsNPs being at the forefront of nanomedicinal efforts.

Indeed, there is still huge potential in advancing this field, as many aspects such as direct functionalization of ChsNPs or ChNCs have not been done. More specifically, thorough in-depth surface characterizations are needed for synthesized ChsNPs to determine factors such as DDA and surface functional groups and how they affect both binding and release capabilities of the drug within ChsNPs. As for the use of ChNCs as a mechanical filler for the reinforcement of gel-like systems, a molecular-level guide on how these nanomaterials behave within these gels must be characterized to its fullest extent. Importantly, the advantages of using ChsNCs which combine aspects of mechanical filler reinforcement as well as the primary amine group for drug binding can be a distinct avenue for future research.

4.1.2. Wound healing and tissue engineering. The use of bulk chitin and chitosan in wound-healing has been extensively highlighted in several reviews.[224–228] In fact, this research has been extended into the nanoscale, as there is strong evidence for further improved properties that make the material even better suited for some applications. ChNCs have been used as "nanofillers," or nanoscale substituents into bulk composites to increase mechanical durability (Section 3.1). Tissue adhesion is one area of research that can also exploit the biocompatibility and mechanical durability of ChNCs. For instance, Xu *et al.* created a nanocomposite adhesive based on a mussel-inspired citrate-based adhesive, POEC-d.[229] This nanocomposite is made from a one-pot polycondensation of citric acid, 1,8-octanediol, and dopamine. With the inclusion of 15 wt% (w/w) ChNCs into the POEC-d adhesive, both the tensile strength and tensile modulus increased by an order of magnitude. Further, increased adhesion strength from lap-shear measurements were also seen with ChNC incorporation (Fig. 14a). With increased ChNC loading, greater shear strength was observed (Fig. 14b). The authors proposed that the ChNC's high tensile strength enabled strengthened cohesion capacity, thereby leading to increased macroscopic adhesion capability (Fig. 14c). ChNCs can improve adhesion strength of certain adhesives, which warrants further study for application as a wound-healing substituent.

Electrospinning is an effective and simple technique for the fabrication of nanofibers from polymers for wound healing.[226] The ultrafine fiber webs formed with this technique allows for good absorption of wound exudates, prevention of dehydration and infection, gas permeability, and a sustained release of loaded drug, making this technology highly suitable for wounded tissue regeneration.[224] While both chitin- and chitosan-based nanomaterials have both been used for wound healing applications, the latter has seen more use due to its higher solubility. Naseri *et al.* developed a crosslinked nanocomposite fiber mat based on chitosan and polyethylene oxide for wound dressing that is also reinforced with 50 wt% ChNCs.[230] This mechanically and thermally strong material also had relatively low water vapor transmission rates (WVTR), controlling water loss while considering the accumulation of exudates from the wound. Besides physical reinforcement, it was hypothesized that the ChNCs improved susceptibility to lysozyme, as the breakdown product of chitin into chitooligomers stimulated macrophage activity and collagen deposition, and thus the entire process of wound healing improved.[66,225] This demonstrates the unique capabilities of ChNCs that other systems would not have, including that of nanocellulose. Fibroblast action and proliferation of injured tissues was also stimulated with wound treated with nanofibrous membranes, due to the high surface area and porosity of the electrospun nanomaterial which simulates the natural extracellular matrix.[230,231] Nanofibrous membranes based on collagen, chitosan, and

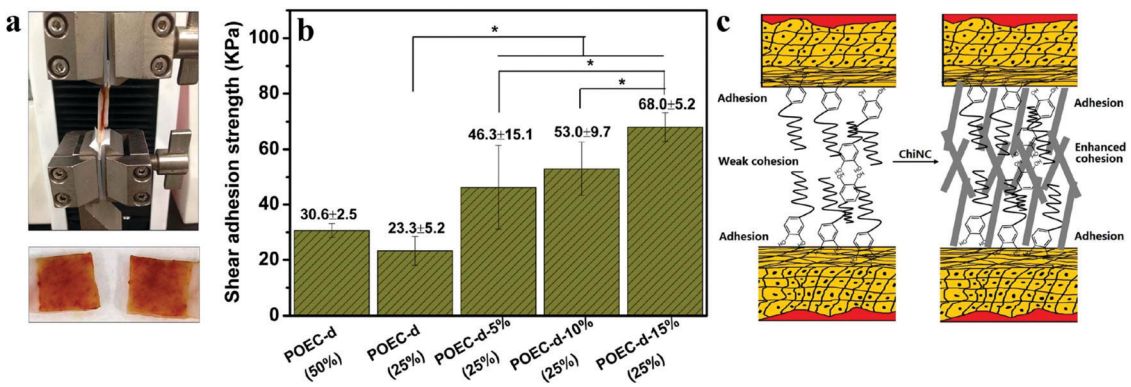

Fig. 14 (a) Image of lap-shear measurement set-up (top) and two pieces of adhered porcine skins after tensile breaking; (b) the lap-shear adhesion strength using wet porcine as the adherent. POEC-d (50%) and POEC-d (25%) are the catechol-based adhesive with aqueous weight concentration in water in brackets. POEC-d-5%, POEC-d-10%, and POEC-d-15% are the POEC-d adhesives with 5, 10 and 15% (w/w) ChNCs with respect to POEC-d. (c) Proposed mechanism of heightened adhesion caused by addition of ChNC. (*$p < 0.05$). Adapted from ref. 229.

polyethylene oxide fabricated by Chen *et al.* also showed similar beneficial effects for wound healing, and authors observed that the nanofibrous membranes reduced wound area faster than traditional gauze and commercial collagen sponges in animal studies.[232]

This accelerated healing demonstrated that the biomaterial promoted the growth of skin tissues in a comparable way to commercial products. Izumi *et al.* also explored using deacetylated ChNFs on wound healing, although they did not use the electrospinning process.[233] The group discovered that much greater fibroblast and collagen proliferation and re-epithelium was induced by the surface-deacetylated ChNFs in a circular excision wound model compared to bulk chitin, ChNFs, and ChsNFs.

In terms of chitosan-based nanomaterials, one study evaluated the healing efficiency of electrospun, chitosan-blend nano-Bioglass through acute skin trauma in rats and diabetic chronic wounds in mice.[234] Accelerated wound healing, complete re-epithelialization, collagen deposition and alignment, and regeneration of skin appendages were observed *in vivo*. The complex and synergistic effect that the chitosan-based nanomaterial exerted at different stages of healing are presented in Fig. 15.[232]

Kossovich *et al.* also found electrospun ChsNFs to be effective for treating burn wounds, most of which are often quite severe, as they involve large skin surface areas and thus have the potential to be lethal.[235] As reviewed by Jayakumar *et al.*, the material seemed to address many crucial aspects of wound healing, including moisture control, wound ventilation, protection from infection, stimulation of tissue regeneration, and degradation of material to minimize mechanical damage.[225] Many other chitosan–blend nanofibers produced by electrospinning have also been explored and found to be effective for the purpose of wound healing and skin cell proliferation, such as with silk fibroin,[236] poly(ethylene oxide),[237] poly(vinyl alcohol),[225,238,239] polyaniline,[240] and gelatin.[241]

Besides nanofiber mats, other forms of nanoscale chitin and chitosan-based wound dressings have also been explored including hydrogels, sprays, films, and sponges.[224,242] For example, Guo *et al.* constructed ChNP-based hydrogels through electro-assembly to be dried into porous and tough aerogels. The observed effects of the aerogel on wound healing *in vivo* included acceleration of macrophage migration, and promotion of granulation and vascularization.[243] Mattioli-Belmonte compared the effectiveness of ChNF/chitosan glycolate-based material of wound healing in the form of a spray, gel, and gauze to find that each form provided optimal treatment effects for different types of wounds.[242]

Similar to epithelial tissue regeneration, chitin-based nanomaterials have also been explored as support for various disease treatments through regenerative medicine. Much work has been done in the use of hydrogels to produce cartilage tissue,[244] bone tissue,[245–248] tracheal tissue,[249] liver tissue,[87] and myocardial tissue, which is usually non-proliferative.[250] The fabricated hydrogel or scaffolding material is often intended to mimic the corresponding extracellular matrix and specific environment

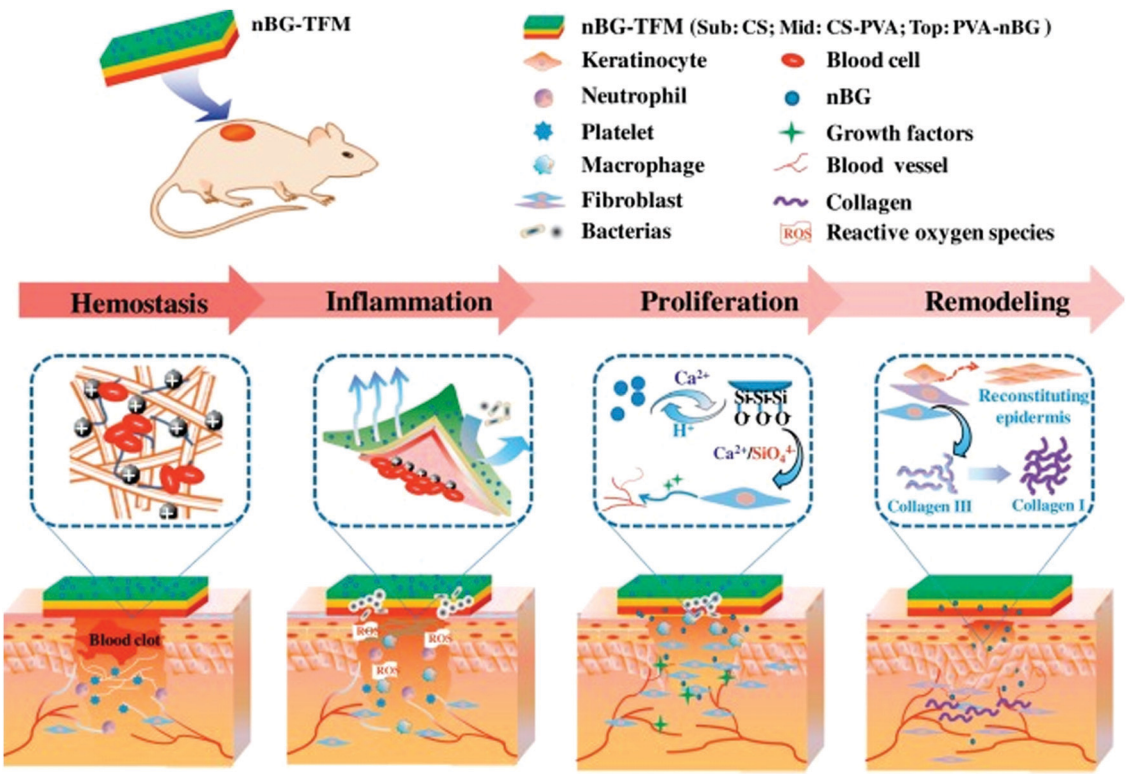

Fig. 15 Mechanism of chitosan-blend nanomaterial at different stages of wound healing leading to accelerated and enhanced wound healing. Adapted from ref. 234.

of the tissue of interest, thus supporting cell proliferation for functional medical purposes.

Based on current literature, it appears that the use of ChsNPs in bone regeneration is relatively more developed than in other areas of regenerative medicine.[251] In fact, Tao *et al.* specifically reviewed bone regeneration applications using nanofibers based on chitin and chitosan.[252] For example, Sedghi *et al.* used the MTT assay, an *in vitro* cell viability test, to find their non-cytotoxic, antibacterial PCL-chitosan/magnesium-hydroxyaptite electrospun nanofiber scaffolds proliferated osteoblast cells at a higher rate compared to the control with no nanofiber scaffolds.[246] Some studies have also addressed the regeneration of cartilage tissues relevant to the treatment of osteoarthritis.[244] As bone regeneration is a main constraint for bone grafting during surgery for bone conditions, this novel, tuneable technology can potentially remove this large limitation.[253]

4.1.3. Cosmetology. Some properties of chitin-based nanomaterials were also shown to be applicable to cosmeceutical functions. Bulk chitin, chitosan, and their derivatives are ideal ingredients for use in the cosmetic industry with beneficial antimicrobial and antioxidant properties.[254,255] Morganti and Morganti discussed how chitin nanofibrils could be applied to cosmetic dermatology.[256] Chitin nanofibrils can be a suitable and active ingredient to protect and restore skin barrier integrity because they can regulate collagen synthesis, capture active ingredients, neutralize free radicals, and retain water in the skin matrix. Morganti *et al.* developed a medical device in an injectable form based on ChNFs, phosphatidylcholine, and hyaluronan to entrap active nutrients, and successfully demonstrated its efficiency in reducing skin wrinkling and signs of aging in photoaged subjects (Fig. 16).[257] The treatment significantly increased fibroblast activity, type-1 collagen synthesis, and ATP activity of keratinocytes *in vitro*, which are the main causes of skin aging.

Out of all derivatives, the results of carboxymethyl caproyl chitosan seem to be especially remarkable as they can form nano-network or nanospheres self-assemblies with strong antioxidant and antibacterial activity and good water retention properties.[254] Jimtaisong *et al.* summarized five major functions for the material to be applied to the cosmetic dermatology: moisture retention, antimicrobial and antioxidant activity, delivery system and natural-derived emulsion stabilizer.[258] In the work of Anitha *et al.*, their carboxymethyl ChsNPs (80–100 nm in diameter) also exhibited stronger antibacterial activity against *S. aureus* compared to ChsNPs.[100] Considering the applicability and versatility of CNCs currently being researched for cosmeceutical applications, nanochitin and nanochitosan have high potential for being used commercially with further research.[259,260]

4.1.4. Antibacterial finishings. Due to their antibacterial properties, nanochitin and nanochitosan there have been some early reports in using them as part of antibacterial finishings for fabrics and textiles. Shirvan *et al.* fabricated ChsNPs on woven cotton fabric with a "layer-by-layer self-assembly" method.[261] Besides the additional antibacterial properties observed with increasing amount of layers, the water drop spreading time, contact angle, and decrease in a whiteness index also had a direct correlation with the number of layers. Villanueva *et al.* enhanced the antimicrobial effect by encapsulating methylparaben in ChNCs to be incorporated into the textile, to provide a more gradual and controlled release of antibiotics.[127] The group assessed the antimicrobial efficiency by quantifying the methylparaben leaching concentration through HPLC, and confirmed that the antimicrobial effect of the textile is laundry-durable for at least 20 washes.

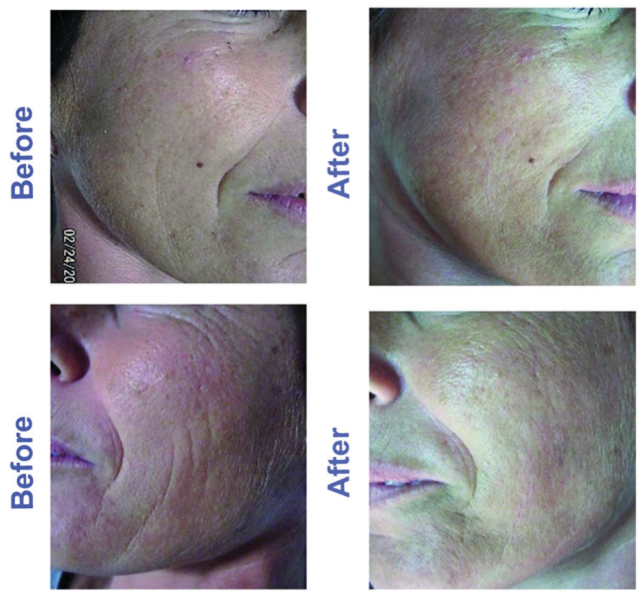

Fig. 16 Changes in skin appearance of subjects before and after *in vivo* treatment of nanocomposite injection. Adapted from ref. 257.

4.2. Agricultural applications

As nanotechnology is starting to play a role in addressing modern agricultural challenges, chitin-based nanomaterials have risen in interest for their unique properties. A recent review by Maluin and Husein highlights the advances of chitinous agronanochemicals capable of promoting plant growth and disease/pest mitigation through controlled release of active ingredients.[262] Agricultural ingredients, whether plant growth promotors or biocidal materials, can be encapsulated in chitinous matrices for controlled release to facilitate uptake by plants and increased efficacy of the agrochemical. At the same time, controlled release can minimize ingredient loss to the environment *via* run-off and leaching. Furthermore, encapsulation can lower the negative impacts of direct application of agrochemicals on plants, which may cause unpredictable environmental and health damage to nearby ecosystems. Although the following examples demonstrate the potential of nanochitin and nanochitosan for agricultural applications, much work is still required to translate laboratory-based results to larger nursery and field trials.

4.2.1. Plant growth. Bulk chitin and chitosan have shown to be have many applications in agriculture, including

stimulating plant growth, seed germination, enhancing crop yield, improving nutrient uptake, and even increasing chlorophyll content.[263] As their desirable properties seem to be enhanced in the nanoscale, it would be logical to explore their uses at the nanoscale for possible amplified results. In the case of plant growth, the two common goals for improvement are increased yield and better product quality. Traditionally, products such as growth regulators, pesticides, and fertilizers are applied for these purposes. The water insolubility of many plant growth promoters and biocides limits their direct use on plants, therefore chitin/chitosan matrices may prevent premature environmental degradation (typically photolysis) and increase plant absorption.[264]

There have been a few studies that propose nanochitin as a more sustainable alternative to pesticides and fertilizers to achieve similar results. Xue *et al.* observed that a low concentration of ChNPs in soil improved yield of winter wheat by 23.0% and 33.4%, for two different varieties.[265] In the grain filling stage of growth, there were also significant increases in rate of photosynthesis, nutrient uptake, and transpiration during growth. Based on their large surface and strong properties, nanoparticles were previously reported to enhance nutrient absorption in plants. This could enable them to promote plant absorption of water from soil, along with possible organic compounds and ions attached to the nanoparticles.[266] In addition, the quality of the winter wheat products in terms of zinc, iron, and grain protein content was found to have improved – one of the most important indexes for grain quality. A follow-up study by Cheng *et al.* concluded that the applications of nanochitin appears to significantly increase nitrogen content and promote its metabolism in the wheat plant, as the increased nitrogen supply enriches the nutritional value and enhances the yield.[267] Protein, zinc, and iron deficiencies are nutrition-related health problems at a global scale.[268] The capability of nanochitin at low doses to enhance the quality of a globally consumed grain provides the material with immense agricultural potential.

Zhou *et al.* has also explored the use of ChNCs in tobacco plants.[269] The group found that low concentrations (0.001–0.005% w/v) of nanochitin suspensions shortened time for tobacco seed germination, increased stem girth and length, and increased leaf number and area (Fig. 17). For example, the incorporation of a 0.001 wt% suspension of ChNCs saw increase in the stem girth, leaf number, and maximum leaf area of tobacco seedlings by 27.28%, 19.12%, and 10.68%, respectively. Interestingly, when the concentration of the ChNC suspension was increased to 0.005 wt%, the increase in seed germination and plant growth decreased in comparison with the 0.001 wt% experiment, indicating that ChNCs have a low-dose dependence effect on plant growth. When mixed with small amounts of fungicides, nanochitin also exhibited synergistic effects on inhibiting tobacco root rot disease. Similar results of reduced time for germination and fungistatic properties are observed in a study on pepper plants (*Capsicum annuum*), where the effects of nanochitin were compared to that of bulk chitosan.[270] Although the exact mechanism of the enhancement is unclear, nanochitin significantly reduced the mean time to germination compared to chitosan. It was hypothesized that this finding could be due to the increased permeability of nanochitin due to its smaller size, causing greater uptake of nutrients into the organelles in seed embryo relevant to germination.[269,270] The use of nanochitin to replace traditional germination methods also provides antifungal properties, which can simultaneously reduce the use of traditional chemical fungicides, which can cause environmental damage.

Fig. 17 Effect of applying nanochitin on tobacco plant seedling growth. Control sample uses tap water, while nanochitin suspensions are applied in NC samples. Adapted from ref. 269.

Similar to studies of nanochitin, many studies of nanochitosan show similar effects of enhanced plant growth and quality. Bulk chitosan has also been shown to contribute to plant growth by enhancing the plant defence system. This appears to occur through stimulating of plant-specific mechanisms, such as hydrogen peroxide production in rice.[271] A few reports indicate that nanochitosan also has this effect. By primarily stimulating activity in plant defence and antioxidant enzymes, Chandra *et al.* found a significantly improved immune response in *C. sinensis*.[272] The enzymes assayed showed a reduction in oxidative stress, *via* reactive oxygen species (ROS) scavenging. ROS are compounds oxidizing the phenolic content responsible for resisting pathogens in plants. Those enzymes include peroxidase, polyphenol oxidase, phenylalanine ammonia lyase, β-1,3-glucanase and superoxide dismutase (SOD), all of which showed 0.3% to more than 400% increase in activity.

This result echoed the study of Choudhary *et al.*, which examined the boost in defence responses in maize upon the application of Cu–ChsNPs.[273] In the same study, Curvularia leaf spot, a common disease in maize, was also significantly controlled, as the authors also stated that the sustained release profile of Cu from the nanomaterial additionally contributed to the result for the metal's antifungal effect. ChsNPs have also been found to be a positive modulator of plant immune response by elevating the total phenolic content of plants. Chandra *et al.* observed that the increased enzyme activity and phenolic content came from increased gene expression of defence enzymes and compounds due to the ChsNP treatment.[272]

The fabrication of ChsNPs using chitosan and TPP is a common strategy for the encapsulation of agricultural plant ingredients such as plant growth regulators (PGRs) and

biocides. PGRs are molecules that can alter plant hormonal homeostasis and signalling to enhance plant development, increase production, improve the visual and nutritional aspects of food, and increase shelf life.[274] Pereira *et al.* used this method to encapsulate a well-known PGR, gibberellic acid (GA3), which can stimulate the synthesis of hydrolases to increase the availability of endosperm reserves for the embryo.[275,276] They evaluated the effects of seed priming on tomatoes (*Solanum lycopersicum*) and found that the nanoALG/CS-GA3 formulation consisting of chitosan and alginate exhibited the best growth for plants cultivated under field conditions, improving fruit production almost 4-fold. The authors hypothesized that the ChsNPs formed a coating on the tomato seeds that maintained hydration and extended the period of release of GA3 after initial seed priming process. Plant uptake of the GA3-loaded ChsNPs continued to release GA3 within the plant tissues which increased the bioavailability of the PGR compared direct application of GA3.

Chauhan *et al.* investigated the fabrication of ChsNPs from chitosan and TPP to encapsulate hexaconazole [(*R*,*S*)-2-(2,4-dichlorophenyl)-1-(1*H*-1,2,4-triazole-1-yl)hexane-2-ol], a fungicide commonly used for controlling fungal pathogens that affect crops.[277] Authors studied different concentrations of chitosan and TPP to produce fungicide-loaded ChsNPs and determined a relationship with the resulting ChsNPs size. Using response surface plot analysis, an optimal nanocapsule formulation was determined to be 100 nm nanocapsules with a 73% encapsulation efficiency at a chitosan concentration of 0.10% and a TPP concentration of 0.08%. As expected, release of hexaconazole from the nanocapsules was fastest in acidic soil due to the solubility of chitosan at lower pH. In comparison to a commercial hexacoanzole formulation which released its fungicidal payload in 5 days, the ChsNPs exhibited a far slower release of hexaconazole in 14 days. The efficacy of the nanocapsules were demonstrated against the soil-borne pathogen, *R. solani*. Maluin *et al.* also used TPP to formulate ChsNPs of different sizes to encapsulate the fungicides hexaconazole and dazomet against the *G. boninense*, a fungus that causes basal stem rot disease in oil palms.[278] Similar to the work by Chauhan, as the concentration of TPP increased, the resulting size of the dual-loaded fungicidal ChsNPs also decreased. The smaller ChsNPs (5 nm) exhibited the highest antifungal efficacy against *G. boninense*, attributed to the higher surface area of the nanoparticles to interact with the fungal cell wall. The synergistic effect for the dual-loaded antifungal ChsNPs resulted in a 4-fold increase in antifungal activity, compared to single-loaded hexaconazole and dazomet ChsNPs.

ChNPs loaded with avermectin have been investigated as a means to control pinewood nematodes that cause the death of millions of pine trees from pine wilt disease.[279] Current control measures to combat pine wilt disease include removal of infected trees, aerial application of insecticides, and direct trunk injection of anti-nematodal compounds such as avermectin. Unfortunately, the poor solubility of avermectin in water and its rapid photolysis results in poor bioavailability. This has led to its excessive application, contributing needlessly to environmental pollution. Liang *et al.* developed a nanocapsule (~60 nm) consisting of anionic poly-γ-glutamic acid and cationic chitosan, crosslinked by TPP, with an encapsulation efficiency of 30.5% for avermectin.[279] Interestingly, in contrast to ChsNPs fabricated from chitosan and TPP alone that breakdown under acidic conditions, these nanoparticles were more resilient under acidic pH which was attributed to the electrostic interaction of chitosan and poly-γ-glutamic acid. The encapsulation matrix was able to protect the avermectin from photolysis loss by 20%, while increasing the efficacy of the biocide from 69.9% in the free form to 98.6% while encapsulated.

4.2.2. Food science. Another large area of applications for chitin and chitosan nanomaterials lies in the food industry. The antimicrobial and antioxidant properties of chitosan makes it attractive to be applied in food products to retain product quality and extend shelf-life.

4.2.2.1. Food preservation. The use of chemical food additives is a modern method of preserving foodstuffs. Examples include sodium nitrate to prevent botulism in meat products, BHA and BHT to delay oxidation in cereal, and sulfites to prevent contamination in wine, most of which are synthetically produced.[280] With increasing consumer demand for more "natural" products, chitosan has been a material of interest.

Research has explored the direct effects of nanochitosan on food quality. The assessment of quality is usually completed microbiologically for bacterial and fungal count, physiochemically for pH and degree of oxidation, and sometimes with sensory evaluation for consumer consideration. Ramezani *et al.* investigated the coating effects of ChsNPs and chitosan on silver carp fish fillets. While both materials enhanced preservation of the fillets, ChsNP had lower antibacterial activity starting at day 9 of refrigerated storage.[281] An overall indicator for spoilage in fish is the total volatile basic nitrogen value (TVB-N). Its value for ChsNP-treated samples was significantly lower than that of chitosan-treated samples on day 9 and 12 – implying that ChsNP may be a more appropriate coating for maximal shelf-life extension (Fig. 18). However, in terms of lipid oxidation, pH, and sensory evaluation, results showed that ChsNP and chitosan shared the same degree of preservative effect.

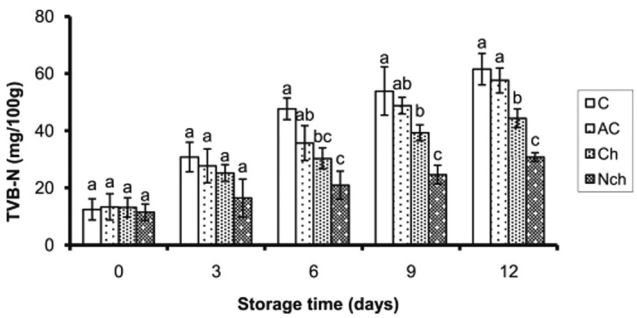

Fig. 18 TVB-N values changes measured at 3-day intervals. Different lower-case letters in the same day represent a statistically significant difference at $P < 0.05$. Adapted from ref. 281.

ChsNP has also been coated onto cucumber,[282] sprayed onto freshly-cut apple slices,[283] incorporated into fish surimi,[284] dispersed in ice for tilapia to be submerged in[285] and all studies found similar results, where ChsNP had significant effects in delaying microbial, oxidative spoilage and retaining quality compared to control samples, measured by respective microbiological and physiochemical assessments. This effect is primarily due to the antimicrobial and antioxidant properties of ChsNPs.

Another rising technology involved in food preservation is loading antibacterial agents, most notably plant essential oils, onto ChsNPs for a controlled release, in an effort to create a more potent and sustained antimicrobial and antioxidative environment for the product.[286] As an alternative to the traditional washing product for sanitation of chlorinated water (NaOCl) Martínez-Hernández *et al.* produced carvacrol-loaded ChsNPs and washed fresh-cut carrot slices with the solution.[286] Carvacrol is a major component in the essential oils of several herbs. Its strong bactericidal action comes from how its phenolic compounds can interact with proteins of microorganisms, leading to their precipitation, cell content leakage, and cell lysis. Nanoencapsulation was achieved through first dissolving carvacrol in ethanol, then adding it dropwise into aqueous chitosan during homogenization, followed by TPP ionic gelation. This emulsified formulation was performed in hopes of improving the dispersibility, solubility, and stability of carvacrol in the aqueous system during application, as the compound is naturally aromatic and hydrophobic. The authors observed that the treatment of carvacrol loaded ChsNPs produced the best sensory and physicochemical qualities in carrot-specific parameters, as well as highly reducing the whitening effect and microbial levels, by 0.6–3.0 log units. The reduced whitening effect of carrots possibly comes from the inactivation of discoloration enzymes, induced by the antioxidant activity of carvacrol and chitosan. While the whitening is equally reduced in samples directly treated with carvacrol solution, this solution leads to more off-flavour and odours.

The release of carvacrol played an important role in the preservative effect of the carrots. Hosseini *et al.* concluded that the release profile of carvacrol in ChsNPs was biphasic. As carvacrol was adsorbed on the nanoparticle surfaces, the faster dissolution at the surface causes the compound to release in an initial burst followed by continuously slower release.[287] For a more optimal extension of carrot shelf-life, the initial burst must be controlled for a slower, more gradual release. Additional research demonstrated that in a more acidic medium, the greater ionic repulsion between cationic amino groups on chitosan chains caused a greater dispersion, and thus longer release.[288] The solution in which the carvacrol-loaded ChsNPs were fabricated was thus adjusted to a higher pH (pH = 4.3), allowing for a more optimal, efficient release of carvacrol and ensuing preservative effect.

Similar positive results for this nanoencapsulation technology of essential oils or other compounds in nanochitosan was observed in many different settings, including cinnamon–ChsNP in beef patties and on cucumber,[289,290] rosemary essential oil in chitosan–benzoic acid nanogel in beef cutlet,[291] nitric oxide–ChsNPs on sweet cherry fruits,[292] and cumin seed essential oil–ChsNP on button mushrooms.[293] All of these studies observed enhanced antibacterial and antioxidant activity, a reduction in microbial population and lipid oxidation, stability in colour and sensation, and shelf-life extension. Many studies have also compared using the essential oil in free form to an encapsulated from. In the case of cinnamon essential oil in beef patties, Ghaderi-Ghahfarokhi *et al.* observed that bacterial counts remained similar for all treatments, but started to significantly differ on day 8 of storage.[289] The 0.1% encapsulated cinnamon essential oil sample had the highest log decrease in *S. aureus* counts, compared to its 0.05% encapsulated oil sample and unencapsulated counterparts. The inhibitory effect for fungal growth, lipid oxidation, and discolouration was also the most notable in the 0.1% encapsulated sample, mostly for its sustained release. Ultimately, this natural and novel additive seemed to provide a promising delivery system that served to effectively preserve many types of food products.

4.2.2.2. Food packaging. Many traditional food packaging materials are derived from petroleum.[294] Biodegradable and eco-friendly food packaging materials have been a growing area of research in recent years due to consumers' concerns over environment waste and food product quality. Similar to food additives, food packaging is used to extend shelf life and improve or retain product quality. The main aspect where different types of packaging differ is the imperative film-forming ability of the material, which is often the biggest hurdle for non-conventional packaging materials.[294,295] The preparation of films typically involves pouring a film-forming solution into a tray or mould, followed by drying.

Specific parameters become crucial in food packaging for its function in food preservation, most notably water-vapor permeability, film tensile strength, light absorption, and thermal degradation. The incorporation of nanomaterials has been found to improve these film properties, and also play an active role in food preservation in the case of nanochitin or nanochitosan. Ifuku *et al.* explored the effects of reinforcing chitosan-based high-strength transparent films with surface-deacetylated ChNFs.[163] With only a 10% blending of the ChNFs, the group observed significant improvements in light transparency and tensile strength, and significant reductions in thermal expansion (Fig. 19). Increasing the content of ChNF was also found to increase the chitosan film's tensile strength. It was hypothesized that the strong extended crystalline structure of the chitin core, along with the slow drying process, lead to the formation of hydrogen bonds between the ChNFs resulting in good mechanical properties of the films. Ultimately, the results show that ChNFs act as an effective filler for novel, biodegradable films that often lack strong properties needed for food packaging. In a study by Satam *et al.*, films with ChNF and CNC blends were found to be mechanically stronger than both neat cellulose and chitin films, as the blending of two materials led to aggregation which supported the fibrous networks.[161] Similar results of reinforcement were observed with ChsNPs as nanofillers for sago

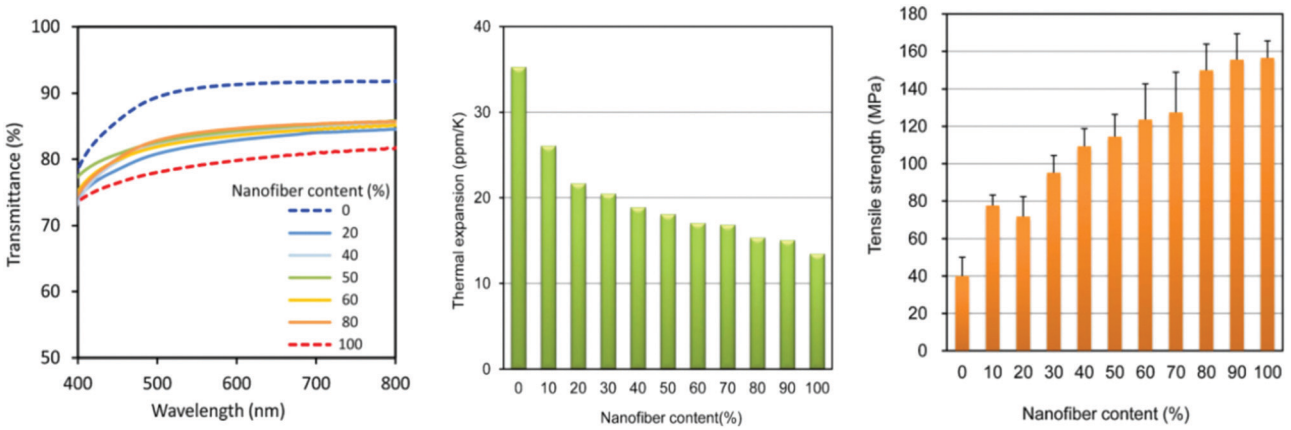

Fig. 19 Changes in (a) light transmittance (b) thermal expansion (c) tensile strength with increasing incorporation of chitin nanofibers in chitosan film. Adapted from ref. 163.

starch film.[296] Due to changes in chemical structure, the nanocomposite film brought significant increases in its mechanical properties including tensile strength, Young's modulus, and elongation at break. This was postulated to be mostly due to the proper dispersion of the nanofillers throughout the film, yielding a strong and reliant film. Thermogravimetric analysis also demonstrated the film to be capable of sustaining heat-sealing applications. Many other studies also showed strengthening effects of ChsNPs on various films, and some even had an enhanced antimicrobial effect.[103,297]

Water-vapor permeability is another property important to applications of food packaging. Often measured by water-vapor diffusion coefficient (WVDC), the incorporation of ChsNPs showed a decrease in WVDC when incorporated in a variety of potential packaging materials, including chitosan/montmorillonite films,[298] propolis–ChsNP films,[299] and banana puree films.[103] This is speculated to be due to the increased compacting of the film as the ChsNPs fill the empty spaces in the porous film matrix, making it less likely for water to permeate and thus enhancing its barrier properties.[103,299,300] On the other hand, Bao *et al.* observed that the addition of ChsNPs increased the water vapor permeability in gelatin films.[301] However, the gelatin film is a protein-based film, while the previously mentioned are all polysaccharide-based films. The group postulated that protein–protein crosslinks became further away from each other due to the dispersion of large nanoparticles in the network, causing penetration of water to be easier.

Azarifar *et al.* studied the shelf-life characteristics of refrigerated raw beef using gelatin–CMC films incorporated with ChNFs.[302] By sealing beef fillet cubes with this active composite film, the samples were shown to inhibit psychotropic bacteria throughout 15 days of storage, delaying lipid oxidation and protein decomposition, and overall prolonging the shelf life of the beef. This is a result of the reduced oxygen permeability of the film. There are many proposed mechanisms for this reduced oxygen permeability, such as the formation of amide and hydrogen bonds between ChNFs and gelatin chains to increase cohesiveness, and the more tortuous film matrix, reducing the speed of oxygen travel through the film. Ultimately, chitin-based nanomaterials have shown to effectively improve film properties, a key feature for the production of more sustainable alternatives to plastic food packaging.

4.2.2.3. Food bioavailability. Another interesting angle to the use of nanochitineous materials in the context of food is their interplay with human digestion itself. In one example, Zhou *et al.* explored a possible adverse impact on this incorporation. They observed that the nanochitin coating can in fact reduce lipid digestion by 30%, reduce vitamin bioaccessibility by 45%, and also decrease overall digestion rate.[303] It is hypothesized that nanochitin acts as a barrier for lipases to contact the lipid molecules to catalyse digestion. Therefore, in this case, nanochitin could act as a functional ingredient at the expense of fat-soluble vitamins bio-accessibility. Conversely, Khorasani *et al.* found that ChNFs contributed to protecting the probiotic population. Prebiotics induce the growth of probiotics in the gut microbiome.[304] By incorporating cellulose and ChNFs into pectin as a prebiotic material, a slower degradation of the biocomposite and a higher survival rate of probiotics was observed. These results demonstrate potential for the usage of ChNFs in improving the delivery of probiotics to the gastrointestinal (GI) tract and also increasing shelf life in probiotic-loaded food products.

Guo *et al.* have also explored the fate of chitin-based nanomaterials in the gastrointestinal tract.[305] The authors assessed the transformations that ChsNPs go through in the GI tract through a simulated digestion and found that while bulk chitosan dissolves in weakly acidic environment and during digestion, TPP-crosslinked ChsNPs do not. These results imply that ChsNPs remain stable from strongly to weakly acidic solutions, indicating that they would be suitable for drug delivery. The group observed that the surface zeta potential of the ChsNPs went from positive to negative when moving from the gastric to the small intestinal phase. This would be important to consider for certain applications, as the positive surface charge is often what provides the material with cell-adhesive

properties. In fact, using ChsNPs, Diop *et al.* managed to increase bioefficiency of insulin by oral administration.[306] Insulin is often destroyed by enzymes and the harsh environment of digestion and therefore cannot be taken orally. By freeze drying insulin-loaded ChsNPs for stabilization, followed by cross-linking with TPP to increase bioefficiency, the procedure appeared to effectively protect insulin and reduce glycemia in insulinopenic rats.[307] This nanoencapsulation technique using chitosan-based nanomaterials has also shown to successfully improved bioavailability of bioactive food components, including carotenoids, vitamins, and essential oils - as reviewed by Akbari-Alavijeh *et al.*[308]

4.3. Water filtration and purification

Many applications for water filtration have been explored using chitosan-based nanofibers, for the prupose of metal and bacterial decontamination.[309] The size and morphology of ChsNFs, along with chitosan's antimicrobial and metal binding ability, makes it a very suitable material for this purpose. Nanofibrous membranes that are typically electrospun have also been found to withstand high fluid flux while also removing particulates from liquids.[310] Cooper *et al.* demonstrates the fabrication of polycaprolactone (PCL) and chitosan composite nanofibers which was then tested for water remediation, specifically for antibacterial filtration of *S. aureus*.[310] By incorporating increasing ratios of chitosan within the nanofibers, less bacteria colonies formed on the nanofibers membranes with higher chitosan concentration, as seen on Fig. 20. With no chitosan incorporation (Fig. 20a and e), dense bacteria colonies were able to proliferate on the surface of the nanofibers, detrimental to filtration systems due to the potential for bio-fouling or decreased filter efficiencies.[311] With 25% chitosan (Fig. 20b and f) and 50% chitosan (Fig. 20c and g) content, fewer bacteria colonies formed, attributed to the antibacterial properties of the chitosan. Even though very few bacterial colonies formed on the 75% chitosan (Fig. 20d and h) nanofiber, excessive swelling of the nanofibers began to develop and were unable to filter water at a high flux for a prolonged period of time. The authors reported an optimized formulation at 25% chitosan incorporation within PLA–chitosan nanofiber membranes, enabling the successful filtration of 100% of >300 nm particles as a prolonged pre-filter. Chitosan inhibited the development of bacteria colonies on the surface of the membrane, which is an important issue for water remediation filtration technologies.

ChsNFs have been used to bind many heavy metals, such as Cr(VI),[312,313] Cu(II) and Pb(II).[314] For instance, Desai *et al.* observed Cr(VI) binding capacities of up to 35 mg chromium per g chitosan and 2–3 log reduction in *E. coli* count.[309] Furthermore, Haider and Park examined the metal adsorption of electrospun ChsNF.[314] Mono-layer adsorption was observed on the nanofiber mats, as there was good erosion stability and high affinity for adsorbing metal ions in aqueous solutions. It was also observed that Cu(II) adsorption with ChsNFs is six times higher than that of chitosan microspheres, and 11 times higher than bulk chitosan, implying that size is another crucial factor responsible for the high adsorption capacity of the material. Desai *et al.* also related the physical filtration efficiency, antimicrobial properties, and metal binding capabilities to the surface chitosan content of the nanofiber mats.[309] Moreover, as Makaremi *et al.* used polyacrylonitrile (PAN) nanofibers for water filtration, they found that an additional layer of electrospun chitosan membrane increased tensile strength and elasticity modulus, while significantly improving heavy metal adsorption, bacteria filtration, and antibacterial action.[315] Bai also explored filtration of porcine parvovirus, a water-borne virus causing diarrhoeal disease, by functionalizing the nanofibers to form chitosan chloride and blending the electrospinning solution with graphene.[316] This modification increased the removal of the virus to a minimum of 99% in solution. In addition to water filtration, electronspun ChsNFs have also been explored to be effective at air filtration.[317]

4.4. Catalysis

Nanochitin and nanochitosan have been used in catalysis, in three main contexts: (1) as a catalyst support for metal

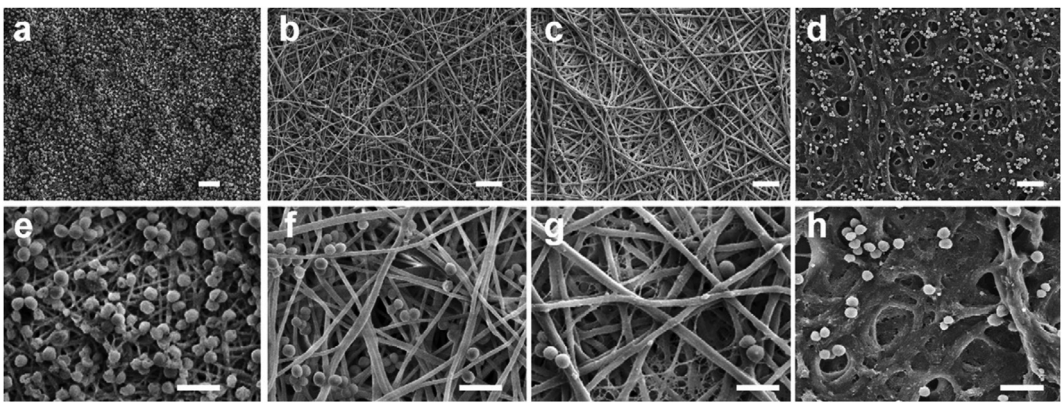

Fig. 20 Scanning electron microscopy (SEM) analysis of *S. aureus* on nanofibrous membranes at low (top row) and high (bottom row) magnifications. (a and e) PCL only, (b and f) 25% chitosan, (c and g) 50% chitosan and (d and h) 75% chitosan. The samples were fixed after 24 h of culture with an initial bacteria density of 5 × 104 cells per mL in tryptic soy broth medium. Scale bars represent 5 μm (top row) and 2.5 μm (bottom row). Note the excessive fiber swelling in h. Adapted from ref. 310.

Table 4 Organic transformations done using nanochitin or nanochitosan as either a support for metal nanoparticle catalysis or as an organocatalyst itself

Reaction	Catalyst	Rate constant, k, s^{-1}	Turnover frequency, h^{-1}	Ref.
Reduction of congo red	Ag NPs supported on ChNCs	50.2×10^{-3}	—	329
Reduction of 4-nitrophenol	Au NPs supported on ChsNCs	4.75×10^{-3}	8557	39
Aldehyde–amine–alkyne coupling	Au NPs supported on ChsNCs	—	8.3	39
Heck coupling	Pd NPs supported on ChNCs	—	4.2	331
Knoevenagel condensation	ChNF aerogel	—	22	330

nanoparticles, (2) as an organocatalyst itself, and (3) as an enzyme immobilization for biocatalysis. Firstly, the use of bulk chitin or chitosan as a catalyst support is well-established and has been extensively reviewed,[318–321] for instance in systems featuring Fe_3O_4,[319] Pd,[320,322,323] Cu,[324] Ni,[325] Rh,[326] and Pt,[327] as the catalytic species. Thanks to the practicality of its primary amine functionality in promoting solubility and metal nanoparticle stabilization, chitosan is often preferred over chitin.[328] The nanoscale counterparts of chitin and chitosan have however been far less explored, despite the inspiring advancements seen while using other types of supports in the nanoregime, such as carbon- and metal oxide-based nanomaterials. Table 4 depicts the various organic transformations that have been done using nanochitin and nanochitosan, as well as their reported rate constants and turnover frequency (TOF) values.

Yang *et al.* used ChNCs as a support for Ag NPs as a catalyst for environmental waste removal, using the reduction of congo red as a model reaction (Scheme 5).[329] Sodium lignosulfonate (NaLS) was combined with ChNCs and $AgNO_3$ to produce Ag NPs with a diameter of 15 ± 5 nm, upon $NaBH_4$ reduction. The authors further showed a good rate constant for the congo red reaction at 50.2×10^{-3} s^{-1}, while also maintaining catalytic efficiency of up to 90% even after 5 reaction cycles.

We recently reported the use of carboxylated ChsNCs as a versatile catalyst support for Au catalysis (Scheme 6).[39] By using the catalytic reduction of 4-nitrophenol as a model reaction, it was demonstrated that Au supported on ChsNCs had better catalytic activity than ChNCs, proving the effectiveness of the amine functionality in stabilizing highly disperse metal NP catalysts. Further comparisons with Au supported on bulk chitin and chitosan also proved that the nanoscale nature of ChsNCs were crucial in yielding high surface area for metal NPs to deposit onto. Interestingly, by comparing with other literature values for the same reaction, ChsNCs were the most effective catalyst support for Au, outperforming all other carbon-based supports including CNCs.

Nanochitin itself has also been used as a base catalyst for the aqueous Knoevenagel condensation reaction, as reported by Isogai and coworkers in 2014 (Scheme 7). A flow system was implemented with ChNF-based hydrogel and aerogels, showing exceptional turnover frequencies of 22 h^{-1} at a flow rate between 0.03–0.04 mL min^{-1}. Importantly, control tests using aerogels made with cellulose showed virtually no product yield, highlighting the importance of the amine units on the ChNFs. Aerogels made from bulk chitosan were also tested to yield no product, further indicating the importance of the increased surface area from making aerogels from ChNFs.[330]

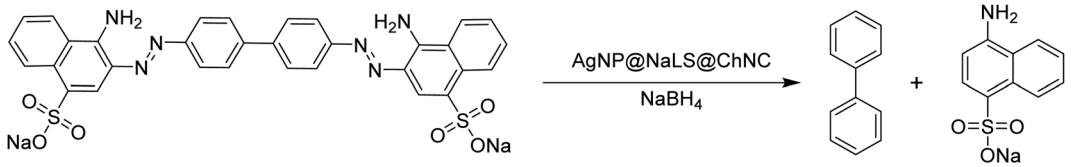

Scheme 5 Catalytic reduction of Congo red *via* AgNPs supported by NaLS@ChNC.

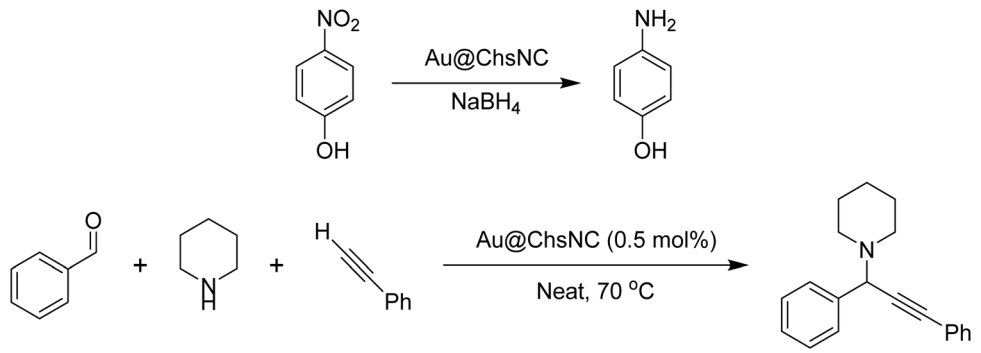

Scheme 6 Catalytic reduction of 4-nitrophenol and multicomponent A^3 coupling reaction catalysed by Au supported on ChsNC.

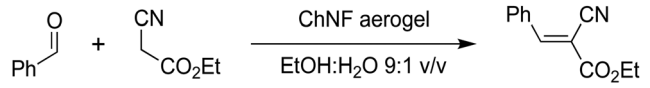

Scheme 7 Knoevenagel condensation reaction catalysed by a ChNF aerogel.

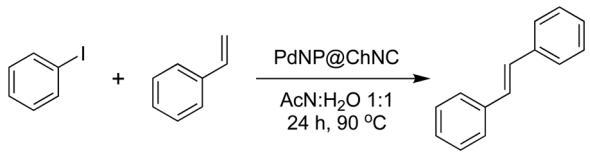

Scheme 8 Heck coupling reaction catalysed by PdNPs supported on ChNCs.

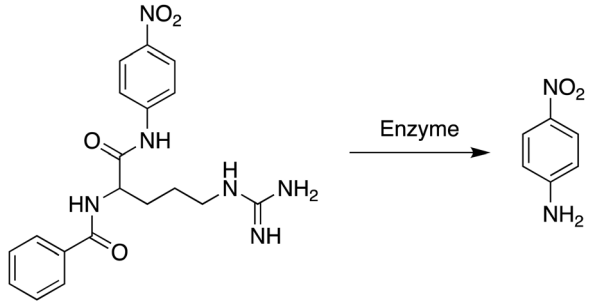

Scheme 9 Enzymatic reduction of *N*-α-benzoyl-D,L-arginine-pnitroanilide to 4-nitroaniline.

Recently, our group has also used ChNCs as a support for PdNPs to catalyse the Heck coupling reaction (Scheme 8). Full product yield was observed after 24 h and 90 °C.[331]

The immobilization of enzymes is a large field under development to promote the sustainable usage of costly enzymes, ensure easy separation from products (akin to heterogeneous catalysis), and prevent deactivation in the presence of deviations from the ideal condition such as pH, temperature, and reaction media.[332] ChNCs have been shown to effectively immobilize enzymes for biocatalysis. For instance, Cao *et al.* immobilized porcine pancrease lipase (PPL) onto ChNC using a crosslinking procedure with glutaraldehyde.[82] In a model reaction, the reduction of *N*-α-benzoyl-D,L-arginine-pnitroanilide to 4-nitroaniline (Scheme 9) showed that ChNC prevented deactivation of the PPL enzyme when subjected to changes in pH and temperature, as compared to free PPL.

Similarly, a chitosan/poly(vinyl alcohol) nanofibrous membrane was prepared by Huang *et al.* for the immobilization of lipase from *Candida rugosa*.[333] The activity after use, pH, and thermal stability were all improved compared to free enzymes. Other enzymes that have been immobilized on electrospun ChsNFs include trypsin and acetylcholinesterase, with trypsin showing long-term activity and recyclability for the reduction of *N*-α-benzoyl-D,L-arginine-pnitroanilide (Scheme 9) compared to free enzyme.[334,335] Park *et al.* also immobilized lysozyme on electrospun, stabilized chitosan/poly(vinyl alcohol) nanofibrous membranes as it was shown to be effective for continuous antibacterial function.[336] While free lysozymes lost all activity after 80 days of room temperature storage, 75.4% of initial activity was retained in the immobilized lysozymes, all while having bacteriostatic properties.

With these few notable examples, it is apparent that there is a huge gap within the literature to expand upon the use of nanoscale chitin and chitosan as metal catalyst supports compared to CNCs or as an organocatalyst themselves. One important aspect to consider is the wide variety of functionalization that can be done *via* the acetamide or amine on chitin and chitosan, respectively. While this has been done with bulk chitin and chitosan, it will be of notable interest to understand how manipulating these nitrogen handles on the nanoscale can drastically alter their properties, as it has been seen within the cellulose literature. Important properties of chitin and chitosan to augment include, but are not limited to, metal binding, solubility, thermal and mechanical durability, and catalytic effectiveness (*e.g.*, by hydrophobic moieties to boost interaction of reacting substrates). A litany of reactions may be used to accomplish this including reductive amination, Schiff base formation, thiolation, among many others that can introduce a variety of unique ligands, which have already been done with bulk chitosan.[328] With this in mind, it is hopeful that this field will offer both the promising advantages of heterogeneity in using a catalyst support, along with green chemistry principles such as sustainability and waste valorisation in making the next generation of catalytic materials.

5. Conclusions and future outlooks

In the present review, we have attempted to showcase the functional properties of nanochitin and nanochitosan and articulate how these materials may address technical challenges in applications across multiple disciplines. In particular, we started by focussing on the current known fabrication procedures for producing nanochitin and nanochitosan. Yet, these materials face significant challenges in catching up to the technology development of nanocellulose. Milder and more economical and sustainable techniques are the focus of intensive research efforts to fine-tune the morphology of these materials, to create consistent batch-to-batch quality in product, and to ease in scale-up production. Current processes to produce nanochitin and nanochitosan use significant amounts of water and chemical reagents, whether they are corrosive mineral acids for hydrolysis or strong bases for chitin deacetylation. Little is known regarding their biodegradation and toxicity, while LCA must be conducted more rigorously to compare known processes to emerging ones. CNC production is currently reaching commercial scale on the strength of years of R&D to reduce water consumption and recover/reuse these chemical reagents to lower the cost of production. One key technical challenge to overcome is the amorphization that occurs with the synthesis of ChsNC, as crystallinity has an important role in many applications related to mechanical and thermal properties. For example,

compromises between crystallinity and DDA may prove to be the pivot point in maximizing the potential of chitosan-based nanomaterials, where only the surface of the nanocrystals should be fully deacetylated while the interior be fully crystalline. The work of the Hsieh group on this topic is particularly inspiring.[90]

The functional properties of nanochitin and nanochitosan may provide these materials the opportunity to supercede nanocellulose. As physical reinforcing agents, the additional nitrogen-bearing groups on nanochitin and nanochitosan are able to contribute to additional electrostatic or chemical crosslinking interactions. We anticipate that nanochitin and nanochitosan will specifically benefit from this increase reactivity imparted by the nitrogen-bearing groups in areas such as wound healing, tissue adhesion, drug delivery, drug encapsulation, and environmental remediation. We anticipate with more refined processing, nanochitosan (specifically ChsNCs and ChsNFs) can have a greater role in food packaging and biomedicine, due to its natural antimicrobial characteristics. Furthermore, the area of organocatalysis also has huge potential for development, as nanochitosan features high surface area characteristics along with amine groups that can be used as a Lewis base, or participate in the formation of imine- and enamine-type organocatalytic reactions. In such a small period of time, the literature has shown a wealth of initial applications using nanochitin and nanochitosan materials, reminiscent of the surge in publications associated with nanocellulose. We anticipate that future research will not only advance some of these identified application areas, but begin to address the core challenges related to economics and sustainability, key factors to commercial viability for nanochitin and nanochitosan.

Funding and acknowledgements

We thank the National Research Council (NRC) New Beginnings Initiative Ideation fund, the Natural Science and Engineering Research Council of Canada (NSERC) Discovery Grant, Discovery Accelerator Supplement and Postgraduate Scholarship-Doctoral (TJ), the Fonds de Recherche du Québec – Nature et Technologies (FRQNT) Centre for Green Chemistry and Catalysis (CGCC) the National Research Council Canada (NRC) and McGill University. Dorelle Hinton is also thanked for her precise and thorough editing.

Conflicts of interest

There are no conflicts to declare.

References

1 S. Eyley and W. Thielemans, *Nanoscale*, 2014, **6**, 7764–7779.
2 M. Mariano, N. El Kissi and A. Dufresne, *J. Polym. Sci., Part B: Polym. Phys.*, 2014, **52**, 791–806.
3 A. Sharma, M. Thakur, M. Bhattacharya, T. Mandal and S. Goswami, *Biotechnol. Rep.*, 2019, **21**, e00316.
4 A. Percot, C. Viton and A. Domard, *Biomacromolecules*, 2003, **4**, 12–18.
5 S.-K. Kim, *Chitin, chitosan, oligosaccharides and their derivatives: biological activities and applications*, CRC Press, 2010.
6 FAO, *Opportunities and challenges*, 2012.
7 N. Yan and X. Chen, *Nature*, 2015, **524**, 155–157.
8 T. Maschmeyer, R. Luque and M. Selva, *Chem. Soc. Rev.*, 2020, **49**, 4527–4563.
9 J. L. Shamshina, T. Oldham and R. D. Rogers, in *Sustainable Agriculture Reviews 36: Chitin and Chitosan: Applications in Food, Agriculture, Pharmacy, Medicine and Wastewater Treatment*, ed. G. Crini and E. Lichtfouse, Springer International Publishing, Cham, 2019, pp. 125–146, DOI: 10.1007/978-3-030-16581-9_4.
10 X. Chen, S. L. Chew, F. M. Kerton and N. Yan, *Green Chem.*, 2014, **16**, 2204–2212.
11 G. Margoutidis, V. H. Parsons, C. S. Bottaro, N. Yan and F. M. Kerton, *ACS Sustainable Chem. Eng.*, 2018, **6**, 1662–1669.
12 E. R. Adlard, *Chromatographia*, 2017, **80**, 1485.
13 Y. Fan, T. Saito and A. Isogai, *Carbohydr. Polym.*, 2010, **79**, 1046–1051.
14 T. Di Nardo, C. Hadad, A. Nguyen Van Nhien and A. Moores, *Green Chem.*, 2019, **21**, 3276–3285.
15 M. Kong, X. G. Chen, K. Xing and H. J. Park, *Int. J. Food Microbiol.*, 2010, **144**, 51–63.
16 M.-T. Yen, J.-H. Yang and J.-L. Mau, *Carbohydr. Polym.*, 2008, **74**, 840–844.
17 Q. Yuan, J. Shah, S. Hein and R. D. K. Misra, *Acta Biomater.*, 2010, **6**, 1140–1148.
18 L.-C. Tsai, M.-L. Tsai, K.-Y. Lu and F.-L. Mi, *Res. Chem. Intermed.*, 2018, **44**, 4855–4871.
19 A. Gamage and F. Shahidi, *Food Chem.*, 2007, **104**, 989–996.
20 R. H. Marchessault, F. F. Morehead and N. M. Walter, *Nature*, 1959, **184**, 632–633.
21 K. J. De France, K. J. W. Chan, E. D. Cranston and T. Hoare, *Biomacromolecules*, 2016, **17**, 649–660.
22 B. L. Tardy, J. J. Richardson, L. G. Greca, J. Guo, H. Ejima and O. J. Rojas, *Adv. Mater.*, 2020, 1906886.
23 K. E. Shopsowitz, H. Qi, W. Y. Hamad and M. J. MacLachlan, *Nature*, 2010, **468**, 422–425.
24 D. Trache, M. H. Hussin, M. K. M. Haafiz and V. K. Thakur, *Nanoscale*, 2017, **9**, 1763–1786.
25 J. Moohan, S. A. Stewart, E. Espinosa, A. Rosal, A. Rodríguez, E. Larrañeta, R. F. Donnelly and J. Domínguez-Robles, *Appl. Sci.*, 2019, **10**, 65.
26 Y. Habibi, L. A. Lucia and O. J. Rojas, *Chem. Rev.*, 2010, **110**, 3479–3500.
27 Y.-R. Seo, J.-W. Kim, S. Hoon, J. Kim, J. H. Chung and K.-T. Lim, *J. Biosyst. Eng.*, 2018, **43**, 59–71.
28 N. Lin and A. Dufresne, *Eur. Polym. J.*, 2014, **59**, 302–325.
29 S. Nandi and P. Guha, *J. Packag. Technol. Res.*, 2018, **2**, 149–166.
30 A. Tran, C. E. Boott and M. J. MacLachlan, *Adv. Mater.*, 2020, **32**, 1905876.

31 J. Li, J. F. Revol and R. H. Marchessault, *J. Appl. Polym. Sci.*, 1997, **65**, 373–380.
32 S. Phongying, S.-i. Aiba and S. Chirachanchai, *Biopolymers*, 2006, **83**, 280–288.
33 S. Kaur and G. S. Dhillon, *Crit. Rev. Biotechnol.*, 2015, **35**, 44–61.
34 M. H. Mohammed, P. A. Williams and O. Tverezovskaya, *Food Hydrocolloids*, 2013, **31**, 166–171.
35 E. S. Abdou, K. S. A. Nagy and M. Z. Elsabee, *Bioresour. Technol.*, 2008, **99**, 1359–1367.
36 P. R. Chang, R. Jian, J. Yu and X. Ma, *Carbohydr. Polym.*, 2010, **80**, 420–425.
37 Y. Fan, T. Saito and A. Isogai, *Carbohydr. Polym.*, 2009, **77**, 832–838.
38 J. F. Revol and R. H. Marchessault, *Int. J. Biol. Macromol.*, 1993, **15**, 329–335.
39 T. Jin, D. Kurdyla, S. Hrapovic, A. C. W. Leung, S. Régnier, Y. Liu, A. Moores and E. Lam, *Biomacromolecules*, 2020, **21**, 2236–2245.
40 X. Deng, M. Cao, J. Zhang, K. Hu, Z. Yin, Z. Zhou, X. Xiao, Y. Yang, W. Sheng, Y. Wu and Y. Zeng, *Biomaterials*, 2014, **35**, 4333–4344.
41 J. D. Schiffman and C. L. Schauer, *Biomacromolecules*, 2007, **8**, 594–601.
42 J. H. Luong, E. Lam, C. W. Leung, S. Hrapovic and K. B. Male, Chitin Nanocrystals and Process for Preparation Thereof, *US Pat.*, US20160272731A1, 2016.
43 M. Kaya, M. Mujtaba, H. Ehrlich, A. M. Salaberria, T. Baran, C. T. Amemiya, R. Galli, L. Akyuz, I. Sargin and J. Labidi, *Carbohydr. Polym.*, 2017, **176**, 177–186.
44 M.-K. Jang, B.-G. Kong, Y.-I. Jeong, C. H. Lee and J.-W. Nah, *J. Polym. Sci., Part A: Polym. Chem.*, 2004, **42**, 3423–3432.
45 D. Carlström, *J. Biophys. Biochem. Cytol.*, 1957, **3**, 669–683.
46 Y. Fan, T. Saito and A. Isogai, *Biomacromolecules*, 2008, **9**, 1919–1923.
47 J. Sugiyama, C. Boisset, M. Hashimoto and T. Watanabe, *J. Mol. Biol.*, 1999, **286**, 247–255.
48 P. S. Barber, C. S. Griggs, J. R. Bonner and R. D. Rogers, *Green Chem.*, 2013, **15**, 601–607.
49 S. Ifuku, M. Nogi, K. Abe, M. Yoshioka, M. Morimoto, H. Saimoto and H. Yano, *Biomacromolecules*, 2009, **10**, 1584–1588.
50 H. Kargarzadeh, M. Mariano, J. Huang, N. Lin, I. Ahmad, A. Dufresne and S. Thomas, *Polymer*, 2017, **132**, 368–393.
51 S. Ifuku, M. Nogi, M. Yoshioka, M. Morimoto, H. Yano and H. Saimoto, *Carbohydr. Polym.*, 2010, **81**, 134–139.
52 H. K. Noh, S. W. Lee, J.-M. Kim, J.-E. Oh, K.-H. Kim, C.-P. Chung, S.-C. Choi, W. H. Park and B.-M. Min, *Biomaterials*, 2006, **27**, 3934–3944.
53 B.-M. Min, S. W. Lee, J. N. Lim, Y. You, T. S. Lee, P. H. Kang and W. H. Park, *Polymer*, 2004, **45**, 7137–7142.
54 D. N. Hon and N. Shiraishi, *Wood and cellulosic chemistry, revised, and expanded*, CRC Press, 2000.
55 P. Lu and Y.-L. Hsieh, *Carbohydr. Polym.*, 2012, **87**, 564–573.
56 J.-B. Zeng, Y.-S. He, S.-L. Li and Y.-Z. Wang, *Biomacromolecules*, 2012, **13**, 1–11.
57 M. Paillet and A. Dufresne, *Macromolecules*, 2001, **34**, 6527–6530.
58 A. Morin and A. Dufresne, *Macromolecules*, 2002, **35**, 2190–2199.
59 Y. Lu, L. Weng and L. Zhang, *Biomacromolecules*, 2004, **5**, 1046–1051.
60 K. Gopalan Nair and A. Dufresne, *Biomacromolecules*, 2003, **4**, 657–665.
61 X. Wu, F. Torres, F. Vilaseca and T. Peijs, *J. Biobased Mater. Bioenergy*, 2007, **1**, 341–350.
62 L. Feng, Z. Zhou, A. Dufresne, J. Huang, M. Wei and L. An, *J. Appl. Polym. Sci.*, 2009, **112**, 2830–2837.
63 P. Hariraksapitak and P. Supaphol, *J. Appl. Polym. Sci.*, 2010, **117**, 3406–3418.
64 J. Sriupayo, P. Supaphol, J. Blackwell and R. Rujiravanit, *Carbohydr. Polym.*, 2005, **62**, 130–136.
65 J. D. Goodrich and W. T. Winter, *Biomacromolecules*, 2007, **8**, 252–257.
66 A. Watthanaphanit, P. Supaphol, H. Tamura, S. Tokura and R. Rujiravanit, *J. Appl. Polym. Sci.*, 2008, **110**, 890–899.
67 J. Junkasem, R. Rujiravanit, B. P. Grady and P. Supaphol, *Polym. Int.*, 2010, **59**, 85–91.
68 A. Watthanaphanit, P. Supaphol, H. Tamura, S. Tokura and R. Rujiravanit, *Carbohydr. Polym.*, 2010, **79**, 738–746.
69 S. Phongying, S.-i. Aiba and S. Chirachanchai, *Polymer*, 2007, **48**, 393–400.
70 P. Wongpanit, N. Sanchavanakit, P. Pavasant, T. Bunaprasert, Y. Tabata and R. Rujiravanit, *Eur. Polym. J.*, 2007, **43**, 4123–4135.
71 M. Mincea, A. Negrulescu and V. Ostafe, *Rev. Adv. Mater. Sci.*, 2012, **30**, 225–242.
72 Y. Qin, S. Zhang, J. Yu, J. Yang, L. Xiong and Q. Sun, *Carbohydr. Polym.*, 2016, **147**, 372–378.
73 S. Ge, Q. Liu, M. Li, J. Liu, H. Lu, F. Li, S. Zhang, Q. Sun and L. Xiong, *Food Hydrocolloids*, 2018, **75**, 1–12.
74 J. Pang, S. Bi, T. Kong, X. Luo, Z. Zhou, K. Qiu, L. Huang, X. Chen and M. Kong, *Carbohydr. Polym.*, 2020, 116138.
75 B. Thomas, M. C. Raj, K. B. Athira, M. H. Rubiyah, J. Joy, A. Moores, G. L. Drisko and C. Sanchez, *Chem. Rev.*, 2018, **118**, 11575–11625.
76 Y. Fan, T. Saito and A. Isogai, *Biomacromolecules*, 2008, **9**, 192–198.
77 J. Jiang, W. Ye, J. Yu, Y. Fan, Y. Ono, T. Saito and A. Isogai, *Carbohydr. Polym.*, 2018, **189**, 178–183.
78 H. Tang, J. Wu, D. Li, C. Shi, G. Chen, M. He and J. Tian, *Int. J. Biol. Macromol.*, 2020, **150**, 885–893.
79 P. Baldrian, *FEMS Microbiol. Rev.*, 2006, **30**, 215–242.
80 M. Fabbrini, C. Galli, P. Gentili and D. Macchitella, *Tetrahedron Lett.*, 2001, **42**, 7551–7553.
81 A. C. W. Leung, S. Hrapovic, E. Lam, Y. Liu, K. B. Male, K. A. Mahmoud and J. H. T. Luong, *Small*, 2011, **7**, 302–305.
82 S.-L. Cao, W.-M. Gu, W.-D. Ou-Yang, D.-C. Chen, B.-Y. Yang, L.-H. Lai, Y.-D. Wu, Y.-J. Liu, J. Zhu, W.-J. Chen, Z.-Q. Gai, X.-D. Hou, Y.-Z. Ma and Y.-X. An, *Carbohydr. Polym.*, 2019, **213**, 304–310.

83 C. Mukesh, D. Mondal, M. Sharma and K. Prasad, *Carbohydr. Polym.*, 2014, **103**, 466–471.
84 K. T. Smitha, A. Anitha, T. Furuike, H. Tamura, S. V. Nair and R. Jayakumar, *Colloids Surf., B*, 2013, **104**, 245–253.
85 P. Geetha, A. J. Sivaram, R. Jayakumar and C. Gopi Mohan, *Carbohydr. Polym.*, 2016, **142**, 240–249.
86 A. Dev, J. C. Mohan, V. Sreeja, H. Tamura, G. R. Patzke, F. Hussain, S. Weyeneth, S. V. Nair and R. Jayakumar, *Carbohydr. Polym.*, 2010, **79**, 1073–1079.
87 R. Jayakumar, M. Prabaharan, S. V. Nair and H. Tamura, *Biotechnol. Adv.*, 2010, **28**, 142–150.
88 H. Homayoni, S. A. H. Ravandi and M. Valizadeh, *Carbohydr. Polym.*, 2009, **77**, 656–661.
89 K. Ohkawa, K.-I. Minato, G. Kumagai, S. Hayashi and H. Yamamoto, *Biomacromolecules*, 2006, **7**, 3291–3294.
90 A. G. B. Pereira, E. C. Muniz and Y.-L. Hsieh, *Carbohydr. Polym.*, 2014, **107**, 158–166.
91 A. G. B. Pereira, E. C. Muniz and Y.-L. Hsieh, *Carbohydr. Polym.*, 2015, **123**, 46–52.
92 S. Chen and D. Chen, *Polym. Bull.*, 2020, **77**, 5345–5355.
93 D. Fengel and G. Wegener, *Wood: chemistry, ultrastructure, reactions*, Walter de Gruyter, 2011.
94 K.-S. Huang, Y.-R. Sheu and I.-C. Chao, *Polym.-Plast. Technol. Eng.*, 2009, **48**, 1239–1243.
95 R. Bodmeier, H. Chen and O. Paeratakul, *Pharm. Res.*, 1989, **6**, 413–417.
96 K. J. Zhu and X. Z. Shu, *J. Microencapsul.*, 2001, **18**, 237–245.
97 H.-C. Yang, W.-H. Wang, K.-S. Huang and M.-H. Hon, *Carbohydr. Polym.*, 2010, **79**, 176–179.
98 Z.-X. Tang, J.-Q. Qian and L.-E. Shi, *Appl. Biochem. Biotechnol.*, 2007, **136**, 77–96.
99 K. Vijayalakshmi, B. Devi, P. Sudha, J. Venkatesan and S. Anil, *J. Nanomed. Nanotechnol.*, 2016, **7**, 2.
100 A. Anitha, V. V. Divya Rani, R. Krishna, V. Sreeja, N. Selvamurugan, S. V. Nair, H. Tamura and R. Jayakumar, *Carbohydr. Polym.*, 2009, **78**, 672–677.
101 M. R. de Moura, F. A. Aouada and L. H. C. Mattoso, *J. Colloid Interface Sci.*, 2008, **321**, 477–483.
102 R. De Lima, L. Feitosa, A. do Espírito Santo Pereira, M. R. De Moura, F. A. Aouada, L. H. C. Mattoso and L. F. Fraceto, *J. Food Sci.*, 2010, **75**, N89–N96.
103 M. R. Martelli, T. T. Barros, M. R. de Moura, L. H. C. Mattoso and O. B. G. Assis, *J. Food Sci.*, 2013, **78**, N98–N104.
104 H. Tokumitsu, H. Ichikawa and Y. Fukumori, *Pharm. Res.*, 1999, **16**, 1830–1835.
105 C. J. Murphy and J. M. Buriak, 2015.
106 J. L. Leuba and P. Stossel, in *Chitin in Nature and Technology*, ed. R. Muzzarelli, C. Jeuniaux and G. W. Gooday, Springer US, Boston, MA, 1986, pp. 215–222, DOI: 10.1007/978-1-4613-2167-5_29.
107 R. Prathapan, R. F. Tabor, G. Garnier and J. Hu, *ACS Appl. Bio Mater.*, 2020, **3**, 1828–1844.
108 T.-D. Nguyen and M. J. MacLachlan, *Adv. Opt. Mater.*, 2014, **2**, 1031–1037.
109 D. G. Gray, *Carbohydr. Polym.*, 1994, **25**, 277–284.
110 M. Giese, L. K. Blusch, M. K. Khan and M. J. MacLachlan, *Angew. Chem., Int. Ed.*, 2015, **54**, 2888–2910.
111 V. Sharma, M. Crne, J. O. Park and M. Srinivasarao, *Science*, 2009, **325**, 449.
112 E. Lizundia, T.-D. Nguyen, R. J. Winnick and M. J. MacLachlan, *J. Mater. Chem. C*, 2021, **9**, 796–817.
113 J. Li, J. F. Revol, E. Naranjo and R. H. Marchessault, *Int. J. Biol. Macromol.*, 1996, **18**, 177–187.
114 E. Belamie, P. Davidson and M. M. Giraud-Guille, *J. Phys. Chem. B*, 2004, **108**, 14991–15000.
115 Z. Luo, H. Song, X. Feng, M. Run, H. Cui, L. Wu, J. Gao and Z. Wang, *Langmuir*, 2013, **29**, 12358–12366.
116 Y. Liu, M. Liu, S. Yang, B. Luo and C. Zhou, *ACS Sustainable Chem. Eng.*, 2018, **6**, 325–336.
117 R. M. Parker, B. Frka-Petesic, G. Guidetti, G. Kamita, G. Consani, C. Abell and S. Vignolini, *ACS Nano*, 2016, **10**, 8443–8449.
118 D. X. Oh, Y. J. Cha, H.-L. Nguyen, H. H. Je, Y. S. Jho, D. S. Hwang and D. K. Yoon, *Sci. Rep.*, 2016, **6**, 23245.
119 A. Narkevicius, L. M. Steiner, R. M. Parker, Y. Ogawa, B. Frka-Petesic and S. Vignolini, *Biomacromolecules*, 2019, **20**, 2830–2838.
120 T.-D. Nguyen, B. U. Peres, R. M. Carvalho and M. J. MacLachlan, *Adv. Funct. Mater.*, 2016, **26**, 2875–2881.
121 D. Raafat, K. von Bargen, A. Haas and H.-G. Sahl, *Appl. Environ. Microbiol.*, 2008, **74**, 3764.
122 J. Xu, L. Liu, J. Yu, Y. Zou, Z. Wang and Y. Fan, *Cellulose*, 2019, **26**, 2279–2290.
123 M. S. Benhabiles, R. Salah, H. Lounici, N. Drouiche, M. F. A. Goosen and N. Mameri, *Food Hydrocolloids*, 2012, **29**, 48–56.
124 K. T. Hwang, S. T. Jung, G. D. Lee, M. S. Chinnan, Y. S. Park and H. J. Park, *J. Agric. Food Chem.*, 2002, **50**, 1876–1882.
125 T. H. Tran, H.-L. Nguyen, D. S. Hwang, J. Y. Lee, H. G. Cha, J. M. Koo, S. Y. Hwang, J. Park and D. X. Oh, *Carbohydr. Polym.*, 2019, **205**, 392–400.
126 S. Shankar, J. P. Reddy, J.-W. Rhim and H.-Y. Kim, *Carbohydr. Polym.*, 2015, **117**, 468–475.
127 M. E. Villanueva, A. Salinas, L. E. Díaz and G. J. Copello, *New J. Chem.*, 2015, **39**, 614–620.
128 E. Gayán, S. Condón and I. Álvarez, *Food Bioprocess Technol.*, 2014, **7**, 1–20.
129 S. Jiang, Y. Qin, J. Yang, M. Li, L. Xiong and Q. Sun, *Food Chem.*, 2017, **221**, 1507–1513.
130 L. Qi, Z. Xu, X. Jiang, C. Hu and X. Zou, *Carbohydr. Res.*, 2004, **339**, 2693–2700.
131 K. Saravanakumar, R. Chelliah, D. MubarakAli, E. Jeevithan, D.-H. Oh, K. Kathiresan and M.-H. Wang, *Int. J. Biol. Macromol.*, 2018, **118**, 1542–1549.
132 M. D. Leonida, S. Belbekhouche, A. Benzecry, M. Peddineni, A. Suria and B. Carbonnier, *Int. J. Biol. Macromol.*, 2018, **120**, 1335–1343.
133 W.-L. Du, S.-S. Niu, Y.-L. Xu, Z.-R. Xu and C.-L. Fan, *Carbohydr. Polym.*, 2009, **75**, 385–389.

134 A. K. T. Chang, R. R. Frias, L. V. Alvarez, U. G. Bigol and J. P. M. D. Guzman, *Biocatal. Agric. Biotechnol.*, 2019, **17**, 189–195.
135 O. M. Darwesh, Y. Y. Sultan, M. M. Seif and D. A. Marrez, *Toxicol. Rep.*, 2018, **5**, 348–356.
136 L. Sun, Y. Du, L. Fan, X. Chen and J. Yang, *Polymer*, 2006, **47**, 1796–1804.
137 K. Xing, X. G. Chen, M. Kong, C. S. Liu, D. S. Cha and H. J. Park, *Carbohydr. Polym.*, 2009, **76**, 17–22.
138 K. Divya, V. Smitha and M. S. Jisha, *Int. J. Biol. Macromol.*, 2018, **114**, 572–577.
139 M. Sathiyabama and R. Parthasarathy, *Carbohydr. Polym.*, 2016, **151**, 321–325.
140 A. González-Saucedo, L. L. Barrera-Necha, R. I. Ventura-Aguilar, Z. N. Correa-Pacheco, S. Bautista-Baños and M. Hernández-López, *Postharvest Biol. Technol.*, 2019, **149**, 74–82.
141 D. MubarakAli, F. LewisOscar, V. Gopinath, N. S. Alharbi, S. A. Alharbi and N. Thajuddin, *Microb. Pathog.*, 2018, **114**, 323–327.
142 H. Alboghbeish and A. Khodanazary, *Turk. J. Fish. Aquat. Sci.*, 2019, **19**, 957–967.
143 R. C. Choudhary, R. V. Kumaraswamy, S. Kumari, A. Pal, R. Raliya, P. Biswas and V. Saharan, in *Nanotechnology: An Agricultural Paradigm*, ed. R. Prasad, M. Kumar and V. Kumar, Springer Singapore, Singapore, 2017, pp. 227–247, DOI: 10.1007/978-981-10-4573-8_10.
144 R. Ikono, A. Vibriani, I. Wibowo, K. E. Saputro, W. Muliawan, B. M. Bachtiar, E. Mardliyati, E. W. Bachtiar, N. T. Rochman, H. Kagami, L. Xianqi, T. Nagamura-Inoue and A. Tojo, *BMC Res. Notes*, 2019, **12**, 383.
145 Z. Shi, K. G. Neoh, E. T. Kang and W. Wang, *Biomaterials*, 2006, **27**, 2440–2449.
146 T. M. P. Ngo, T. H. Nguyen, T. M. Q. Dang, T. X. Tran and P. Rachtanapun, *Int. J. Mol. Sci.*, 2020, **21**, 2224.
147 W. Chen, X. Rong, J. Peng, Q. Tang, H. Luo, L. Fan, K. Feng and H. Zheng, *Chemosphere*, 2020, **239**, 124736.
148 S. Bahrami, S. Esmaeilzadeh, M. Zarei and F. Ahmadi, *Parasitol. Res.*, 2015, **114**, 4617–4624.
149 V. Sekar, K. Rajendran, S. Vallinayagam, V. Deepak and S. Mahadevan, *J. Ind. Eng. Chem.*, 2018, **62**, 239–249.
150 E. Lam, S. Hrapovic, E. Majid, J. H. Chong and J. H. T. Luong, *Nanoscale*, 2012, **4**, 997–1002.
151 Q. Wang, S. Chen and D. Chen, *J. Mech. Behav. Biomed. Mater.*, 2017, **65**, 466–477.
152 F. Brandl, F. Sommer and A. Goepferich, *Biomaterials*, 2007, **28**, 134–146.
153 D. J. Huey, J. C. Hu and K. A. Athanasiou, *Science*, 2012, **338**, 917–921.
154 S. Ifuku, S. Morooka, A. Norio Nakagaito, M. Morimoto and H. Saimoto, *Green Chem.*, 2011, **13**, 1708–1711.
155 Y. Fan, H. Fukuzumi, T. Saito and A. Isogai, *Int. J. Biol. Macromol.*, 2012, **50**, 69–76.
156 A. M. Salaberria, J. Labidi and S. C. M. Fernandes, *Chem. Eng. J.*, 2014, **256**, 356–364.
157 M. N. Anglès and A. Dufresne, *Macromolecules*, 2000, **33**, 8344–8353.
158 A. Kaushik, M. Singh and G. Verma, *Carbohydr. Polym.*, 2010, **82**, 337–345.
159 P. Hassanzadeh, M. Kazemzadeh-Narbat, R. Rosenzweig, X. Zhang, A. Khademhosseini, N. Annabi and M. Rolandi, *J. Mater. Chem. B*, 2016, **4**, 2539–2543.
160 C. Chen, Y. Wang, Y. Yang, M. Pan, T. Ye and D. Li, *Carbohydr. Polym.*, 2018, **195**, 387–392.
161 C. C. Satam, C. W. Irvin, C. J. Coffey, R. K. Geran, R. Ibarra-Rivera, M. L. Shofner and J. C. Meredith, *Biomacromolecules*, 2020, **21**, 545–555.
162 C. C. Satam, C. W. Irvin, A. W. Lang, J. C. R. Jallorina, M. L. Shofner, J. R. Reynolds and J. C. Meredith, *ACS Sustainable Chem. Eng.*, 2018, **6**, 10637–10644.
163 S. Ifuku, A. Ikuta, M. Egusa, H. Kaminaka, H. Izawa, M. Morimoto and H. Saimoto, *Carbohydr. Polym.*, 2013, **98**, 1198–1202.
164 S. Ifuku, A. Ikuta, H. Izawa, M. Morimoto and H. Saimoto, *Carbohydr. Polym.*, 2014, **101**, 714–717.
165 Y. S. Nam, W. H. Park, D. Ihm and S. M. Hudson, *Carbohydr. Polym.*, 2010, **80**, 291–295.
166 R. Senthil Kumar, N. Ravikumar, S. Kavitha, S. Mahalaxmi, R. Jayasree, T. S. Sampath Kumar and M. Haneesh, *Int. J. Biol. Macromol.*, 2017, **104**, 1860–1865.
167 M. S. Sivakami, T. Gomathi, J. Venkatesan, H.-S. Jeong, S.-K. Kim and P. N. Sudha, *Int. J. Biol. Macromol.*, 2013, **57**, 204–212.
168 K. Karuppasamy, S. Thanikaikarasan, R. Antony, S. Balakumar and X. S. Shajan, *Ionics*, 2012, **18**, 737–745.
169 P. T. Anastas and J. C. Warner, *Green chemistry: Theory and practice*, 1998, pp. 29–56.
170 J. H. Clark, V. Budarin, F. E. I. Deswarte, J. J. E. Hardy, F. M. Kerton, A. J. Hunt, R. Luque, D. J. Macquarrie, K. Milkowski, A. Rodriguez, O. Samuel, S. J. Tavener, R. J. White and A. J. Wilson, *Green Chem.*, 2006, **8**, 853–860.
171 G. Finnveden, M. Z. Hauschild, T. Ekvall, J. Guinée, R. Heijungs, S. Hellweg, A. Koehler, D. Pennington and S. Suh, *J. Environ. Manage.*, 2009, **91**, 1–21.
172 N. Yang, W. Zhang, C. Ye, X. Chen and S. Ling, *Biotechnol. J.*, 2019, **14**, 1700754.
173 I. Muñoz, C. Rodríguez, D. Gillet and B. M. Moerschbacher, *Int. J. Life Cycle Assess.*, 2018, **23**, 1151–1160.
174 B. Subramaniam, P. Licence, A. Moores and D. T. Allen, *ACS Sustainable Chem. Eng.*, 2021, **9**, 3977–3978.
175 T. Iwata, *Angew. Chem., Int. Ed.*, 2015, **54**, 3210–3215.
176 I. Makarios-Laham and T.-C. Lee, *J. Environ. Polym. Degrad.*, 1995, **3**, 31–36.
177 R. Jayakumar, D. Menon, K. Manzoor, S. V. Nair and H. Tamura, *Carbohydr. Polym.*, 2010, **82**, 227–232.
178 E. Khor and L. Y. Lim, *Biomaterials*, 2003, **24**, 2339–2349.
179 H. Sashiwa and S.-i. Aiba, *Prog. Polym. Sci.*, 2004, **29**, 887–908.
180 A. Bernkop-Schnürch and S. Dünnhaupt, *Eur. J. Pharm. Biopharm.*, 2012, **81**, 463–469.
181 R. Riva, H. Ragelle, A. des Rieux, N. Duhem, C. Jérôme and V. Préat, in *Chitosan for Biomaterials II*, ed. R. Jayakumar,

M. Prabaharan and R. A. A. Muzzarelli, Springer Berlin Heidelberg, Berlin, Heidelberg, 2011, pp. 19–44, DOI: 10.1007/12_2011_137.
182 O. Felt, P. Buri and R. Gurny, *Drug Dev. Ind. Pharm.*, 1998, **24**, 979–993.
183 A. Anitha, S. Sowmya, P. T. S. Kumar, S. Deepthi, K. P. Chennazhi, H. Ehrlich, M. Tsurkan and R. Jayakumar, *Prog. Polym. Sci.*, 2014, **39**, 1644–1667.
184 M. Dash, F. Chiellini, R. M. Ottenbrite and E. Chiellini, *Prog. Polym. Sci.*, 2011, **36**, 981–1014.
185 P. Chen, H. Song, S. Yao, X. Tu, M. Su and L. Zhou, *RSC Adv.*, 2017, **7**, 29025–29034.
186 M. Rahimi, K. D. Safa, E. Alizadeh and R. Salehi, *New J. Chem.*, 2017, **41**, 3177–3189.
187 Z. Karimi Ghezeli, M. Hekmati and H. Veisi, *Appl. Organomet. Chem.*, 2019, **33**, e4833.
188 B. Rastegari, H. R. Karbalaei-Heidari, S. Zeinali and H. Sheardown, *Colloids Surf., B*, 2017, **158**, 589–601.
189 G. Unsoy, S. Yalcin, R. Khodadust, P. Mutlu, O. Onguru and U. Gunduz, *Biomed. Pharmacother.*, 2014, **68**, 641–648.
190 P. Mukhopadhyay, R. Mishra, D. Rana and P. P. Kundu, *Prog. Polym. Sci.*, 2012, **37**, 1457–1475.
191 S. Naskar, K. Kuotsu and S. Sharma, *J. Drug Targeting*, 2019, **27**, 379–393.
192 M. A. Mohammed, J. Syeda, K. M. Wasan and E. K. Wasan, *Pharmaceutics*, 2017, **9**, 53.
193 J. J. Wang, Z. W. Zeng, R. Z. Xiao, T. Xie, G. L. Zhou, X. R. Zhan and S. L. Wang, *Int. J. Nanomed.*, 2011, **6**, 765.
194 V. Arulmozhi, K. Pandian and S. Mirunalini, *Colloids Surf., B*, 2013, **110**, 313–320.
195 M. T. A. Qashqoosh, F. A. M. Alahdal, Y. K. Manea, S. M. Zakariya and S. Naqvi, *Chem. Phys.*, 2019, **527**, 110462.
196 P. Balan, J. Indrakumar, P. Murali and P. S. Korrapati, *Int. J. Biol. Macromol.*, 2020, **142**, 201–211.
197 R. Kavi Rajan, M. Z. Hussein, S. Fakurazi, K. Yusoff and M. J. Masarudin, *Int. J. Mol. Sci.*, 2019, **20**, 4667.
198 A. Lalatsa, N. L. Garrett, T. Ferrarelli, J. Moger, A. G. Schätzlein and I. F. Uchegbu, *Mol. Pharmaceutics*, 2012, **9**, 1764–1774.
199 L. Yang, S. Gao, S. Asghar, G. Liu, J. Song, X. Wang, Q. Ping, C. Zhang and Y. Xiao, *Int. J. Biol. Macromol.*, 2015, **72**, 1391–1401.
200 O. A. Attallah, A. Shetta, F. Elshishiny and W. Mamdouh, *RSC Adv.*, 2020, **10**, 8703–8708.
201 J. Khanifar, A. H. Salmanian, R. Haji Hosseini, J. Amani and R. Kazemi, *Artif. Cells, Nanomed., Biotechnol.*, 2019, **47**, 2593–2604.
202 K. Zhao, X. Shi, Y. Zhao, H. Wei, Q. Sun, T. Huang, X. Zhang and Y. Wang, *Vaccine*, 2011, **29**, 8549–8556.
203 S. Sudhakar, S. V. Chandran, N. Selvamurugan and R. A. Nazeer, *Int. J. Biol. Macromol.*, 2020, **150**, 281–288.
204 N. Jabbari, Z. Eftekhari, N. H. Roodbari and K. Parivar, *Int. Immunopharmacol.*, 2020, **85**, 106554.
205 C. Feng, J. Li, M. Kong, Y. Liu, X. J. Cheng, Y. Li, H. J. Park and X. G. Chen, *Colloids Surf., B*, 2015, **128**, 439–447.
206 P. Yousefpour, F. Atyabi, E. Vasheghani-Farahani, A.-A. M. Movahedi and R. Dinarvand, *Int. J. Nanomed.*, 2011, **6**, 1977–1990.
207 W.-H. Tsai, K.-H. Yu, Y.-C. Huang and C.-I. Lee, *Int. J. Nanomed.*, 2018, **13**, 903–916.
208 W.-T. Huang, M. Larsson, Y.-J. Wang, S.-H. Chiou, H.-Y. Lin and D.-M. Liu, *Mol. Pharmaceutics*, 2015, **12**, 1242–1249.
209 X. Tian, H. Yin, S. Zhang, Y. Luo, K. Xu, P. Ma, C. Sui, F. Meng, Y. Liu, Y. Jiang and J. Fang, *Eur. J. Pharm. Biopharm.*, 2014, **87**, 445–453.
210 Q. Xu, L. Guo, X. Gu, B. Zhang, X. Hu, J. Zhang, J. Chen, Y. Wang, C. Chen, B. Gao, Y. Kuang and S. Wang, *Biomaterials*, 2012, **33**, 3909–3918.
211 S. Maya, L. G. Kumar, B. Sarmento, N. Sanoj Rejinold, D. Menon, S. V. Nair and R. Jayakumar, *Carbohydr. Polym.*, 2013, **93**, 661–669.
212 A. Dev, N. S. Binulal, A. Anitha, S. V. Nair, T. Furuike, H. Tamura and R. Jayakumar, *Carbohydr. Polym.*, 2010, **80**, 833–838.
213 X. Ou, J. Zheng, X. Zhao and M. Liu, *ACS Appl. Nano Mater.*, 2018, **1**, 6790–6799.
214 Y. Matsumura and H. Maeda, *Cancer Res.*, 1986, **46**, 6387.
215 J. Fang, H. Nakamura and H. Maeda, *Adv. Drug Delivery Rev.*, 2011, **63**, 136–151.
216 H. Maeda, H. Nakamura and J. Fang, *Adv. Drug Delivery Rev.*, 2013, **65**, 71–79.
217 J. Zempleni, S. S. K. Wijeratne and Y. I. Hassan, *BioFactors*, 2009, **35**, 36–46.
218 P.-H. Yin, X. Liu, Y.-Y. Qiu, J.-F. Cai, J.-M. Qin, H.-R. Zhu and Q. Li, *Asian Pac. J. Cancer Prev.*, 2012, **13**, 5339–5343.
219 A. Aruffo, I. Stamenkovic, M. Melnick, C. B. Underhill and B. Seed, *Cell*, 1990, **61**, 1303–1313.
220 C. Feng, Z. Wang, C. Jiang, M. Kong, X. Zhou, Y. Li, X. Cheng and X. Chen, *Int. J. Pharm.*, 2013, **457**, 158–167.
221 R. Jayakumar, K. P. Chennazhi, R. A. A. Muzzarelli, H. Tamura, S. V. Nair and N. Selvamurugan, *Carbohydr. Polym.*, 2010, **79**, 1–8.
222 N. D. Al-Jbour, M. D. Beg, J. Gimbun and A. M. Alam, *Curr. Drug Delivery*, 2019, **16**, 272–294.
223 V. A. Petrova, V. Y. Elokhovskiy, S. V. Raik, D. N. Poshina, D. P. Romanov and Y. A. Skorik, *Biomolecules*, 2019, **9**, 291.
224 B. R. Rizeq, N. N. Younes, K. Rasool and G. K. Nasrallah, *Int. J. Mol. Sci.*, 2019, **20**, 5776.
225 R. Jayakumar, M. Prabaharan, P. T. Sudheesh Kumar, S. V. Nair and H. Tamura, *Biotechnol. Adv.*, 2011, **29**, 322–337.
226 S. Chen, B. Liu, M. A. Carlson, A. F. Gombart, D. A. Reilly and J. Xie, *Nanomedicine*, 2017, **12**, 1335–1352.
227 A. Memic, T. Abudula, H. S. Mohammed, K. Joshi Navare, T. Colombani and S. A. Bencherif, *ACS Appl. Bio Mater.*, 2019, **2**, 952–969.
228 M. Alavi, in *Nanotechnology in Skin, Soft Tissue, and Bone Infections*, ed. M. Rai, Springer International Publishing, Cham, 2020, pp. 169–181, DOI: 10.1007/978-3-030-35147-2_10.

229 Y. Xu, K. Liang, W. Ullah, Y. Ji and J. Ma, *Carbohydr. Polym.*, 2018, **190**, 324–330.
230 N. Naseri, C. Algan, V. Jacobs, M. John, K. Oksman and A. P. Mathew, *Carbohydr. Polym.*, 2014, **109**, 7–15.
231 S. Ramakrishna, K. Fujihara, W.-E. Teo, T. Yong, Z. Ma and R. Ramaseshan, *Mater. Today*, 2006, **9**, 40–50.
232 J.-P. Chen, G.-Y. Chang and J.-K. Chen, *Colloids Surf., A*, 2008, **313–314**, 183–188.
233 R. Izumi, S. Komada, K. Ochi, L. Karasawa, T. Osaki, Y. Murahata, T. Tsuka, T. Imagawa, N. Itoh, Y. Okamoto, H. Izawa, M. Morimoto, H. Saimoto, K. Azuma and S. Ifuku, *Carbohydr. Polym.*, 2015, **123**, 461–467.
234 Q. Chen, J. Wu, Y. Liu, Y. Li, C. Zhang, W. Qi, K. W. K. Yeung, T. M. Wong, X. Zhao and H. Pan, *Mater. Sci. Eng., C*, 2019, **105**, 110083.
235 L. Y. Kossovich, Y. Salkovskiy and I. V. Kirillova, in *6th World Congress of Biomechanics (WCB)*, ed. C. T. Lim and J. C. H. Goh, Springer, Berlin, Heidelberg, 2010, pp. 1212–1214.
236 Z.-X. Cai, X.-M. Mo, K.-H. Zhang, L.-P. Fan, A.-L. Yin, C.-L. He and H.-S. Wang, *Int. J. Mol. Sci.*, 2010, **11**, 3529–3539.
237 Z. Xie, C. B. Paras, H. Weng, P. Punnakitikashem, L.-C. Su, K. Vu, L. Tang, J. Yang and K. T. Nguyen, *Acta Biomater.*, 2013, **9**, 9351–9359.
238 Y. Zhou, D. Yang, X. Chen, Q. Xu, F. Lu and J. Nie, *Biomacromolecules*, 2008, **9**, 349–354.
239 A. Naeimi, M. Payandeh, A. R. Ghara and F. E. Ghadi, *Carbohydr. Polym.*, 2020, **240**, 116315.
240 P. Moutsatsou, K. Coopman and S. Georgiadou, *Polymers*, 2017, **9**, 687.
241 B. Dhandayuthapani, U. M. Krishnan and S. Sethuraman, *J. Biomed. Mater. Res., Part B*, 2010, **94**, 264–272.
242 M. Mattioli-Belmonte, A. Zizzi, G. Lucarini, F. Giantomassi, G. Biagini, G. Tucci, F. Orlando, M. Provinciali, F. Carezzi and P. Morganti, *J. Bioact. Compat. Polym.*, 2007, **22**, 525–538.
243 X. Guo, D. Xu, Y. Zhao, H. Gao, X. Shi, J. Cai, H. Deng, Y. Chen and Y. Du, *ACS Appl. Mater. Interfaces*, 2019, **11**, 34766–34776.
244 G. Nour-Eldeen, M. Abdel-Rasheed, A. M. El-Rafei, O. Azmy and G. T. El-Bassyouni, *Cell Regener.*, 2020, **9**, 7.
245 F. Moradikhah, M. Doosti-Telgerd, I. Shabani, S. Soheili, B. Dolatyar and E. Seyedjafari, *Life Sci.*, 2020, **254**, 117768.
246 R. Sedghi, A. Shaabani and N. Sayyari, *Carbohydr. Polym.*, 2020, **230**, 115707.
247 R. Sruthi, K. Balagangadharan and N. Selvamurugan, *Colloids Surf., B*, 2020, **193**, 111110.
248 Y. P. Singh, S. Dasgupta, S. Nayar and R. Bhaskar, *J. Biomater. Sci., Polym. Ed.*, 2020, **31**, 781–803.
249 C. O'Leary, L. Soriano, A. Fagan-Murphy, I. Ivankovic, B. Cavanagh, F. J. O'Brien and S.-A. Cryan, *Front. Bioeng. Biotechnol.*, 2020, **8**, 190.
250 Y. Fang, T. Zhang, Y. Song and W. Sun, *Biomed. Mater.*, 2020, **15**, 045003.
251 A. Bharadwaz and A. C. Jayasuriya, *Mater. Sci. Eng., C*, 2020, **110**, 110698.
252 F. Tao, Y. Cheng, X. Shi, H. Zheng, Y. Du, W. Xiang and H. Deng, *Carbohydr. Polym.*, 2020, **230**, 115658.
253 J. Henkel, M. A. Woodruff, D. R. Epari, R. Steck, V. Glatt, I. C. Dickinson, P. F. M. Choong, M. A. Schuetz and D. W. Hutmacher, *Bone Res.*, 2013, **1**, 216–248.
254 I. Aranaz, N. Acosta, C. Civera, B. Elorza, J. Mingo, C. Castro, M. D. L. L. Gandía and A. Heras Caballero, *Polymers*, 2018, **10**, 213.
255 S. Hirano, K. Hirochi, K.-I. Hayashi, T. Mikami and H. Tachibana, *Cosmetic and Pharmaceutical Applications of Polymers*, Springer, 1991, pp. 95–104.
256 P. Morganti and G. Morganti, *Clin. Dermatol.*, 2008, **26**, 334–340.
257 P. Morganti, P. Palombo, M. Palombo, G. Fabrizi, A. Cardillo, F. Svolacchia, L. Guevara and P. Mezzana, *Clin., Cosmet. Invest. Dermatol.*, 2012, **5**, 213–220.
258 A. Jimtaisong and N. Saewan, *Int. J. Cosmet. Sci.*, 2014, **36**, 12–21.
259 Z. Zhang, B. Zhang, N. Grishkewich, R. Berry and K. C. Tam, *Adv. Sustainable Syst.*, 2019, **3**, 1800156.
260 F. Awan, M. S. Islam, Y. Ma, C. Yang, Z. Shi, R. M. Berry and K. C. Tam, *ACS Omega*, 2018, **3**, 12403–12411.
261 A. R. Shirvan, N. H. Nejad and A. Bashari, *Fibers Polym.*, 2014, **15**, 1908–1914.
262 F. N. Maluin and M. Z. Hussein, *Molecules*, 2020, **25**, 1611.
263 S. Nguyen Van, H. Dinh Minh and D. Nguyen Awnh, *Biocatal. Agric. Biotechnol.*, 2013, **2**, 289–294.
264 A. R. Dudhani and S. L. Kosaraju, *Carbohydr. Polym.*, 2010, **81**, 243–251.
265 W. Xue, Y. Han, J. Tan, Y. Wang, G. Wang and H. Wang, *J. Agric. Food Chem.*, 2018, **66**, 6637–6645.
266 S. Mura, G. Seddaiu, F. Bacchini, P. P. Roggero and G. Greppi, *Ital. J. Agron.*, 2013, **8**, e18.
267 Y. Cheng, Y. Wang, Y. Han, D. Li, Z. Zhang, X. Zhu, J. Tan and H. Wang, *Molecules*, 2019, **24**, 1752.
268 U. B. Kutman, B. Yildiz and I. Cakmak, *Plant Soil*, 2011, **342**, 149–164.
269 Y. Zhou, S. Jiang, Y. Jiao and H. Wang, *Int. J. Biol. Macromol.*, 2017, **99**, 205–212.
270 N. Samarah, H. Wang and G. Welbaum, *Seed Sci. Technol.*, 2016, **44**, 609–623.
271 W. Lin, X. Hu, W. Zhang, W. J. Rogers and W. Cai, *J. Plant Physiol.*, 2005, **162**, 937–944.
272 S. Chandra, N. Chakraborty, A. Dasgupta, J. Sarkar, K. Panda and K. Acharya, *Sci. Rep.*, 2015, **5**, 15195.
273 R. C. Choudhary, R. V. Kumaraswamy, S. Kumari, S. S. Sharma, A. Pal, R. Raliya, P. Biswas and V. Saharan, *Sci. Rep.*, 2017, **7**, 9754.
274 W. Rademacher, *J. Plant Growth Regul.*, 2015, **34**, 845–872.
275 A. d. E. S. Pereira, H. C. Oliveira and L. F. Fraceto, *Sci. Rep.*, 2019, **9**, 7135.
276 W. E. Finch-Savage and G. W. Bassel, *J. Exp. Bot.*, 2016, **67**, 567–591.
277 N. Chauhan, N. Dilbaghi, M. Gopal, R. Kumar, K.-H. Kim and S. Kumar, *Int. J. Biol. Macromol.*, 2017, **97**, 616–624.

278 F. N. Maluin, M. Z. Hussein, N. A. Yusof, S. Fakurazi, I. Abu Seman, N. H. Zainol Hilmi and L. D. Jeffery Daim, *RSC Adv.*, 2019, **9**, 27083–27095.
279 W. Liang, A. Yu, G. Wang, F. Zheng, J. Jia and H. Xu, *Int. J. Biol. Macromol.*, 2018, **112**, 258–263.
280 Z. E. Sikorski, *J. Food Biochem.*, 2018, **42**, e12483.
281 Z. Ramezani, M. Zarei and N. Raminnejad, *Food Control*, 2015, **51**, 43–48.
282 F. Dong, S. Li, C. Jin, Z. Liu, K. Zhu, H. Zou and X. Wang, *Toxicol. Environ. Chem.*, 2016, **98**, 450–461.
283 L. Pilon, P. C. Spricigo, M. Miranda, M. R. de Moura, O. B. G. Assis, L. H. C. Mattoso and M. D. Ferreira, *Int. J. Food Sci. Technol.*, 2015, **50**, 440–448.
284 S. Hajji, M. Hamdi, S. Boufi, S. Li and M. Nasri, *Cellulose*, 2019, **26**, 6825–6847.
285 N. G. Abhirama, P. S. Nugraheni and W. Budhijanto, 2019, DOI: 10.1063/1.5095013.
286 G. B. Martínez-Hernández, M. L. Amodio and G. Colelli, *Innovative Food Sci. Emerging Technol.*, 2017, **41**, 56–63.
287 S. F. Hosseini, M. Zandi, M. Rezaei and F. Farahmandghavi, *Carbohydr. Polym.*, 2013, **95**, 50–56.
288 A. Anitha, V. G. Deepagan, V. V. Divya Rani, D. Menon, S. V. Nair and R. Jayakumar, *Carbohydr. Polym.*, 2011, **84**, 1158–1164.
289 M. Ghaderi-Ghahfarokhi, M. Barzegar, M. A. Sahari, H. Ahmadi Gavlighi and F. Gardini, *Int. J. Biol. Macromol.*, 2017, **102**, 19–28.
290 A. Mohammadi, M. Hashemi and S. M. Hosseini, *Postharvest Biol. Technol.*, 2015, **110**, 203–213.
291 M. Hadian, A. Rajaei, A. Mohsenifar and M. Tabatabaei, *LWT*, 2017, **84**, 394–401.
292 Y. Ma, L. Fu, Z. Hussain, D. Huang and S. Zhu, *Food Chem.*, 2019, **285**, 10–21.
293 R. Karimirad, M. Behnamian and S. Dezhsetan, *LWT*, 2019, **106**, 218–228.
294 Z. Li, R. Yang, F. Yang, M. Zhang and B. Wang, *BioResources*, 2015, **10**, 2995–3004.
295 J. Jeevahan and M. Chandrasekaran, *J. Mater. Sci.*, 2019, **54**, 12290–12318.
296 B. Fauzi, M. G. M. Nawawi, R. Fauzi and S. N. L. Mamauod, *BioResources*, 2019, **14**, 8324–8330.
297 H. Cui, D. Surendhiran, C. Li and L. Lin, *Food Packag. Shelf Life*, 2020, **24**, 100511.
298 W. Yan, W. Chen, U. Muhammad, J. Zhang, H. Zhuang and G. Zhou, *Food Control*, 2019, **104**, 132–138.
299 Z. N. Correa-Pacheco, S. Bautista-Baños, M. de Lorena Ramos-García, M. del Carmen Martínez-González and J. Hernández-Romano, *Prog. Org. Coat.*, 2019, **137**, 105326.
300 P. T. S. Melo, J. C. Nunes, C. G. Otoni, F. A. Aouada and M. R. de Moura, *J. Food Sci.*, 2019, **84**, 2228–2233.
301 S. Bao, S. Xu and Z. Wang, *J. Sci. Food Agric.*, 2009, **89**, 2692–2700.
302 M. Azarifar, B. Ghanbarzadeh, M. Sowti Khiabani, A. Akhondzadeh Basti and A. Abdulkhani, *Int. J. Food Microbiol.*, 2020, **318**, 108493.
303 H. Zhou, Y. Tan, S. Lv, J. Liu, J. L. Muriel-Mundo, L. Bai, O. J. Rojas and D. J. McClements, *Food Hydrocolloids*, 2020, **106**, 105878.
304 A. C. Khorasani and S. A. Shojaosadati, *Int. J. Biol. Macromol.*, 2017, **94**, 131–144.
305 Z. Guo, X. Cao, G. M. DeLoid, K. Sampathkumar, K. W. Ng, S. C. J. Loo and P. Demokritou, *J. Agric. Food Chem.*, 2020, **68**, 358–368.
306 M. Diop, N. Auberval, A. Viciglio, A. Langlois, W. Bietiger, C. Mura, C. Peronet, A. Bekel, D. Julien David, M. Zhao, M. Pinget, N. Jeandidier, C. Vauthier, E. Marchioni, Y. Frere and S. Sigrist, *Int. J. Pharm.*, 2015, **491**, 402–408.
307 A. Makhlof, Y. Tozuka and H. Takeuchi, *Eur. J. Pharm. Sci.*, 2011, **42**, 445–451.
308 S. Akbari-Alavijeh, R. Shaddel and S. M. Jafari, *Food Hydrocolloids*, 2020, **105**, 105774.
309 K. Desai, K. Kit, J. Li, P. Michael Davidson, S. Zivanovic and H. Meyer, *Polymer*, 2009, **50**, 3661–3669.
310 A. Cooper, R. Oldinski, H. Ma, J. D. Bryers and M. Zhang, *Carbohydr. Polym.*, 2013, **92**, 254–259.
311 M. Botes and T. Eugene Cloete, *Crit. Rev. Microbiol.*, 2010, **36**, 68–81.
312 L. Li, Y. Li and C. Yang, *Carbohydr. Polym.*, 2016, **140**, 299–307.
313 L. Li, J. Zhang, Y. Li and C. Yang, *J. Membr. Sci.*, 2017, **544**, 333–341.
314 S. Haider and S.-Y. Park, *J. Membr. Sci.*, 2009, **328**, 90–96.
315 M. Makaremi, C. X. Lim, P. Pasbakhsh, S. M. Lee, K. L. Goh, H. Chang and E. S. Chan, *RSC Adv.*, 2016, **6**, 53882–53893.
316 B. Bai, Master's dissertation, Michigan Technological University, 2012.
317 L. Wang, C. Zhang, F. Gao and G. Pan, *RSC Adv.*, 2016, **6**, 105988.
318 Y. Su, L. Ma, J. Chen and J. Xu, *Carbohydr. Polym.*, 2017, **175**, 113–121.
319 M. Zarghani and B. Akhlaghinia, *RSC Adv.*, 2016, **6**, 31850–31860.
320 N. V. Kramareva, A. Y. Stakheev, O. P. Tkachenko, K. V. Klementiev, W. Grünert, E. D. Finashina and L. M. Kustov, *J. Mol. Catal. A: Chem.*, 2004, **209**, 97–106.
321 E. Guibal, *Prog. Polym. Sci.*, 2005, **30**, 71–109.
322 J. J. E. Hardy, S. Hubert, D. J. Macquarrie and A. J. Wilson, *Green Chem.*, 2004, **6**, 53–56.
323 H. Song, N. Zhang, C. Zhong, Z. Liu, M. Xiao and H. Gai, *New J. Chem.*, 2017, **41**, 9170–9177.
324 A. V. Kucherov, N. V. Kramareva, E. D. Finashina, A. E. Koklin and L. M. Kustov, *J. Mol. Catal. A: Chem.*, 2003, **198**, 377–389.
325 Y. Chang, Y. Wang and Z. Su, *J. Appl. Polym. Sci.*, 2002, **83**, 2188–2194.
326 D.-Q. Zhou, M. He, Y.-H. Zhang, M.-Y. Huang and Y.-Y. Jiang, *Polym. Adv. Technol.*, 2003, **14**, 287–291.
327 J. W. Bae, I. G. Kim, J. S. Lee, K. H. Lee and E. J. Jang, *Appl. Catal., A*, 2003, **240**, 129–142.

328 D. J. Macquarrie and J. J. E. Hardy, *Ind. Eng. Chem. Res.*, 2005, **44**, 8499–8520.
329 J. Yang, X. An, L. Liu, F. T. Seta, H. Zhang, S. Nie, S. Yao, H. Cao, Q. Xu, H. Liu and Y. Ni, *Cellulose*, 2020, **27**, 5071–5087.
330 Y. Tsutsumi, H. Koga, Z.-D. Qi, T. Saito and A. Isogai, *Biomacromolecules*, 2014, **15**, 4314–4319.
331 T. Jin, M. Hicks, D. Kurdyla, S. Hrapovic, E. Lam and A. Moores, *Beilstein J. Org. Chem.*, 2020, **16**, 2477–2483.
332 R. A. Sheldon, *Adv. Synth. Catal.*, 2007, **349**, 1289–1307.
333 X.-J. Huang, D. Ge and Z.-K. Xu, *Eur. Polym. J.*, 2007, **43**, 3710–3718.
334 J. Srbová, M. Slováková, Z. Křípalová, M. Žárská, M. Špačková, D. Stránská and Z. Bílková, *React. Funct. Polym.*, 2016, **104**, 38–44.
335 N. Dorraki, N. N. Safa, M. Jahanfar, H. Ghomi and S.-O. Ranaei-Siadat, *Appl. Surf. Sci.*, 2015, **349**, 940–947.
336 J.-M. Park, M. Kim, H.-S. Park, A. Jang, J. Min and Y.-H. Kim, *Int. J. Biol. Macromol.*, 2013, **54**, 37–43.

